2018

WILDFIRE EMISSIONS IN THE CONTEXT OF GLOBAL CHANGE AND THE IMPLICATIONS FOR MERCURY POLLUTION

Aditya Kumar
Michigan Technological University, adityak@mtu.edu

WILDFIRE EMISSIONS IN THE CONTEXT OF GLOBAL CHANGE AND THE IMPLICATIONS FOR MERCURY POLLUTION

By

Aditya Kumar

A DISSERTATION

Submitted in partial fulfillment of the requirements for the degree of

DOCTOR OF PHILOSOPHY

In Environmental Engineering

MICHIGAN TECHNOLOGICAL UNIVERSITY

2018

This dissertation has been approved in partial fulfillment of the requirements for the Degree of DOCTOR OF PHILOSOPHY in Environmental Engineering.

Department of Geological and Mining Engineering and Sciences

Dissertation Advisor: *Dr. Shiliang Wu*

Committee Member: *Dr. Judith Perlinger*

Committee Member: *Dr. Hugh Gorman*

Committee Member: *Dr. Noel Urban*

Department Chair: *Dr. John Gierke*

Dedicated

to

God

Contents

Acknowledgements

I would like to thank my advisor Dr. Shiliang Wu for his continuous support during the course of my study period at Michigan Tech. It has been a great learning experience working on all the research projects and it has been a great experience working in his group. I learnt a lot working on the Michigan Tech ASEP project working with team members from such a diverse group of disciplines and multiple institutions. Thanks to Dr. Judith Perlinger for her leadership during the project, being on my doctoral committee and feedback and support during the past several years. Special thanks to Dr. Hugh Gorman for being on my doctoral committee and support. I would also like to thank Dr. Noel Urban for being on my doctoral committee and providing feedback.

I would like to acknowledge the support provided by the Michigan Tech ASEP project (award #ICER-1313755), U.S. EPA (grant # 83518901) and the Michigan Tech Earth and Planetary Sciences Institute grant that has made this dissertation possible and helped me bring my graduate education close to completion. Thanks to Michigan Tech Center for Water and Society, Graduate Student Government, Great Lakes Research Center and Harvard University Atmospheric Chemistry Modeling Group for supporting my conference travels. It has been great attending the GEOS-Chem meetings at Harvard and participating in all the Michigan Tech World Water Day events and the Graduate Research Colloquiums.

Furthermore, a word of thanks for the Michigan Tech ASEP project team members, my research group members, friends in Houghton and my family.

Special mention for DOW 853 for housing me for the past 7.5 years and the machines (C08-0853-05.ad) and ctm.geo.mtu.edu on which I have done all my graduate work.

Abstract

Wildfires are episodic disturbances that exert a significant influence on the Earth system. They emit substantial amounts of atmospheric pollutants, which can impact atmospheric chemistry/composition and the Earth's climate at the global and regional scales. This work presents a collection of studies aimed at better estimating wildfire emissions of atmospheric pollutants, quantifying their impacts on remote ecosystems and determining the implications of 2000s-2050s global environmental change (land use/land cover, climate) for wildfire emissions following the Intergovernmental Panel on Climate Change (IPCC) A1B socioeconomic scenario.

A global fire emissions model is developed to compile global wildfire emission inventories for major atmospheric pollutants [greenhouse gases (CO_2, CH_4, N_2O), air pollutants and tropospheric O_3 precursors (nitrogen oxides (NO_x), carbon monoxide (CO), volatile organic compounds (VOCs) (alkanes, alkenes)), aerosols and their precursors (particulate matter ($PM_{2.5}$), black carbon (BC), organic carbon (OC), sulfur dioxide (SO_2)) and mercury (Hg)] and quantify the impacts of 2000s-2050s global change. The estimated Hg wildfire emissions (2000s) are used in a global chemical transport model (GEOS-Chem) to determine the contribution of wildfire emissions to Hg pollution in the Arctic.

Significant perturbations to wildfire emissions of atmospheric pollutants in the context of global change are estimated, mainly driven by the projected changes in climate, land use/land cover and in the case of Hg, anthropogenic emissions as well. A continuing increase in anthropogenic influence on wildfires in the coming decades is predicted.

Greater human occupation of the African continent and increase in cropland coverage cause significant declines in wildfire emissions of atmospheric pollutants from the continent. Anthropogenic factors play an important role in the changes in emissions from other continents as well. Future changes in climate and land cover contribute to significant increases in global emissions for all the species.

Wildfires are estimated to contribute 10% of global annual deposition to the Arctic with boreal fires in Asia contributing the most. Wildfires in Eurasia contribute 5.3% of annual Hg deposition followed by Africa (2.5%) and North America (1%). Wildfires contribute to Arctic Hg deposition throughout the year with the highest deposition occurring during the boreal fire season.

Chapter 1: Introduction

Human alterations of the Earth's environment can be dated back to several thousand years ago. For example, Lu et al. (2017) reported evidence of land use change and deforestation occurring 11,500 years ago. The findings of Hong et al. (1994) showed that lead (Pb) pollution was significant 2500-1700 years ago. These alterations mainly consisted of land use change, mining activities and igniting fires. However, the Industrial Revolution marked the beginning of a period of unprecedented changes in the interactions of humans with the Earth's environment that have continued till present day. The accelerated pace of socioeconomic development, use of non-renewable energy sources (e.g. fossil fuels) to advance economic development and provide a more affluent lifestyle have contributed to major degradation of the global environment (Weiss et al., 1999)] including the composition of the atmosphere (IPCC, 2014).

Substantial amounts of CO_2 and a myriad of other pollutants (e.g. CH_4, NO_x, N_2O, aerosols, CO, VOCs, Hg) have been emitted to the atmosphere as a result of anthropogenic activities driven by the quest for economic growth and efforts to sustain a growing human population. The cumulative CO_2 emissions to the atmosphere during 1750 – 2011 were estimated at 2040 ± 310 Gt CO_2 with about half of these emissions occurring in the last 40 years (IPCC, 2014). These emissions have caused atmospheric levels of pollutants to reach unprecedented levels at an alarming rate (Canadell et al., 2007; Davidson, 2009; Dickinson and Cicerone, 1986; Forster et al., 2007; Horowitz, 2006; Machida et al., 1995; Siegenthaler and Sarmiento, 1993). The levels of atmospheric concentrations of CO_2, CH_4

and N_2O (as of 2011) have not been observed at least in the past 800,000 years (IPCC, 2014). The natural biogeochemical cycles of several elements (e.g. carbon, nitrogen, sulfur, phosphorus, and mercury) have been altered substantially (Magnani et al., 2007; Schlesinger et al., 2017; Vitousek et al., 1997). Tropospheric O_3 levels have increased since the pre-industrial times with the most likely cause being the concordant increase in anthropogenic emissions of O_3 precursors (NO_x, CO, VOCs) (Anfossi et al., 1991; Horowitz, 2006; Logan, 1985; Staehelin et al., 1994; Volz and Kley, 1988; Wang and Jacob, 1998). Several air pollution episodes have occurred in the past few decades [e.g. 1930 Meuse Valley (Anderson, 2009; Firket, 1936; Nemery et al., 2001; Roholm, 1937), 1939 Saint Louis, 1948 (Donora) (Ciocco and Thompson, 1961; Schrenk et al., 1949), 1952 & 1991 (London) (Anderson, 2009; Anderson et al., 1995; Bell and Davis, 2001; Bell et al., 2004; Lawler et al., 2014), 1997 (Indonesian forest fires) (Kim et al., 2017; Kunii et al., 2002)] with each resulting in grave impacts on human health and a significant number of fatalities. Moreover, anthropogenic land use change in the form of clearing forests to expand agricultural croplands/pastoral lands and support human population expansion has resulted in major alterations to the Earth's natural land cover (Foley et al., 2005). The destruction of ecosystems at the global and regional scales (e.g. the tropical rainforests in the Amazon and South Asia (Achard et al., 2002; Laurance, 2007; Skole and Tucker, 1993)) has continued unabated for long periods. For example, in the tropics, more than 80% of new agricultural land during the 1980s and 1990s was derived at the expense of the rainforests (Gibbs et al., 2010).

These anthropogenic forcings have not only caused significant environmental pollution but have also resulted in long term/potentially irreversible impacts on the Earth system, its constituent reservoirs (atmospheric, terrestrial and oceanic) and modified the mutual interactions between them. The impacts have been of such magnitude and extent that this geological era has been referred to as the Anthropocene (Crutzen, 2002; Lewis and Maslin, 2015). Furthermore, due to the coupled nature of the Earth system, alterations to one component can cause major changes in the others and can also result in the initiation of feedback loops (positive/negative). For example, elevated atmospheric CO_2 levels could promote natural vegetation growth through the process of CO_2 fertilization (Donohue et al., 2013; Farquhar, 1997). Higher atmospheric greenhouse gas [CO_2, CH_4, N_2O] concentrations have contributed to a global increase in surface temperatures and major shifts in the climate in general (e.g. precipitation patterns, extreme events). A warmer climate could result in favorable conditions for wildfire activity. Wildfires themselves are significant sources of greenhouse gases which can further exacerbate the warming, thus forming a positive feedback loop.

Considering the substantial alterations to the Earth system that have resulted from human activities in the past few centuries, it is imperative to determine how the future will look and make continuous efforts to improve our understanding of the Earth system in order to better appreciate the implications of various anthropogenic activities. What will be the future trajectories of human population, land use, economic development and technological changes and how will they impact greenhouse gas and other pollutant emissions? How will these socioeconomic/technological changes and the resulting emissions impact the Earth

system? How sensitive is the Earth system to perturbations caused by various forcings it is subjected to and how does the presence/absence of these forcings affect its state? These are important questions from the perspective of devising strategies and policies aimed at preventing/minimizing further environmental degradation, facilitate the recovery of the Earth system from the anthropogenic forcings of the past few centuries, derive estimates of the times needed for recovery and improving our understanding of the Earth system. However, future predictions are inherently uncertain and predicting future global environmental change/global change and its potential impacts is no different. There are significant complexities associated with the driving forces of global change and the various components of the Earth system/interactions between them and their constituent species. Moreover, there are prevailing uncertainties in our understanding of the Earth system. For example, future changes in climate would primarily be a function of the greenhouse gas emissions trajectories. These emissions involve a large number of driving forces [e.g. population and economic growth]. It is difficult to provide accurate future emissions estimates given the large number of variables involved.

Scenario based analysis serves as a particularly useful tool in this case. A scenario is defined as a postulated sequence of events that could lead to certain outcomes. It allows us to construct potential cases of driving forces for a variable and paint a plausible future picture with respect to the variable. There are no probabilities attached to these scenarios and their sole purpose is to provide a picture of the future for several possible cases. In the context of global change, scenarios can be employed to study various trajectories of future global development and the resulting impacts on the variable of interest. They also

facilitate the assessment of future developments in complex systems that are either inherently unpredictable or have high scientific uncertainties (Nakicenovic et al., 2000). A number of scenarios have been developed in the past [e.g. The Intergovernmental Panel on Climate Change (IPCC) scenarios of future greenhouse gas/aerosol precursor emissions (IS 92 (Houghton et al., 1992) and Special Report Emission Scenarios (SRES) (Nakicenovic et al., 2000)) and concentrations (Representative Concentration Pathways (RCP)), Hg anthropogenic emissions scenarios based on the IPCC SRES scenarios (Corbitt et al., 2011; Streets et al., 2009), United Nations Minamata Convention (Giang et al., 2015) and other developments (Glodek et al., 2010; Pacyna et al., 2016; Rafaj et al., 2013), climate scenarios (Giorgi et al., 1992)], land use scenarios (Lawler et al., 2014)] and have been utilized extensively to study the impacts of various forcings on the Earth system and present possible pictures of the future at the regional and global scales [e.g. (Huang et al., 2015; Kumar et al., 2018; Leibensperger et al., 2012a, b; Mickley et al., 2012; Mitchell et al., 1995; Perlinger et al., 2018; Wu et al., 2007; 2008a; 2012; 2008b; Zhang et al., 2016)].

A scenario based analysis aimed at studying the effects of various forcings on the Earth system generally involves the use of one/more computational models simulating the Earth system and its components [e.g. atmosphere (e.g. atmospheric circulation, atmospheric chemistry, biogeochemical cycling of elements) and the coupled reservoirs (marine and terrestrial)] or a coupled human-natural systems model]. Models are representations of the physical/chemical processes occurring in the system considered. They solve the governing mathematical formulations of the physical and chemical behavior of the system considered at discrete time intervals over a discretized spatial domain. Models can be used to study

and quantify the effects of various forcings on the system considered, better understand the physical/chemical interactions between the constituent species and the response and sensitivity of system dynamics and chemistry to alterations in the system composition. A plethora of models have been created to simulate the Earth system [e.g. atmospheric dynamics (e.g. NASA GISS GCM 3 (Hansen et al., 1988; Rind et al., 2007; Wu et al., 2007; Wu et al., 2008a; Wu et al., 2008b)), chemistry (e.g. GEOS-Chem (Bey et al., 2001; Park et al., 2003; Park et al., 2004; Parrella et al., 2012)) and coupling to other reservoirs (e.g. terrestrial biogeochemical cycling of elements (Carnegie Ames Stanford Approach carbon cycling model (CASA) (Potter et al., 1993), Global Terrestrial Mercury Model (GTMM) (Smith-Downey et al., 2010)), global vegetation cover (e.g. Lund Potsdam Jena –Dynamic Global Vegetation Model (LPJ-DGVM) (Sitch et al., 2003; Wu et al., 2012))]. Several previous studies have used a scenario and modeling approach to predict the impacts of future global change on the atmospheric, terrestrial and marine reservoirs employing scenarios of climate change, anthropogenic emissions and associated policies, land cover, land use [e.g. (Jiang et al., 2013; Mickley et al., 2004; Pye et al., 2009; Spracklen et al., 2009; Wu et al., 2008a; Wu et al., 2012; Wu et al., 2008b)]. Thus, a general scenario based approach to predict a future variable of interest would begin with identifying the factors this variable depends upon, deciding on all possible trajectories the variable of interest could follow in the future depending on various directions of changes in the underlying factors followed by defining the scenarios and finally using models to make quantitative predictions of the variable. Scenario based analyses coupled with the use of models have been an integral part of research aiming to delineate the impacts of human activities on the Earth system and studying the sensitivity of atmospheric chemistry and air

quality to atmospheric composition and emission sources. However, models are only as good as the inputs they receive and the scientific understanding of the system they represent along with the associated physical/chemical processes. Therefore, continuous efforts to improve inputs to these models and the physical/chemical processes simulated by them are imperative.

This study presents an effort to provide better estimates of currently uncertain atmospheric model inputs, study the impacts of pollution in different global regions and quantify the effects of future (2000s-2050s) global change on atmospheric forcings along with the resulting impacts on atmospheric chemistry and composition. It employs scenario based and sensitivity analyses together with models of the atmosphere [NASA GISS GCM 3], land cover [LPJ DGVM], coupled human natural systems [IMAGE model (IMAGE Team, 2001)] and a fire emissions model (Kumar et al., 2018). The forcings studied in this work are atmospheric pollutant emissions from wildfires and anthropogenic sources while the atmospheric species of interest include major greenhouse gases [CO_2, CH_4, and N_2O], air pollutants [CO, O_3, NO_x, aerosols, VOCs] and Atmosphere-Surface Exchangeable Pollutants (ASEPs (Perlinger et al., 2016)) [Hg]. 2000s-2050s global change in this work follows the IPCC SRES A1B scenario and encompasses human population changes, changes in climate caused by anthropogenic forcings, alterations in natural vegetation coverage and distribution driven by climate change and changes in anthropogenic land use.

Chapter 2 presents the development of a global fire emissions model. The model is used to estimate the global wildfire emissions of atmospheric Hg, which are highly uncertain and constitute an important input to atmospheric models simulating Hg. Subsequently, the

model is employed to investigate the impacts of 2000s-2050s global change on Hg wildfire emissions with an emphasis on changes in climate, land use/land cover and Hg anthropogenic emissions following the IPCC A1B scenario.

Chapter 3 presents further use of the fire emissions model to estimate global emissions of the major atmospheric pollutants emitted from wildfires (e.g. NO_x, CO_2, CO, VOCs, $PM_{2.5}$) for the 2000s and discusses the impacts of 2000s-2050s global change on the emissions and its implications for atmospheric chemistry and air quality at the global and regional scales. In order to estimate the emissions for these species, a recently published wildfire emission factors compilation (Akagi et al., 2011) is used.

Chapter 4 aims to determine the contributions of Hg wildfire emissions from different geographical regions to annual atmospheric gross Hg deposition in the Arctic. This work uses the global Hg emissions inventory from Chapter 1 to drive the atmospheric Hg simulation in GEOS-Chem.

References

Achard, F., Eva, H.D., Stibig, H.-J., Mayaux, P., Gallego, J., Richards, T., Malingreau, J.-P. (2002) Determination of deforestation rates of the world's humid tropical forests. Science 297, 999-1002.

Akagi, S., Yokelson, R.J., Wiedinmyer, C., Alvarado, M., Reid, J., Karl, T., Crounse, J., Wennberg, P. (2011) Emission factors for open and domestic biomass burning for use in atmospheric models. Atmospheric Chemistry and Physics 11, 4039-4072.

Anderson, H.R. (2009) Air pollution and mortality: A history. Atmospheric environment 43, 142-152.

Anderson, H.R., Limb, E.S., Bland, J.M., De Leon, A.P., Strachan, D.P., Bower, J.S. (1995) Health effects of an air pollution episode in London, December 1991. Thorax 50, 1188-1193.

Anfossi, D., Sandroni, S., Viarengo, S. (1991) Tropospheric ozone in the nineteenth century: the Moncalieri series. Journal of Geophysical Research: Atmospheres 96, 17349-17352.

Bell, M.L., Davis, D.L. (2001) Reassessment of the lethal London fog of 1952: novel indicators of acute and chronic consequences of acute exposure to air pollution. Environmental health perspectives 109, 389.

Bell, M.L., Davis, D.L., Fletcher, T. (2004) A retrospective assessment of mortality from the London smog episode of 1952: the role of influenza and pollution. Environmental health perspectives 112, 6.

Bey, I., Jacob, D.J., Yantosca, R.M., Logan, J.A., Field, B.D., Fiore, A.M., Li, Q., Liu, H.Y., Mickley, L.J., Schultz, M.G. (2001) Global modeling of tropospheric chemistry with assimilated meteorology: Model description and evaluation. Journal of Geophysical Research: Atmospheres 106, 23073-23095.

Canadell, J.G., Le Quéré, C., Raupach, M.R., Field, C.B., Buitenhuis, E.T., Ciais, P., Conway, T.J., Gillett, N.P., Houghton, R., Marland, G. (2007) Contributions to accelerating atmospheric CO2 growth from economic activity, carbon intensity, and efficiency of natural sinks. Proceedings of the National Academy of Sciences 104, 18866-18870.

Ciocco, A., Thompson, D.J. (1961) A follow-up of Donora ten years after: methodology and findings. American Journal of Public Health and the Nations Health 51, 155-164.

Corbitt, E.S., Jacob, D.J., Holmes, C.D., Streets, D.G., Sunderland, E.M. (2011) Global source–receptor relationships for mercury deposition under present-day and 2050 emissions scenarios. Environmental science & technology 45, 10477-10484.

Crutzen, P.J. (2002) Geology of mankind. Nature 415, 23.

Davidson, E.A. (2009) The contribution of manure and fertilizer nitrogen to atmospheric nitrous oxide since 1860. Nature Geoscience 2, 659.

Dickinson, R.E., Cicerone, R.J. (1986) Future global warming from atmospheric trace gases. Nature 319, 109.

Donohue, R.J., Roderick, M.L., McVicar, T.R., Farquhar, G.D. (2013) Impact of CO2 fertilization on maximum foliage cover across the globe's warm, arid environments. Geophysical Research Letters 40, 3031-3035.

Farquhar, G.D. (1997) Carbon dioxide and vegetation. Science 278, 1411-1411.

Firket, J. (1936) Fog along the Meuse valley. Transactions of the Faraday Society 32, 1192-1196.

Foley, J.A., DeFries, R., Asner, G.P., Barford, C., Bonan, G., Carpenter, S.R., Chapin, F.S., Coe, M.T., Daily, G.C., Gibbs, H.K. (2005) Global consequences of land use. Science 309, 570-574.

Forster, P., Ramaswamy, V., Artaxo, P., Berntsen, T., Betts, R., Fahey, D.W., Haywood, J., Lean, J., Lowe, D.C., Myhre, G., (2007) Changes in atmospheric constituents and in radiative forcing. Chapter 2, Climate Change 2007. The Physical Science Basis.

Giang, A., Stokes, L.C., Streets, D.G., Corbitt, E.S., Selin, N.E. (2015) Impacts of the minamata convention on mercury emissions and global deposition from coal-fired power generation in Asia. Environmental science & technology 49, 5326-5335.

Gibbs, H.K., Ruesch, A.S., Achard, F., Clayton, M.K., Holmgren, P., Ramankutty, N., Foley, J.A. (2010) Tropical forests were the primary sources of new agricultural land in the 1980s and 1990s. Proceedings of the National Academy of Sciences 107, 16732-16737.

Giorgi, F., Marinucci, M., Visconti, G. (1992) A 2XCO2 climate change scenario over Europe generated using a limited area model nested in a general circulation model 2. Climate change scenario. Journal of Geophysical Research: Atmospheres 97, 10011-10028.

Glodek, A., Panasiuk, D., Pacyna, J.M. (2010) Mercury emission from anthropogenic sources In Poland and their scenarios to the year 2020. Water, Air, & Soil Pollution 213, 227-236.

Hansen, J., Fung, I., Lacis, A., Rind, D., Lebedeff, S., Ruedy, R., Russell, G., Stone, P. (1988) Global climate changes as forecast by Goddard Institute for Space Studies three-dimensional model. Journal of Geophysical Research: Atmospheres 93, 9341-9364.

Hong, S., Candelone, J.-P., Patterson, C.C., Boutron, C.F. (1994) Greenland ice evidence of hemispheric lead pollution two millennia ago by Greek and Roman civilizations. Science 265, 1841-1843.

Horowitz, L.W. (2006) Past, present, and future concentrations of tropospheric ozone and aerosols: Methodology, ozone evaluation, and sensitivity to aerosol wet removal. Journal of Geophysical Research: Atmospheres 111.

Houghton, J.T., Callander, B.A., Varney, S.K. (1992) Climate Change 1992: The Supplementary Report to the IPCC Scientific Assessment Cambridge University Press, Great Britain, New York, NY, USA, and Victoria , Australia, 218 pp.

Huang, Y., Wu, S., Kaplan, J.O. (2015) Sensitivity of global wildfire occurrences to various factors in the context of global change. Atmospheric environment 121, 86-92.

IMAGE Team, H. (2001) The IMAGE 2.2 implementation of the SRES scenarios: a comprehensive analysis of emissions, climate change and impacts in the 21st century. RIVM CD-ROM Publication 481508018.

IPCC (2014) Climate Change 2014: Synthesis Report. Contribution of Working Groups I, II and III to the Fifth Assessment Report of the Intergovernmental Panel on Climate Change [Core Writing Team, R.K. Pachauri and L.A. Meyer (eds.)]. IPCC Geneva, Switzerland, 151 pp.

Jiang, H., Liao, H., Pye, H., Wu, S., Mickley, L., Seinfeld, J., Zhang, X. (2013) Projected effect of 2000-2050 changes in climate and emissions on aerosol levels in China and associated transboundary transport. Atmospheric Chemistry and Physics 13, 7937-7960.

Kim, Y., Knowles, S., Manley, J., Radoias, V. (2017) Long-run health consequences of air pollution: Evidence from Indonesia's forest fires of 1997. Economics & Human Biology 26, 186-198.

Kumar, A., Wu, S., Huang, Y., Liao, H., Kaplan, J.O. (2018) Mercury from wildfires: Global emission inventories and sensitivity to 2000–2050 global change. Atmospheric environment 173, 6-15.

Kunii, O., Kanagawa, S., Yajima, I., Hisamatsu, Y., Yamamura, S., Amagai, T., Ismail, I.T.S. (2002) The 1997 haze disaster in Indonesia: its air quality and health effects. Archives of Environmental Health: An International Journal 57, 16-22.

Laurance, W.F. (2007) Forest destruction in tropical Asia. Current Science, 1544-1550.

Lawler, J.J., Lewis, D.J., Nelson, E., Plantinga, A.J., Polasky, S., Withey, J.C., Helmers, D.P., Martinuzzi, S., Pennington, D., Radeloff, V.C. (2014) Projected land-use change impacts on ecosystem services in the United States. Proceedings of the National Academy of Sciences 111, 7492-7497.

Leibensperger, E., Mickley, L.J., Jacob, D.J., Chen, W.-T., Seinfeld, J., Nenes, A., Adams, P., Streets, D., Kumar, N., Rind, D. (2012a) Climatic effects of 1950–2050 changes in US anthropogenic aerosols–Part 1: Aerosol trends and radiative forcing. Atmospheric Chemistry and Physics 12, 3333-3348.

Leibensperger, E., Mickley, L.J., Jacob, D.J., Chen, W.-T., Seinfeld, J., Nenes, A., Adams, P., Streets, D., Kumar, N., Rind, D. (2012b) Climatic effects of 1950–2050 changes in US

anthropogenic aerosols–Part 2: Climate response. Atmospheric Chemistry and Physics 12, 3349-3362.

Lewis, S.L., Maslin, M.A. (2015) Defining the anthropocene. Nature 519, 171.

Logan, J.A. (1985) Tropospheric ozone: Seasonal behavior, trends, and anthropogenic influence. Journal of Geophysical Research: Atmospheres 90, 10463-10482.

Lu, Y., Waldmann, N., Nadel, D., Marco, S. (2017) Increased sedimentation following the Neolithic Revolution in the Southern Levant. Global and Planetary Change 152, 199-208.

Machida, T., Nakazawa, T., Fujii, Y., Aoki, S., Watanabe, O. (1995) Increase in the atmospheric nitrous oxide concentration during the last 250 years. Geophysical Research Letters 22, 2921-2924.

Magnani, F., Mencuccini, M., Borghetti, M., Berbigier, P., Berninger, F., Delzon, S., Grelle, A., Hari, P., Jarvis, P.G., Kolari, P. (2007) The human footprint in the carbon cycle of temperate and boreal forests. Nature 447, 849.

Mickley, L.J., Jacob, D.J., Field, B., Rind, D. (2004) Effects of future climate change on regional air pollution episodes in the United States. Geophysical Research Letters 31.

Mickley, L.J., Leibensperger, E., Jacob, D.J., Rind, D. (2012) Regional warming from aerosol removal over the United States: Results from a transient 2010–2050 climate simulation. Atmospheric environment 46, 545-553.

Mitchell, J.F., Johns, T., Gregory, J.M., Tett, S. (1995) Climate response to increasing levels of greenhouse gases and sulphate aerosols. Nature 376, 501.

Nakicenovic, N., Alcamo, J., Davis, G., De Vries, B., Fenhann, J., Gaffin, S., Gregory, K., Griibler, A., Jung, T.Y., Kram, T. (2000) Emissions scenarios.

Nemery, B., Hoet, P.H., Nemmar, A. (2001) The Meuse Valley fog of 1930: an air pollution disaster. The lancet 357, 704-708.

Pacyna, J.M., Travnikov, O., De Simone, F., Hedgecock, I.M., Sundseth, K., Pacyna, E.G., Steenhuisen, F., Pirrone, N., Munthe, J., Kindbom, K. (2016) Current and future levels of mercury atmospheric pollution on a global scale. Atmospheric Chemistry and Physics 16, 12495.

Park, R.J., Jacob, D.J., Chin, M., Martin, R.V. (2003) Sources of carbonaceous aerosols over the United States and implications for natural visibility. Journal of Geophysical Research: Atmospheres 108.

Park, R.J., Jacob, D.J., Field, B.D., Yantosca, R.M., Chin, M. (2004) Natural and transboundary pollution influences on sulfate-nitrate-ammonium aerosols in the United States: Implications for policy. Journal of Geophysical Research: Atmospheres 109.

Parrella, J., Jacob, D.J., Liang, Q., Zhang, Y., Mickley, L.J., Miller, B., Evans, M., Yang, X., Pyle, J., Theys, N. (2012) Tropospheric bromine chemistry: implications for present and pre-industrial ozone and mercury. Atmospheric Chemistry and Physics 12, 6723-6740.

Perlinger, J., Urban, N., Giang, A., Selin, N., Hendricks, A., Zhang, H., Kumar, A., Wu, S., Gagnon, V., Gorman, H. (2018) Responses of deposition and bioaccumulation in the Great Lakes region to policy and other large-scale drivers of mercury emissions. Environmental Science: Processes & Impacts 20, 195-209.

Perlinger, J.A., Gorman, H.S., Norman, E.S., Obrist, D., Selin, N.E., Urban, N.R., Wu, S., (2016) Measurement and Modeling of Atmosphere-Surface Exchangeable Pollutants (ASEPs) To Better Understand their Environmental Cycling and Planetary Boundaries. ACS Publications.

Potter, C.S., Randerson, J.T., Field, C.B., Matson, P.A., Vitousek, P.M., Mooney, H.A., Klooster, S.A. (1993) Terrestrial ecosystem production: a process model based on global satellite and surface data. Global Biogeochemical Cycles 7, 811-841.

Pye, H., Liao, H., Wu, S., Mickley, L.J., Jacob, D.J., Henze, D.K., Seinfeld, J. (2009) Effect of changes in climate and emissions on future sulfate-nitrate-ammonium aerosol levels in the United States. Journal of Geophysical Research: Atmospheres 114.

Rafaj, P., Bertok, I., Cofala, J., Schoepp, W. (2013) Scenarios of global mercury emissions from anthropogenic sources. Atmospheric environment 79, 472-479.

Rind, D., Lerner, J., Jonas, J., McLinden, C. (2007) Effects of resolution and model physics on tracer transports in the NASA Goddard Institute for Space Studies general circulation models. Journal of Geophysical Research: Atmospheres 112.

Roholm, K. (1937) The fog disaster in the Meuse Valley, 1930: A fluorine intoxication. The Journal of Industrial Hygiene and Toxicology 19, 126-137.

Schlesinger, W.H., Klein, E.M., Vengosh, A. (2017) Global biogeochemical cycle of vanadium. Proceedings of the National Academy of Sciences, 201715500.

Schrenk, H.H., Heimann, H., Clayton, G.D., Gafafer, W., Wexler, H. (1949) Air Pollution in Donora, Pa. Epidemiology of the Unusual Smog Episode of October 1948. Preliminary Report. Air Pollution in Donora, Pa. Epidemiology of the Unusual Smog Episode of October 1948. Preliminary Report.

Siegenthaler, U., Sarmiento, J. (1993) Atmospheric carbon dioxide and the ocean. Nature 365, 119.

Sitch, S., Smith, B., Prentice, I.C., Arneth, A., Bondeau, A., Cramer, W., Kaplan, J., Levis, S., Lucht, W., Sykes, M.T. (2003) Evaluation of ecosystem dynamics, plant geography and

terrestrial carbon cycling in the LPJ dynamic global vegetation model. Global Change Biology 9, 161-185.

Skole, D., Tucker, C. (1993) Tropical deforestation and habitat fragmentation in the Amazon: satellite data from 1978 to 1988. Science 260, 1905-1910.

Smith-Downey, N.V., Sunderland, E.M., Jacob, D.J. (2010) Anthropogenic impacts on global storage and emissions of mercury from terrestrial soils: Insights from a new global model. Journal of Geophysical Research: Biogeosciences 115.

Spracklen, D.V., Mickley, L.J., Logan, J.A., Hudman, R.C., Yevich, R., Flannigan, M.D., Westerling, A.L. (2009) Impacts of climate change from 2000 to 2050 on wildfire activity and carbonaceous aerosol concentrations in the western United States. Journal of Geophysical Research: Atmospheres 114.

Staehelin, J., Thudium, J., Buehler, R., Volz-Thomas, A., Graber, W. (1994) Trends in surface ozone concentrations at Arosa (Switzerland). Atmospheric environment 28, 75-87.

Streets, D.G., Zhang, Q., Wu, Y. (2009) Projections of global mercury emissions in 2050. Environmental science & technology 43, 2983-2988.

Vitousek, P.M., Aber, J.D., Howarth, R.W., Likens, G.E., Matson, P.A., Schindler, D.W., Schlesinger, W.H., Tilman, D.G. (1997) Human alteration of the global nitrogen cycle: sources and consequences. Ecological applications 7, 737-750.

Volz, A., Kley, D. (1988) Evaluation of the Montsouris series of ozone measurements made in the nineteenth century. Nature 332, 240.

Wang, Y., Jacob, D.J. (1998) Anthropogenic forcing on tropospheric ozone and OH since preindustrial times. Journal of Geophysical Research: Atmospheres 103, 31123-31135.

Weiss, D., Shotyk, W., Appleby, P.G., Kramers, J.D., Cheburkin, A.K. (1999) Atmospheric Pb deposition since the industrial revolution recorded by five Swiss peat profiles: enrichment factors, fluxes, isotopic composition, and sources. Environmental science & technology 33, 1340-1352.

Wu, S., Mickley, L.J., Jacob, D.J., Logan, J.A., Yantosca, R.M., Rind, D. (2007) Why are there large differences between models in global budgets of tropospheric ozone? Journal of Geophysical Research: Atmospheres 112.

Wu, S., Mickley, L.J., Jacob, D.J., Rind, D., Streets, D.G. (2008a) Effects of 2000–2050 changes in climate and emissions on global tropospheric ozone and the policy-relevant background surface ozone in the United States. Journal of Geophysical Research: Atmospheres 113.

Wu, S., Mickley, L.J., Kaplan, J., Jacob, D.J. (2012) Impacts of changes in land use and land cover on atmospheric chemistry and air quality over the 21st century. Atmospheric Chemistry and Physics 12, 1597-1609.

Wu, S., Mickley, L.J., Leibensperger, E.M., Jacob, D.J., Rind, D., Streets, D.G. (2008b) Effects of 2000–2050 global change on ozone air quality in the United States. Journal of Geophysical Research: Atmospheres 113.

Zhang, H., Holmes, C., Wu, S. (2016) Impacts of changes in climate, land use and land cover on atmospheric mercury. Atmospheric environment 141, 230-244.

Chapter 2: Mercury from Wildfires: Global Emission Inventories and Sensitivity to 2000-2050 Global Change[1]

[1] The contents of this chapter have been published as a journal article in Atmospheric Environment. *Kumar, A., Wu, S., Huang, Y., Liao, H., & Kaplan, J. O. (2018). Mercury from wildfires: Global emission inventories and sensitivity to 2000–2050 global change. Atmospheric Environment, 173, 6-15*.

2.1. Abstract

We estimate the global Hg wildfire emissions for the 2000s and the potential impacts from the 2000-2050 changes in climate, land use and land cover and Hg anthropogenic emissions by combining statistical analysis with global data on vegetation type and coverage as well as fire activities. Global Hg wildfire emissions are estimated to be 612 Mg $year^{-1}$. Africa is the dominant source region (43.8% of global emissions), followed by Eurasia (31%) and South America (16.6%). We find significant perturbations to wildfire emissions of Hg in the context of global change, driven by the projected changes in climate, land use and land cover and Hg anthropogenic emissions. 2000-2050 climate change could increase Hg emissions by 14% globally and regionally by 18% for South America, 14% for Africa and 13% for Eurasia. Projected changes in land use by 2050 could decrease the global Hg emissions from wildfires by 13% mainly driven by a decline in African emissions due to significant agricultural land expansion. Future land cover changes could lead to significant increases in Hg emissions over some regions (+32% North America, +14% Africa, +13% Eurasia). Potential enrichment of terrestrial ecosystems in 2050 in response to changes in Hg anthropogenic emissions could increase Hg wildfire emissions globally (+28%) and regionally (+19% North America, +20% South America, +24% Africa, +41% Eurasia). Our results indicate that the future evolution of climate, land use and land cover and Hg anthropogenic emissions are all important factors affecting Hg wildfire emissions in the coming decades.

2.2. Introduction

Mercury (Hg) is a toxic and persistent pollutant in the global environment. Hg emitted to the atmosphere can be transported long distances before depositing to terrestrial and aquatic systems. The atmospheric emissions of Hg include both anthropogenic sources such as fossil fuel combustion, smelting of ores, cement production, waste incineration, and artisanal gold mining, (Chen et al., 2014; Pacyna et al., 2010; Pirrone et al., 2010; Streets et al., 2011; Veiga et al., 2006), natural emissions from erupting and passively degassing volcanoes, geothermal hot springs, topsoil enriched in Hg (Ferrara et al., 2000; Nimick et al., 2013; Nriagu and Becker, 2003; Pyle and Mather, 2003; Varekamp and Buseck, 1986), and biomass burning/wildfires (Friedli et al., 2009a; Friedli et al., 2001; Sigler et al., 2003; Turetsky et al., 2006; Veiga et al., 1994; Weiss-Penzias et al., 2007; Wiedinmyer and Friedli, 2007).

Terrestrial vegetation plays an important role in the biogeochemical cycling of Hg, and is considered a significant reservoir for atmospheric Hg. Obrist (2007) estimated the global uptake of atmospheric Hg by vegetation could be more than 1000 Mg per year. Retention of atmospheric Hg by vegetation delays its transport to soils and aquatic systems (Graydon et al., 2012). Hence, vegetation plays an important role in Hg sequestration by terrestrial ecosystems. Wildfires, through the burning of biomass, can effectively mobilize the Hg stored in terrestrial ecosystems and lead to massive emissions of Hg and other pollutants into the atmosphere (Andreae and Merlet, 2001; Biswas et al., 2007; Ito and Penner, 2004; Turetsky et al., 2006; van der Werf et al., 2006; Veiga et al., 1994). Multiple studies have

estimated Hg wildfire emissions at the global and regional scales (Table 2) with global total emissions in the range of 104-1330 Mg Hg $year^{-1}$ indicating large uncertainty in the estimated Hg emissions from wildfires. A number of studies have developed wildfire emission inventories for Hg based on CO or CO_2 emission inventories by applying fixed emission ratios between Hg and CO/CO_2 [e.g. (Brunke et al., 2001; Ebinghaus et al., 2007; Sigler et al., 2003)]. To our knowledge, Friedli et al. (2009a) is the only study so far that have compiled a multi-year (1997-2006) emission inventory for Hg from wildfires at the global scale by accounting for the variations in Hg emission factors across geographical regions and ecosystems. The emission factor (EF) for a given species (Hg in this case) can be expressed as the mass of that species emitted per unit dry biomass burned (Andreae and Merlet, 2001). It is affected by both the vegetation type and geographical region.

Significant changes in global vegetation coverage are expected in the coming decades driven by either climate change (referred to as land cover change hereon) or anthropogenic land use change (referred to as land use change hereon) (Bachelet et al., 2003; Bachelet et al., 2001; Cox et al., 2000; Falloon et al., 2012; Notaro et al., 2007; O'ishi and Abe-Ouchi, 2009; Tilman et al., 2001; Wu et al., 2012). Wu et al. (2012) predicted significant changes in forests and grassland coverage by 2050 with the northern mid-latitudes being affected the most. Notaro et al. (2007) predicted reduced forest cover over the Amazon, South Africa and Australia due to the radiative effect of rising CO_2 and poleward shift of the boreal forest due to both radiative and physiological effects. In addition, continued anthropogenic conversion of forested land for agriculture in the future to support a growing global human population and the resulting food and energy demand could result in

significant degradation of natural vegetation. Tilman et al. (2001) projected an 18% increase in global agricultural (cropland & pastureland) area in 2050 relative to 2000. By 2050 (IPCC A1B scenario), significant degradation of natural vegetation for agricultural purposes is predicted in Eastern US, Central Africa, Southern and Equatorial Asia and Western Europe while agricultural land area could decrease in South America, East Asia, Western parts of Australia and Russia (IPCC, 2001; MNP, 2006).

The changes in vegetation type and density associated with future land use/land cover change could have a direct influence on future wildfire activity. Huang et al. (2015) predicted a 15% increase in global wildfire frequency in 2050 due to land cover change alone with major increases in Africa and North America. On the contrary, land use change could result in significant declines in fire occurrence in Africa and Western US whereas increases are predicted in Australia and South America (Huang et al., 2015). Furthermore, Hg emissions from wildfires are affected by the Hg content in the vegetation (biomass) (Biswas et al., 2007) making Hg emissions particularly sensitive to future alterations in land use and land cover. In addition to land use/land cover change, future changes in climate would also influence global fire activity. Predicted warmer temperatures in the future together with alterations in precipitation patterns driven by climate change could result in significantly different fire regimes from the 2000s (Cochrane and Barber, 2009; Flannigan et al., 2009; Yue et al., 2013). Huang et al. (2015) predicted a 19% increase in global fire frequency in 2050 caused by changes in meteorology due to climate change. Yue et al. (2013) predicted that summertime surface aerosol concentrations resulting from wildfire emissions over the Western US could increase by 46-70% for organic carbon and

20-27% for black carbon by 2050 relative to the 2000s driven by climate change. Finally, the changes in anthropogenic emissions of Hg can significantly affect Hg emissions from wildfires by affecting the atmospheric deposition of Hg. Because atmospheric deposition is a major source of Hg enrichment in terrestrial vegetation and soils, future alterations in Hg atmospheric deposition to terrestrial environments could play a key role in determining the emission factors of Hg from wildfires. In this study, we estimate the atmospheric Hg emissions from global wildfires by accounting for the regional variations in both fire activities and Hg emission factors and examining the impacts from 2000-2050 changes in climate, land use/land cover and anthropogenic emissions.

2.3. Methodology

Hg emissions from wildfires are calculated based on the classical equation for biomass burning emissions (Seiler and Crutzen, 1980) and accounting for various factors including vegetation type and density, Hg content in biomass, and fire characteristics. Considering the significant variation in fire characteristics, land cover and climate across geographical regions, the analyses for various regions is carried out separately. We use geographical region definitions that have been commonly used in the literature (Aldersley et al., 2011; Friedli et al., 2009a; Giglio et al., 2010a; Giglio et al., 2013; Giglio et al., 2006b; Li et al., 2012; Van der Werf et al., 2010; van der Werf et al., 2006).

Figure 1 shows a map of the geographical regions. The Hg emissions model is developed at a spatial resolution of 4° x 5° (latitude x longitude). The monthly mean Hg emissions from wildfires at a grid cell (i, j), $E_{(i,j)}$, are calculated as:

$$\mathbf{E_{(i,j)}} = \sum_{\mathbf{k=1}}^{\mathbf{9}} \mathbf{EF_{k_{(i,j)}}} * \mathbf{M_{k_{(i,j)}}} * \left(\left(\frac{\mathbf{f_{k_{(i,j)}}}}{\sum_{\mathbf{k=1}}^{\mathbf{9}} \mathbf{f_{k_{(i,j)}}}} \right) * \mathbf{A_{(i,j)}} \right) * \mathbf{CF_{(i,j)}} \quad (1)$$

Where:

$\mathbf{EF_{k_{(i,j)}}}$: Hg emission factors (grams of Hg emitted/grams of dry biomass burned) for land cover type k at grid cell (i, j)

$\mathbf{A_{(i,j)}}$: Burned area at (i, j) (square meters)

$\mathbf{f_{k_{(i,j)}}}$: Fractional areal coverage for land cover type k at (i, j) (unitless)

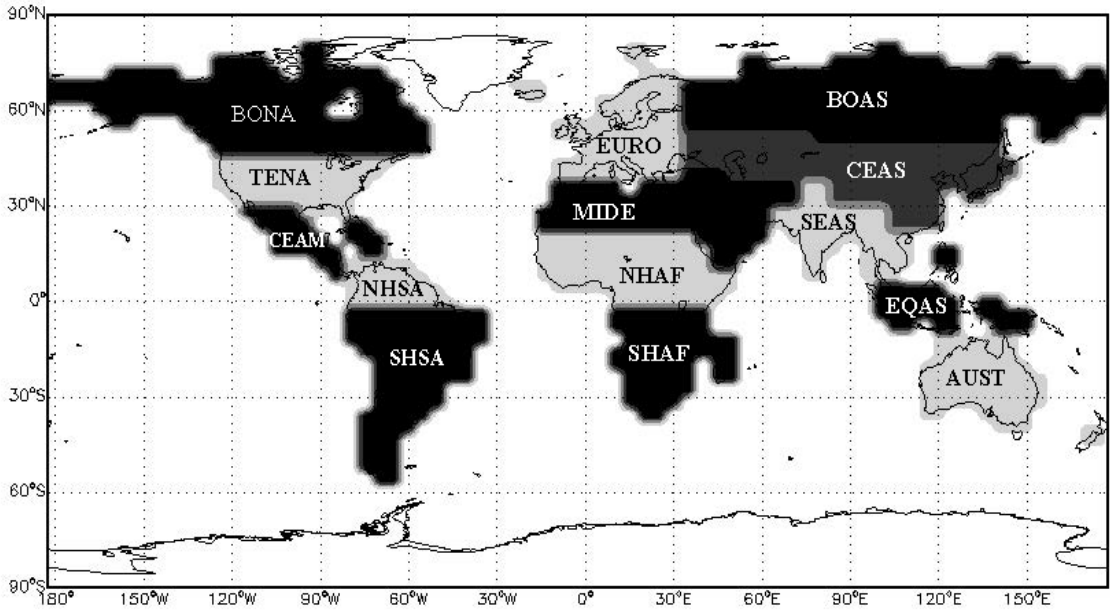

Figure 1: Definition of global regions used in this study. BONA: Boreal North America, TENA: Temperate North America, CEAM: Central North America, NHSA: Northern Hemisphere South America, SHSA: Southern Hemisphere South America, EURO: Europe, MIDE: Middle East, NHAF: Northern Hemisphere Africa, SHAF: Southern Hemisphere Africa, BOAS: Boreal Asia, CEAS: Central Asia, SEAS: South East Asia, EQAS: Equatorial Asia, AUST: Australia.

$\mathbf{M_{k_{(i,j)}}}$: Available biomass density for vegetation type k at grid cell (i, j) (grams of biomass/square meters)

$\mathbf{CF_{(i,j)}}$**:** Combustion fraction at (i, j) (unitless)

For the Hg emission factors for the 2000s, we follow Friedli et al. (2009a) to assign region-specific EF for various regions but update the tropical forests EFs with data from Melendez-Perez et al. (2014). The final EF (122 ng Hg/g biomass burned) for tropical forests is the average of values reported by Friedli et al. (2009a) (198 ng Hg/g biomass burned) and Melendez-Perez et al. (2014) (47 ng Hg/g biomass burned). Boreal regions

(BONA and BOAS) and Equatorial Asia (EQAS) have the highest EF values (315 ng Hg/g biomass burned) due to high soil mercury pools present there (Friedli et al., 2009a) followed by temperate forests (242 ng Hg/g biomass burned), tropical forests (122 ng Hg/g biomass burned) and grasslands (41 ng Hg/g biomass burned).

Available biomass density (M) is the amount of dead/live plant material available for consumption by fires per unit area. The available biomass in a grid cell includes herbaceous vegetation, non-woody and woody tree parts and plant litter (decomposable and resistant). Available biomass estimates for forest and non-forest ecosystems from Jain et al. (2006), generated using the terrestrial component of the Integrated Science Assessment Model (ISAM) (Jain and Yang, 2005) are used here. These estimates are provided for nine geographical regions and four land cover types (tropical, temperate, boreal forests and non-forested ecosystems). Combustion fraction (CF) represents the fraction of available biomass that burns during a fire. It is a function of vegetation type, its spatial arrangement and moisture content (Ito and Penner, 2004). We follow the scheme used by Wiedinmyer et al. (2006) to estimate the CF. This scheme, based on the percentage of tree cover (TC) in a grid cell, classifies the vegetation into different types and assigns corresponding CF estimates for trees and herbaceous vegetation therein, as:

$$\mathrm{CF} = \begin{cases} 0.30 \text{ for trees and } 0.90 \text{ for herbs} & \text{if } \%\mathrm{TC} > 60\% \\ 0.30 \text{ for trees and } \exp^{-0.013*\%\mathrm{TC}} \text{ for herbs} & \text{if } 40\% \leq \%\mathrm{TC} \leq 60\% \\ 0.00 \text{ for trees and } 0.98 \text{ for herbs} & \text{if } \%\mathrm{TC} < 40\% \end{cases} \quad (2)$$

Land cover data used in this work consists of fractional areal vegetation coverage output (2000 and 2050) from the Lund-Potsdam Jena Dynamic Global Vegetation (LPJ DGVM) model (Gerten et al., 2004; Hickler et al., 2006; Schaphoff et al., 2006; Sitch et al., 2003; Thonicke et al., 2001; Wu et al., 2012). The LPJ model is a process based global model of vegetation dynamics. It simulates the production and loss of plant biomass, competition amongst different plant species for resources, vegetation structural properties and soil biogeochemistry (Gerten et al., 2004; Thonicke et al., 2001) based on the inputs of meteorology, soil type and atmospheric CO_2 concentration. Natural vegetation in each grid cell is described in terms of fractional coverage of 9 plant functional types (PFTs), which include *tropical broadleaved evergreen tree (TrBE)*, *tropical broadleaved raingreen tree (TrBR), temperate needleleaved evergreen tree (TeNE)*, *temperate broadleaved evergreen tree (TeBE)*, *temperate broadleaved summergreen tree (TeBS), boreal needleleaved evergreen tree (BNE)*, *boreal needleleaved summergreen tree (BNS)*, *C3 and C4 herbs*. Each woody PFT is either evergreen, summergreen or raingreen depending on water availability and temperature whereas herbaceous PFTs are C3 or C4 based on the type of photosynthesis activity associated with them. The fractional natural vegetation coverage output used here was obtained by driving the LPJ DGVM with meteorology fields (2000 and 2050) generated from the GISS Global Climate Model Version 3 (GISS GCM v3) (Rind et al., 2007; Wu et al., 2007; Wu et al., 2008a; Wu et al., 2008b) following the IPCC A1B scenario for future greenhouse gas concentrations. Further simulation details are provided in Wu et al. (2012). Here 10-year average vegetation data (1991-2000 vs 2041-2050) is used to examine the long-term changes in vegetation.

Data for anthropogenic land use consists of cropland areal coverage (2000 and 2050) from the IMAGE model following the IPCC A1B scenario (IMAGE Team, 2001; MNP, 2006). The data were regridded from a spatial resolution of 1° x 1° to 4° x 5° in this work. For each grid cell, fractional coverage of each of the LPJ PFTs was uniformly reduced in proportion to the crop fraction to accommodate for cropland coverage. For the 2000s, the LPJ PFT and crop fractions are at the 2000s level. The 2000-2050 land use and land cover scenario includes both natural vegetation and crop coverage as predicted for 2050. The land cover change scenario has natural vegetation changing in response to climate change but the cropland coverage is kept fixed at the 2000s level whereas in the land use change scenario natural vegetation is kept fixed at the 2000s level and cropland coverage following land use trends for 2050 is used. The climate change scenario involves changes in meteorology only (using GISS GCM v3 meteorology fields for 2000 and 2050).

The burned area $\mathbf{A_{(i,j)}}$ was estimated as:

$$\mathbf{A_{(i,j)}} = \boldsymbol{\alpha}_{\mathbf{(i,j)}}\left(\mathbf{T_{f_{(i,j)}}}, \mathbf{H_{f_{(i,j)}}}, \mathbf{B_{f_{(i,j)}}}, \mathbf{T_{s_{(i,j)}}}, \mathbf{P_{s_{(i,j)}}}\right) * \mathbf{N_{c_{(i,j)}}} \quad (3)$$

where the proportionality factor $\boldsymbol{\alpha}_{\mathbf{(i,j)}}$is a function of land cover type and coverage (represented by tree cover ($\mathbf{T_{f_{(i,j)}}}$), herb cover ($\mathbf{H_{f_{(i,j)}}}$) and barren land $\mathbf{B_{f_{(i,j)}}}$ in grid cell (i, j)) and climate (represented by surface temperature $\mathbf{T_{s_{(i,j)}}}$ and precipitation $\mathbf{P_{s_{(i,j)}}}$ in grid cell (i, j)). N_c is the fire frequency which is affected by fire ignition sources such as lightning strikes and anthropogenic ignitions, meteorological conditions, vegetation density and human population density. Huang et al. (2015) accounted for all these factors and estimated the changes in fire frequency (at a spatial resolution of 4° x 5° and monthly temporal resolution) in response to changes in climate, land cover, land use and population density

considering a suite of scenarios (land use/land cover change, climate change, changes in ignition agents and anthropogenic suppression of fires). Their results for the 2050 climate change, land use and land cover change scenarios are used here.

Our burned area estimation methodology involves building a statistical model relating fire activity (independent variable) and burned area (dependent variable), which was subsequently used with the fire model generated fire frequencies to predict burned area (for 2000 and 2050). We use available global fire frequencies and burned area datasets from satellite observations and consider land cover (% tree cover (% TC), % herb cover (% HC) and % barren land (% BL)) and meteorology (T_s and P_s) as the major factors influencing the relationship between fire activity and burned area. In order to account for this dependence, regression tree models are employed. A regression tree is a decision–tree-based statistical model (Breiman et al., 1984; Breiman and Meisel, 1976; Loh, 2008, 2011). It recursively partitions the input data space $\{y, x_1, \ldots x_n\}$ (y is the dependent variable and x's are the independent variables) consisting of training data for the dependent and independent variables into subsets and fits separate linear regression models to each subset. The independent variables can be used as splitting variables (used to make univariate splits at each node of the tree), predictive variables (used to predict the dependent variable) or both. The splitting of input data space into subsets allows application of regression relations to a homogeneous data space with respect to the splitting variables and thus improves the applicability of the relations to the data space. The dependence of burned area on land cover has been highlighted by Van Der Werf et al. (2003) and Giglio et al. (2006b) and regression trees for predicting global burned area from fire frequencies have been previously used [e.g. (Giglio et al., 2010a; Giglio et al., 2006b)]. Separate regression trees

were developed for each of the 14 geographical regions in Figure 1. This approach allows modeling the effects of fuel type (tree/herbaceous), configuration and availability and favorable/unfavorable weather conditions on wildfire spread.

The splitting variables include %TC, %HC, %BL, T_s and P_s. Each terminal node of the tree consists of a linear regression model with fire frequencies as the independent variable and burned area as the dependent variable. Training data used for constructing the regression trees is described below. Observed fire frequencies (2001-2015) are from the Collection 5 Terra MODIS Climate Modeling Grid (CMG) fire product (data at ftp://fuoco.geog.umd.edu/modis/C5/cmg/) available at a 0.5° x 0.5° spatial and monthly temporal resolution (Giglio et al., 2006a; Justice et al., 2002). For burned area, estimates from the Global Fire Emissions Database Version 4 (GFEDv4) (data at ftp://fuoco.geog.umd.edu/gfed4/monthly/) ((2001-2015)) (Giglio et al., 2013) are used. The spatial resolution of this product is 0.5° x 0.5° (monthly temporal resolution). Both datasets were regridded to a 4° x 5° spatial resolution for use in this work. LPJ land cover data (accounting for cropland coverage as described earlier) was used for the 2000s land cover. The PFTs were combined to obtain %TC (sum of all tree PFTs), %HC (sum of all herbaceous PFTs) and the remainder after accounting for natural vegetation and cropland yielded the %BL (non-vegetated land). Surface temperature and precipitation datasets consisted of monthly means generated from 3 hourly averaged (A-3) fields from the GEOS-4 (2001-2003) (Suarez et al., 2005), GEOS-5 (2004-2012) (Rienecker, 2008) and hourly average (A-1) fields from the GEOS-FP (2013-2015) (Lucchesi, 2013; Molod et al., 2012) meteorology products (4° x 5° spatial resolution). The datasets for MODIS fire frequency,

GFEDv4 burned area, LPJ land cover and GEOS meteorology at 4° x 5° were prepared for each of the 14 geographical regions as defined in Figure 1. Thus, training data for each regional regression tree consisted of a 15-year (2001-2015) time series of MODIS Terra fire frequencies, GFEDv4 burned area estimates, LPJ land cover data for the 2000s and GEOS meteorology fields. These data were used to construct regression trees for each of the 14 geographical regions. Subsequently, these regression tree models were applied to estimate the monthly-burned area for 2000 and 2050 scenarios based on fire frequencies estimated from the fire model along with land cover data from the LPJ model and surface temperature and precipitation fields (monthly means from 3 hourly averaged (A-3) fields) from the GISS GCM v3 model. With all the input data available, the Hg emissions (with monthly and 4° x 5° resolution) from wildfires for various regions and scenarios are calculated using the fire emissions model (i.e. Eq. 1).

To examine the perturbations to wildfire emissions of Hg from changes in anthropogenic emissions of Hg, we assume a linear relationship between the Hg emission factors from wildfires and the atmospheric deposition of mercury (Dep): $EF_{2000}/ DEP_{2000} = EF_{2050}/DEP_{2050}$. The actual response of Hg enrichment in vegetation and soils to changes in atmospheric deposition could be very complicated and non-linear, but without detailed data available, the linear simplification allows us to estimate the sensitivity of wildfire emissions of Hg to changes in anthropogenic emissions. The atmospheric deposition of mercury for the 2000s and 2050 were estimated using the global mercury simulation in the GEOS-Chem model (Bey et al., 2001). The GEOS-Chem mercury simulation (Corbitt et al., 2011; Giang et al., 2015; Holmes et al., 2010; Jaeglé et al., 2009; Selin and Jacob, 2008;

Selin et al., 2007; Selin et al., 2008; Smith-Downey et al., 2010; Strode et al., 2007; Zhang et al., 2016) includes three Hg species (elemental (Hg (0)), divalent (Hg (II)) and particulate bound Hg (Hg (P)). It includes coupled land-ocean-atmosphere cycling of Hg. Hg emissions include anthropogenic and natural sources and re-emission of previously deposited mercury from terrestrial and aquatic systems. Sinks for Hg include dry deposition, wet deposition (for Hg (II) and Hg (P)) and sea salt uptake (for Hg (II)). This work uses v9-02 of the model and years 2005-2011 were simulated with the GEOS-5 meteorology. The years 2005-2007 were used to initialize the model and the results presented are averages for 2008-2011. The model was driven by anthropogenic emissions for 2050 following the IPCC A1B scenario (Corbitt et al., 2011; Streets et al., 2009). Hg GDEP was calculated as the sum of deposition for all Hg species (Hg (0), Hg (II) and Hg (P) dry deposition + Hg (II) and Hg (P) wet deposition).

2.4. Results

2.4.1. Burned area estimates

Table 1(a). Estimated regional[a] and global wildfire burned area (in Mha year^{-1}) for the 2000s.

Study	Study Period	NA	SA	AFR	EURAS	AUS	GLOB
This work	**1998-2002**	**10**	**47**	**170**	**78**	**29**	**334**
GFEDv4 (Giglio et al., 2013)	1996-2015	6	21	238	28	49	342
GFEDv3 (Giglio et al., 2010a)	1997-2011	5	23	253	30	52	363
GLOBSCAR 2000 (Simon et al., 2004)	2000	11.1		121		18	200
GBA 2000[b,] (Tansey et al., 2004a) (Tansey et al., 2004b)	2000	7	10.5	224	52.5	56	350
L3JRC (Tansey et al., 2008)	2000-2007						392
(Randerson et al., 2012)	2000-2010	8.7	33.8	323.7	49.5	48.5	464.3
Li et al. (2012)	1997-2004			180			330
MCD45A1	2002-2010						338

(Roy et al., 2008)							
FINNv1	2005-2010	18.4	74.5	302.9	64.7	16.6	477.1
(Wiedinmyer et al., 2011)							

[a] Regional definitions: NA = North America (BONA+TENA+CEAM); SA = South America (NHSA+SHSA); AFR=Africa (MIDE+NHAF+SHAF); EURAS= Eurasia (Europe (EURO) + Asia (BOAS+CEAS+SEAS+EQAS)); AUS=Australia (AUST); GLOB = global total. The subcontinental regions such as BONA etc. are as defined in Figure 1.

[b] Continental estimates calculated from percent distribution in Tansey et al. (2004b) [North America: 2%, South America: 3%, Eurasia (Europe + Asia (including Russia)): 15%, Africa: 64%, Australia + Papua New Guinea: 16%].

Using the regression tree models described above, the calculated 2000s (1998-2002 average) annual burned area estimates for various regions, are shown in Table 1(a). The regression tree models were able to explain a significant part of the variability observed in the burned area for all of the geographical regions (R^2 = 0.81 (BONA), 0.72 (TENA), 0.68 (CEAM), 0.75 (NHSA), 0.86 (SHSA), 0.82 (EURO), 0.81 (MIDE), 0.91 (NHAF), 0.94 (SHAF), 0.81 (BOAS), 0.85 (CEAS), 0.73 (SEAS), 0.77 (EQAS), 0.96 (AUST). R^2 values calculated based on GFEDv4 burned area estimates for the region and regression tree predicted burned area based on MODIS Terra fire frequencies). Global annual burned area for the 2000s is estimated at ~334 Mha $year^{-1}$ with maximum (51%) contribution from the African continent (MIDE + NHAF + SHAF ~170 Mha $year^{-1}$) followed by Eurasia (23%) (EURO + BOAS + CEAS + SEAS + EQAS ~ 78 Mha $year^{-1}$), South America (14%)

(NHSA + SHSA ~ 47 Mha year^{-1}), Australia (9%) (AUST ~ 29 Mha year^{-1}) and North America (3%) (BONA + TENA + CEAM ~10 Mha year^{-1}). Table 1(a) contains burned area estimates from this work together with available literature estimates for comparison. There is considerable variability in the global and continental burned area estimates in the literature due to different approaches used (e.g., process-based fire modeling vs. satellite observations) and different year/time period examined. However, our results reproduce the major burned area patterns common to most of the studies (e.g. maximum-burned area in Africa). Overall, estimates of both global and regional wildfire burned area in this work are in reasonable agreement with the literature and represent the spatial distribution of burned area well.

Table 1(b). Projected 2000-2050 changes in wildfire burned area driven by changes in climate, land use, and land cover at global and regional[a] scales. Estimated burned area for the 2000s is shown in Mha year^{-1}.

Scenario	NA	SA	AFR	EURAS	AUS	GLOB
2000s	10	47	170	78	29	334
climate change	+23%	+16%	+28%	+6%	+32%	+22%
land use change	-13%	+12%	-7%	-13%	+31%	-3%
land cover change	+28%	+2%	+16%	-3%	-5%	+8%
land use and land cover change	+16%	+18%	+6%	-11%	+32%	+6%

[a] The regional definitions are the same as in Table 1a.

Our calculated changes in wildfire burned area driven by changes in climate, land use, land cover are shown in Table 1(b). We find that the 2000-2050 climate change could increase the global fire frequencies by 19% (Huang et al., 2015), which would cause significant increases in burned area at both global (+22%) and regional (Africa (+28%), Australia (+32%), North America (+23%), South America (+16%) and Eurasia (+6%)) scales. An increase of 6% (+8% (land cover change), -3% (land use change)) in global burned area is predicted due to the 2000-2050 changes in land use/land cover. However, at the continental scale, more pronounced changes are observed. Burned areas in North America and Africa are predicted to decline by 13% and 7%, respectively, due to reduction in natural vegetation coverage caused by agricultural land expansion. Lesser natural vegetation coverage could significantly reduce wildfire activity and limit wildfire spread. On the other hand, greater vegetation density and the resulting higher fire frequencies due to land cover change could increase burned area in both continents (+28% North America, +16% Africa). Agricultural land expansion is predicted to decline in South America and Australia by 2050 resulting in more natural vegetation and greater fire frequencies increasing the burned area by 12% and 31% respectively. In Eurasia, burned area could decline by 13% due to increase in agricultural land coverage. The combined effects of 2000-2050 land use/land cover change contribute to greater burned area in all continents (North America (+16%), South America (+18%), Africa (+6%), Australia (+32%)) except Eurasia (-11%).

2.5. Hg emissions from wildfires for the 2000s

Table 2. Model calculated 2000s wildfire emissions of Hg (in Mg year^{-1}) for the global total and various regions[a,b].

Study	Study Period	NA	SA	AFR	EURAS	AUS	GLOB
This work	**1998-2002**	**48**	**102**	**268**	**190**	**4**	**612**
Brunke et al. (2001)							510-1140[c]
							380-1330[d]
Chen et al. (2013)[e]	2000-2010				6.20		
Cinnirella and Pirrone (2006)[f]					4.3-28.4		
Delacerda (1995)[g]			17				
De Simone et al. (2015)	2006-2010						600-678
Ebinghaus et al. (2007)	1996-2000						210-750
Friedli et al. (2009a)	1997-2006	50	108	141	357	19	675 (435-915)
Huang et al. (2011)[e]	2000-2007				27		
Michelazzo et al. (2010)[g]	2000-2008		7				

Nelson et al. (2012)	2006					21-63	
Roulet et al. (1999)[g]	(range for the 1980s)		6-9				
Sigler et al. (2003)							250-430
Streets et al. (2009)	(for 1996 and 2006)	28.6[h]-28.7[i]	146.9[i]-156.5[h]	252.7[h]-229[i]	176.3[h] – 181.4[i]		586[i] – 614[h]
Veiga et al. (1994)[g]	1988		88				
Wiedinmyer and Friedli (2007)[j]	2002-2006	44(20-65)					
Weiss-Penzias et al. (2007)	Late 1990s						670 (340-1000)

[a] The regional definitions are the same as in Table 1a.

[b] The specific values shown for this work represent our best estimates; refer to Table 3 and the corresponding discussion in the text for uncertainty analyses.

[c] Based on Hg/CO emission ratio

[d] Based on Hg/CO_2 emission ratio

[e] Emission estimates only for China

[f] Emissions for Europe (1990-2004) and Russian federation (1996-2002) only

[g] For Amazon only

[h] for 1996, [i] for 2006

[j] Emissions for lower 48 states of North America & Alaska only

Our calculated Hg emissions from wildfires for the 2000s are shown in Table 2. Results from previous literature on Hg emissions from biomass burning are included in the table for comparison. Our best estimated global total Hg wildfire emissions for the 2000s is 612 Mg year^{-1} with 43.8 % emissions from the African continent (MIDE + NHAF + SHAF = 268 Mg year^{-1}) followed by Eurasia (EURO + BOAS + CEAS + SEAS + EQAS =31%, 190 Mg year^{-1}), South America (NHSA + SHSA = 16.6%, 102 Mg year^{-1}), North America (BONA + TENA + CEAM = 7.9%, 48 Mg year^{-1}) and Australia (AUST=0.7%, 4 Mg year^{-1}). Africa and Eurasia are the dominant source regions for Hg emissions from wildfires. High emissions from Africa can be attributed to the high fire activity, which results in more than half of the global burned area occurring in the continent. The significant contribution from Eurasia primarily reflects the high Hg pools present over the boreal parts of the continent (Friedli et al., 2009a). Globally, tropical (43.3%) and boreal (33%) forest burning contribute the most to wildfire emissions of Hg followed by temperate forests (16.4%) and grasslands (7.3%).

The calculated global total wildfire emissions of Hg in this work compare very well with the climatological values reported in the literature. However, at the continental scale, there are some significant differences. Equatorial Asia is not the major source of wildfire

emissions of Hg, as found by Friedli et al. (2009a). In addition, the calculated emissions for Africa are much higher, although we follow the same regional emission factor assignment methodology used by them. This could be due to differences in other inputs to the fire emissions model (e.g. predicted burned area from simulated fire frequencies, available biomass density and different combustion fraction schemes used). The calculated global Hg emissions and the source distribution show much better agreement with Streets et al. (2009) with Africa being the most important source region followed by Eurasia + Oceania and South America.

Table 3. Sensitivity of calculated wildfire Hg emissions (in Mg year^{-1}) to various model parameters used in this study.

Region	Emission factors	Burned area	Available biomass density	Meteorology[a] (SE/Mean)
North America	44 – 50	41 - 52	44 - 54	46-51 (2.08%)
South America	95 – 120	86 - 116	91 - 109	95-111 (4.04%)
Africa	251 – 311	238 - 279	230 - 293	255-281 (2.51%)
Eurasia	163 – 197	175 - 203	182 - 202	180-199 (2.58%)
Australia	3.8 – 4.4	3.9 – 4.2	3.4 – 4.8	3.4-4.5 (6.75%)
Global	556 - 683	544 – 654	551-662	598-630 (1.32%)

[a] Ranges of Hg emissions represent the 95% confidence intervals

Our fire emissions model uses inputs from a large number of data sources. For example, the values for Hg emission factors are average values that have been compiled from several studies in the literature; estimates of the burned area involves regression tree models, which were developed based on data from MODIS-Terra, GFEDv4 , the LPJ model as well as the GEOS meteorology. Thus, it is very difficult to quantify the uncertainty in our final results associated with all the model parameters. Nevertheless, we have carried out some simple analyses to examine the sensitivities of our results to various model parameters. We first use the bootstrap methods (Efron, 1979; Efron and Tibshirani, 1993) to evaluate the uncertainties in our calculated Hg emissions from wildfires associated with the inter-annual variability in meteorology. Bootstrap methods belong to the class of nonparametric Monte Carlo methods. In this work, nonparametric bootstrapping is used which regards the data sample as the pseudo-population distribution with similar characteristics as the true population. It involves estimating the sampling distribution of a statistic (e.g. mean of the sample) by repeated sampling (with replacement) from the data sample and subsequent determination of the properties of the statistic (e.g. standard error of the mean). We apply bootstrap methods to the 5-year (1998-2002) emissions sample (global and continental) to determine the standard error of the mean as a measure of the uncertainty in the emissions. In order to provide a range for the mean, the 95% better bootstrap confidence intervals (BCa) (Efron and Tibshirani, 1993) are reported. Random samples (size n = 5) were selected from the original emissions sample and the mean was calculated. This procedure was repeated 10000 times to create a sample of 10000 means. The standard deviation of these 10000 means (standard error (SE) of the mean) was computed to estimate the uncertainty. The standard errors range from 1.3% - 7% (SE/mean;

Table 3), reflecting the relatively small inter-annual variability in the simulated meteorology from the GISS GCM.

We then examine the sensitivities of our calculated Hg emissions from wildfires to the uncertainties in model parameters including burned area, Hg emission factors and available biomass density. Based on literature studies (e.g. Andreae and Merlet, 2001; Brunke et al., 2001; Friedli et al., 2003; Ebinghaus et al., 2007; Weiss-Penzias et al., 2007; Friedli et al., 2009), it appears an uncertainty of 20-30% is typical for these model parameters. Therefore, we have performed two additional simulations for each model parameter by assuming a 20% uncertainty (case 1: -20 to 0% change in the parameter, case 2: 0 to 20% change in the parameter). For each case, a sequence of random numbers between the range [-20, 0] or [0, 20]) were generated with a uniform distribution function. These numbers represent the percentage changes to be applied to the model parameters. Therefore, for case 1, all the random numbers would be between -20 to 0 and 0 to 20 for case 2. For burned area, the random number sequence length equaled to one number representing a particular region (1: BONA, 2: TENA …14: AUST). For emission factors and biomass density, the sequence consisted of different numbers for each vegetation type in a region. Based on these perturbation tests, we have summarized the sensitivities of our final results to various model parameters, as shown in Table 3. We find that the sensitivities of calculated Hg emissions to the three model parameters (Hg emission factors, available biomass density, and the burned area) are similar and a 20% uncertainty in each of the parameter would lead to around 20% uncertainty in our final results.

2.6. Changes in Hg emissions driven by climate, land use /land cover and anthropogenic emissions change

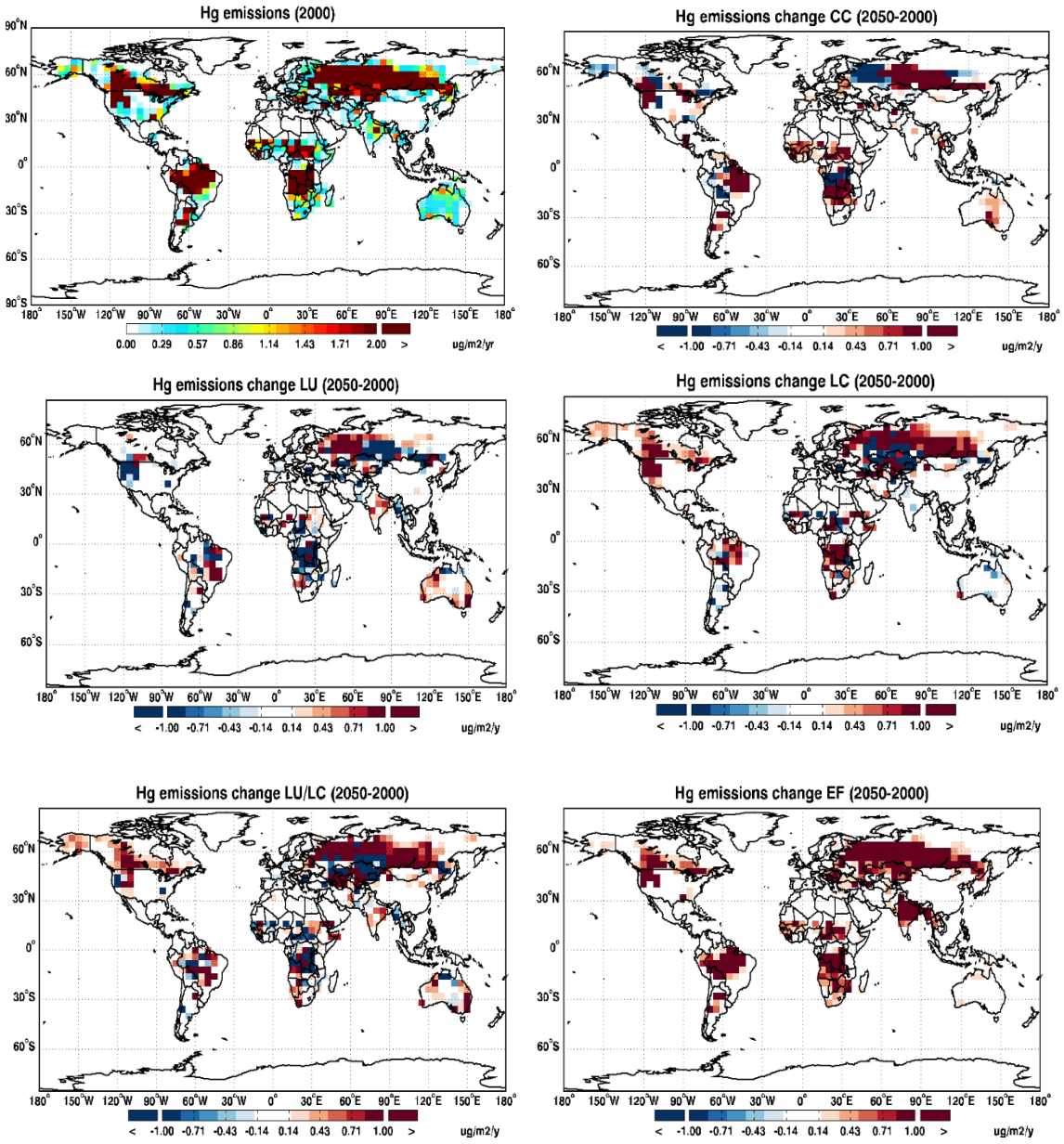

Figure 2(a): Wildfire emissions of Hg for 2000 (µg/m^2/year) (top left), and projected changes by 2050 (µg/m^2/year) due to climate change (CC) (top right), land use change (LU) (middle left), land cover change (LC) (middle right), land use/land cover change (bottom left) and anthropogenic emissions change (EF change) (bottom right).

Table 4. Projected 2000-2050 changes in wildfire emissions of Hg driven by changes in climate, land use, and land cover. Estimated 2000s Hg emissions are shown in Mg year^{-1}.

Scenario/Region[a]	NA	SA	AFR	EURAS	AUS	GLOB
2000s	48	102	268	190	4	612
climate change	+8%	+18%	+14%	+13%	+34%	+14%
land use change	-12%	+19%	-36%	-1%	+58%	-13%
land cover change	+32%	-5%	+14%	+13%	-11%	+12%
land use and land cover change	+19%	+21%	-24%	+17%	+182%	+0.8%
anthropogenic emissions	+19%	+20%	+24%	+41%	+18%	+28%

[a]The regional definitions are the same as in Table 1a.

The perturbations to wildfire emissions of Hg due to 2000-2050 changes in climate, land use and land cover and anthropogenic emissions are shown in Figures 2(a), 2(b) (supplementary material) and Table 4. We find significant increases in wildfire emissions of Hg due to 2000-2050 changes in climate. Global emissions increase by 14% mainly driven by increases in Africa (+14%), South America (+18%), and Eurasia (+13%). In Africa, emissions increase mainly in the southern and northern parts, which could experience significantly warmer and drier conditions than the 2000s resulting in greater and more severe wildfires. Greater precipitation in Central Africa on the other hand causes a decline in wildfire activity and emissions. Eurasian emissions increase is primarily due to higher wildfire activity caused by warmer conditions in the boreal parts of the region (14% increase in BOAS). However, emissions in Equatorial Asia could decline due to suppression of wildfire activity caused by greater precipitation. Significant increases in

wildfires is predicted over the boreal parts of North America due to warmer temperatures and over Western US due to warmer and drier conditions than the 2000s. These changes in climate result in increasing Hg emissions from North America by 8%. Australia (34% increase in emissions) and South America could mainly experience greater wildfire activity in the eastern parts due to higher temperatures and less precipitation in 2050.

In response to the projected changes in land use and land cover by 2050, we find that land use change would be a major driving force in Africa. Substantial conversion of forests to croplands causes wildfire emissions to decline by 36% in the continent, outweighing a 14% increase in emissions due to greater forest coverage and resulting fire frequencies caused by land cover change. Overall, the combined effects of land use and land cover result in a 24% decline in Hg wildfire emissions from Africa. Land use change could also be the dominant factor influencing emissions in South America and Australia. Land use is projected to decline in both the continents resulting in more forest coverage and wildfires than the 2000s. Hence, emissions increase significantly in both continents (+19% (South America), +58% (Australia)). However, land cover change could cause a decline in emissions in both continents (-5% (South America), -11% (Australia)), primarily due to reduction in temperate forest (high Hg emission factors) coverage in sub-tropical South America and decrease in wildfire frequency in Australia. Overall, 2000-2050 land use/land cover change results in increasing Hg wildfire emissions by 21% in South America and 182% in Australia.

On the contrary, future changes in land cover in North America are found to have a greater influence on Hg emissions from wildfires (32% emissions increase) than the

changes in anthropogenic land use (12% emissions decrease). Increase in boreal and temperate forest coverage in the high and mid-latitudes of the continent and the resulting greater fire frequencies lead to increases in Hg emissions over boreal North America (+29%) and the US (+35%). Land use change would have negligible impacts on emissions in boreal North America; however, it could result in a significant decrease in emissions from the US (-23%). In Eurasia as well, land cover change acts as a major factor causing a 13% increase in emissions, primarily caused by boreal forest expansion and the resulting increase in wildfires. Land use change would have negligible overall effects partly reflecting the diverging trends in anthropogenic land use in this region (e.g. decreases in Eastern Asia and parts of Russia but increases in Equatorial Asia).

Following the IPCC A1B scenario, the global anthropogenic emissions are predicted to increase with Hg(II) being the dominant emissions constituent in 2050 (Corbitt et al., 2011; Streets et al., 2009). As a consequence, we find that the Hg enrichment of terrestrial ecosystems driven by changes in atmospheric Hg deposition by 2050 would lead to increases in global wildfire emissions of Hg by 28%. The most significant increases are calculated over Eurasia (+41%) and Africa (+24%) which together account for about 75% of global Hg wildfire emissions for the 2000s. Wildfire emissions of Hg from South East, Central and East Asian countries increase significantly in response to greater Hg anthropogenic emissions in these countries and the resulting deposition to terrestrial environments. South America (+20%), North America (+19%) and Australia (+18%) experience significant increases in emissions as well. Greater Hg deposition to the boreal regions results in an increase of 19% in wildfire emissions from boreal North America and

35% from boreal Asia. Emissions from tropical peatlands in Equatorial Asia also increase due to greater Hg deposition in 2050. It should be noted that new developments in technology (such as the mercury control technology being used by coal-fired power plants) and policy (such as the Minamata Convention) can significantly affect the future trends of anthropogenic emissions of Hg, but these factors are not accounted for in this study.

2.7. Conclusions

We investigate the Hg emissions from wildfires in this study. We first develop the global and regional emission inventories for the 2000s and then examine the perturbations from the projected 2000-2050 changes in climate, land use, land cover and anthropogenic Hg emissions. Africa (43.8%), Eurasia (31%) and South America (16.6%) are found to be the major sources of Hg wildfire emissions in the 2000s. Following the IPCC A1B scenario, the 2000-2050 climate change would lead to more frequent and severe wildfires in most regions around the world resulting in significant increases in wildfire emissions of Hg at both the global and continental scales. Climate change driven alterations in natural vegetation could also increase global emissions particularly in the boreal regions, the US and Africa. However, these impacts of a future favorable climate for fires and land cover change on global emissions are suppressed by continued anthropogenic destruction of natural vegetation in order to support agricultural development. As a result, emissions in Africa, which is a major source of wildfire emissions, decline in 2050 due to reduced forest cover. In addition, destruction of forests in Equatorial Asia and the Western US reduces

Hg wildfire emissions from these regions. On the other hand, a projected rise in anthropogenic emissions in 2050 and the resulting greater Hg contamination of terrestrial environments contributes to increasing emissions globally and regionally. Wildfire emissions of Hg in the boreal regions are predicted to increase in response to the 2000-2050 changes in climate, land cover and anthropogenic Hg emissions which could have significant implications for Hg deposition to the Arctic.

Acknowledgements

This study is supported by NSF (grant #1313755) and U.S. EPA (grant # 83518901). S. Wu acknowledges the sabbatical fellowship from Peking University. Superior, a high performance computing cluster at Michigan Technological University, was used in obtaining results presented in this publication.

Competing interests:

The authors declare that they have no conflict of interest.

References

Aldersley, A., Murray, S.J., Cornell, S.E. (2011) Global and regional analysis of climate and human drivers of wildfire. Science of the Total Environment 409, 3472-3481.

Andreae, M.O., Merlet, P. (2001) Emission of trace gases and aerosols from biomass burning. Global biogeochemical cycles 15, 955-966.

Bachelet, D., Neilson, R.P., Hickler, T., Drapek, R.J., Lenihan, J.M., Sykes, M.T., Smith, B., Sitch, S., Thonicke, K. (2003) Simulating past and future dynamics of natural ecosystems in the United States. Global biogeochemical cycles 17.

Bachelet, D., Neilson, R.P., Lenihan, J.M., Drapek, R.J. (2001) Climate change effects on vegetation distribution and carbon budget in the United States. Ecosystems 4, 164-185.

Bey, I., Jacob, D.J., Yantosca, R.M., Logan, J.A., Field, B.D., Fiore, A.M., Li, Q., Liu, H.Y., Mickley, L.J., Schultz, M.G. (2001) Global modeling of tropospheric chemistry with assimilated meteorology: Model description and evaluation. Journal of Geophysical Research: Atmospheres 106, 23073-23095.

Biswas, A., Blum, J.D., Klaue, B., Keeler, G.J. (2007) Release of mercury from Rocky Mountain forest fires. Global biogeochemical cycles 21.

Breiman, L., Friedman, J., Olshen, R., Stone, C. (1984) Classification and Regression Trees–CRC Press. Boca Raton, Florida.

Breiman, L., Meisel, W. (1976) General estimates of the intrinsic variability of data in nonlinear regression models. Journal of the American Statistical Association 71, 301-307.

Brunke, E.G., Labuschagne, C., Slemr, F. (2001) Gaseous mercury emissions from a fire in the Cape Peninsula, South Africa, during January 2000. Geophysical Research Letters 28, 1483-1486.

Chen, C., Wang, H., Zhang, W., Hu, D., Chen, L., Wang, X. (2013) High-resolution inventory of mercury emissions from biomass burning in China for 2000–2010 and a projection for 2020. Journal of Geophysical Research: Atmospheres 118.

Chen, Y., Wang, R., Shen, H., Li, W., Chen, H., Huang, Y., Zhang, Y., Chen, Y., Su, S., Lin, N. (2014) Global mercury emissions from combustion in light of international fuel trading. Environmental science & technology 48, 1727-1735.

Cinnirella, S., Pirrone, N. (2006) Spatial and temporal distributions of mercury emissions from forest fires in Mediterranean region and Russian federation. Atmospheric Environment 40, 7346-7361.

Cochrane, M.A., Barber, C.P. (2009) Climate change, human land use and future fires in the Amazon. Global Change Biology 15, 601-612.

Corbitt, E.S., Jacob, D.J., Holmes, C.D., Streets, D.G., Sunderland, E.M. (2011) Global source–receptor relationships for mercury deposition under present-day and 2050 emissions scenarios. Environmental science & technology 45, 10477-10484.

Cox, P.M., Betts, R.A., Jones, C.D., Spall, S.A., Totterdell, I.J. (2000) Acceleration of global warming due to carbon-cycle feedbacks in a coupled climate model. Nature 408, 184-187.

De Simone, F., Cinnirella, S., Gencarelli, C.N., Yang, X., Hedgecock, I.M., Pirrone, N. (2015) Model study of global mercury deposition from biomass burning. Environmental science & technology 49, 6712-6721.

Delacerda, L.D. (1995) Amazon mercury emissions. Nature 374, 20-21.

Ebinghaus, R., Slemr, F., Brenninkmeijer, C., Van Velthoven, P., Zahn, A., Hermann, M., O'Sullivan, D., Oram, D. (2007) Emissions of gaseous mercury from biomass burning in South America in 2005 observed during CARIBIC flights. Geophysical Research Letters 34.

Efron, B. (1979) Bootstrap methods: another look at the jackknife Annals of Statistics 7, 1–26.

Efron, B., Tibshirani, R.J. (1993) An Introduction to the Bootstrap: Monographs on Statistics and Applied Probability, Vol. 57. New York and London: Chapman and Hall/CRC.

Falloon, P., Dankers, R., Betts, R., Jones, C., Booth, B., Lambert, F. (2012) Role of vegetation change in future climate under the A1B scenario and a climate stabilisation scenario, using the HadCM3C Earth system model. Biogeosciences 9, 4739.

Ferrara, R., Mazzolai, B., Lanzillotta, E., Nucaro, E., Pirrone, N. (2000) Volcanoes as emission sources of atmospheric mercury in the Mediterranean basin. Science of the Total Environment 259, 115-121.

Flannigan, M.D., Krawchuk, M.A., de Groot, W.J., Wotton, B.M., Gowman, L.M. (2009) Implications of changing climate for global wildland fire. International journal of wildland fire 18, 483-507.

Friedli, H., Arellano, A., Cinnirella, S., Pirrone, N. (2009) Initial estimates of mercury emissions to the atmosphere from global biomass burning. Environmental science & technology 43, 3507-3513.

Friedli, H.R., Radke, L.F., Lu, J.Y. (2001) Mercury in smoke from biomass fires. Geophysical Research Letters 28, 3223-3226.

Gerten, D., Schaphoff, S., Haberlandt, U., Lucht, W., Sitch, S. (2004) Terrestrial vegetation and water balance—hydrological evaluation of a dynamic global vegetation model. Journal of Hydrology 286, 249-270.

Giang, A., Stokes, L.C., Streets, D.G., Corbitt, E.S., Selin, N.E. (2015) Impacts of the minamata convention on mercury emissions and global deposition from coal-fired power generation in Asia. Environmental science & technology 49, 5326-5335.

Giglio, L., Csiszar, I., Justice, C.O. (2006a) Global distribution and seasonality of active fires as observed with the Terra and Aqua Moderate Resolution Imaging Spectroradiometer (MODIS) sensors. Journal of Geophysical Research: Biogeosciences 111.

Giglio, L., Randerson, J., Van der Werf, G., Kasibhatla, P., Collatz, G., Morton, D., DeFries, R. (2010) Assessing variability and long-term trends in burned area by merging multiple satellite fire products. Biogeosciences 7.

Giglio, L., Randerson, J.T., Werf, G.R. (2013) Analysis of daily, monthly, and annual burned area using the fourth-generation global fire emissions database (GFED4). Journal of Geophysical Research: Biogeosciences 118, 317-328.

Giglio, L., Van der Werf, G., Randerson, J., Collatz, G., Kasibhatla, P. (2006b) Global estimation of burned area using MODIS active fire observations. Atmospheric Chemistry and Physics 6, 957-974.

Graydon, J.A., St Louis, V.L., Lindberg, S.E., Sandilands, K.A., Rudd, J.W., Kelly, C.A., Harris, R., Tate, M.T., Krabbenhoft, D.P., Emmerton, C.A. (2012) The role of terrestrial

vegetation in atmospheric Hg deposition: Pools and fluxes of spike and ambient Hg from the METAALICUS experiment. Global biogeochemical cycles 26.

Hickler, T., Prentice, I.C., Smith, B., Sykes, M.T., Zaehle, S. (2006) Implementing plant hydraulic architecture within the LPJ Dynamic Global Vegetation Model. Global Ecology and Biogeography 15, 567-577.

Holmes, C.D., Jacob, D.J., Corbitt, E.S., Mao, J., Yang, X., Talbot, R., Slemr, F. (2010) Global atmospheric model for mercury including oxidation by bromine atoms. Atmospheric Chemistry and Physics 10, 12037-12057.

Huang, X., Li, M., Friedli, H.R., Song, Y., Chang, D., Zhu, L. (2011) Mercury emissions from biomass burning in China. Environmental science & technology 45, 9442-9448.

Huang, Y., Wu, S., Kaplan, J.O. (2015) Sensitivity of global wildfire occurrences to various factors in the context of global change. Atmospheric Environment 121, 86-92.

IMAGE Team, H. (2001) The IMAGE 2.2 implementation of the SRES scenarios: a comprehensive analysis of emissions, climate change and impacts in the 21st century. RIVM CD-ROM Publication 481508018.

IPCC (2001) Climate Change 2001: The Scientific Basis, contribution of Working Group I to the Third Assessment Report of the Intergovernmental Panel on Climate Change, edited by: Houghton, J. T., Ding, Y., Griggs, D. J., Noguer, M., van der, P. J. Linden. Cambridge University Press, Cambridge United Kingdom and New York, NY, USA.

Ito, A., Penner, J.E. (2004) Global estimates of biomass burning emissions based on satellite imagery for the year 2000. Journal of Geophysical Research: Atmospheres 109.

Jaeglé, L., Strode, S.A., Selin, N.E., Jacob, D.J., (2009) The geos-chem model, Mercury Fate and Transport in the Global Atmosphere. Springer, pp. 533-545.

Jain, A.K., Tao, Z., Yang, X., Gillespie, C. (2006) Estimates of global biomass burning emissions for reactive greenhouse gases (CO, NMHCs, and NOx) and CO2. Journal of Geophysical Research: Atmospheres 111.

Jain, A.K., Yang, X. (2005) Modeling the effects of two different land cover change data sets on the carbon stocks of plants and soils in concert with CO2 and climate change. Global biogeochemical cycles 19.

Justice, C., Giglio, L., Korontzi, S., Owens, J., Morisette, J., Roy, D., Descloitres, J., Alleaume, S., Petitcolin, F., Kaufman, Y. (2002) The MODIS fire products. Remote Sensing of Environment 83, 244-262.

Li, F., Zeng, X., Levis, S. (2012) A process-based fire parameterization of intermediate complexity in a Dynamic Global Vegetation Model. Biogeosciences 9, 2761-2780.

Loh, W.Y. (2008) Classification and regression tree methods. Encyclopedia of statistics in quality and reliability.

Loh, W.Y. (2011) Classification and regression trees. Wiley Interdisciplinary Reviews: Data Mining and Knowledge Discovery 1, 14-23.

Lucchesi, R. (2013) File Specification for GEOS-5 FP (Forward Processing).

Melendez-Perez, J.J., Fostier, A.H., Carvalho, J.A., Windmöller, C.C., Santos, J.C., Carpi, A. (2014) Soil and biomass mercury emissions during a prescribed fire in the Amazonian rain forest. Atmospheric Environment 96, 415-422.

Michelazzo, P.A.M., Fostier, A.H., Magarelli, G., Santos, J.C., Carvalho, J.A. (2010) Mercury emissions from forest burning in southern Amazon. Geophysical Research Letters 37.

MNP (2006) Integrated modelling of global environmental change, an overview of IMAGE 2.4. edited by: Bouwman, A. F., Kram,T., and Klein Goldewijk, K. Netherlands Environmental Assessment Agency (MNP), Bilthoven, The Netherlands.

Molod, A., Takacs, L., Suarez, M., Bacmeister, J., Song, I.-S., Eichmann, A. (2012) The GEOS-5 atmospheric general circulation model: Mean climate and development from MERRA to Fortuna.

Nelson, P.F., Morrison, A.L., Malfroy, H.J., Cope, M., Lee, S., Hibberd, M.L., Meyer, C.M., McGregor, J. (2012) Atmospheric mercury emissions in Australia from anthropogenic, natural and recycled sources. Atmospheric Environment 62, 291-302.

Nimick, D.A., Caldwell, R.R., Skaar, D.R., Selch, T.M. (2013) Fate of geothermal mercury from Yellowstone National Park in the Madison and Missouri Rivers, USA. Science of the Total Environment 443, 40-54.

Notaro, M., Vavrus, S., Liu, Z. (2007) Global vegetation and climate change due to future increases in CO2 as projected by a fully coupled model with dynamic vegetation. Journal of Climate 20, 70-90.

Nriagu, J., Becker, C. (2003) Volcanic emissions of mercury to the atmosphere: global and regional inventories. Science of the Total Environment 304, 3-12.

O'ishi, R., Abe-Ouchi, A. (2009) Influence of dynamic vegetation on climate change arising from increasing CO2. Climate Dynamics 33, 645-663.

Obrist, D. (2007) Atmospheric mercury pollution due to losses of terrestrial carbon pools? Biogeochemistry 85, 119-123.

Pacyna, E.G., Pacyna, J., Sundseth, K., Munthe, J., Kindbom, K., Wilson, S., Steenhuisen, F., Maxson, P. (2010) Global emission of mercury to the atmosphere from anthropogenic sources in 2005 and projections to 2020. Atmospheric Environment 44, 2487-2499.

Pirrone, N., Cinnirella, S., Feng, X., Finkelman, R., Friedli, H., Leaner, J., Mason, R., Mukherjee, A., Stracher, G., Streets, D. (2010) Global mercury emissions to the atmosphere from anthropogenic and natural sources. Atmospheric Chemistry and Physics 10, 5951-5964.

Pyle, D.M., Mather, T.A. (2003) The importance of volcanic emissions for the global atmospheric mercury cycle. Atmospheric Environment 37, 5115-5124.

Randerson, J., Chen, Y., Werf, G., Rogers, B., Morton, D. (2012) Global burned area and biomass burning emissions from small fires. Journal of Geophysical Research: Biogeosciences 117.

Rienecker, M. (2008) File specification for GEOS-5 DAS gridded output. NASA Goddard Space Flight Center.

Rind, D., Lerner, J., Jonas, J., McLinden, C. (2007) Effects of resolution and model physics on tracer transports in the NASA Goddard Institute for Space Studies general circulation models. Journal of Geophysical Research: Atmospheres 112.

Roulet, M., Lucotte, M., Farella, N., Serique, G., Coelho, H., Sousa Passos, C., De Jesus da Silva, E., Scavone de Andrade, P., Mergler, D., Guimarães, J.-R. (1999) Effects of recent human colonization on the presence of mercury in Amazonian ecosystems. Water, Air, & Soil Pollution 112, 297-313.

Roy, D.P., Boschetti, L., Justice, C.O., Ju, J. (2008) The collection 5 MODIS burned area product—Global evaluation by comparison with the MODIS active fire product. Remote Sensing of Environment 112, 3690-3707.

Schaphoff, S., Lucht, W., Gerten, D., Sitch, S., Cramer, W., Prentice, I.C. (2006) Terrestrial biosphere carbon storage under alternative climate projections. Climatic Change 74, 97-122.

Seiler, W., Crutzen, P.J. (1980) Estimates of gross and net fluxes of carbon between the biosphere and the atmosphere from biomass burning. Climatic Change 2, 207-247.

Selin, N.E., Jacob, D.J. (2008) Seasonal and spatial patterns of mercury wet deposition in the United States: Constraints on the contribution from North American anthropogenic sources. Atmospheric Environment 42, 5193-5204.

Selin, N.E., Jacob, D.J., Park, R.J., Yantosca, R.M., Strode, S., Jaeglé, L., Jaffe, D. (2007) Chemical cycling and deposition of atmospheric mercury: Global constraints from observations. Journal of Geophysical Research: Atmospheres 112.

Selin, N.E., Jacob, D.J., Yantosca, R.M., Strode, S., Jaeglé, L., Sunderland, E.M. (2008) Global 3-D land-ocean-atmosphere model for mercury: Present-day versus preindustrial cycles and anthropogenic enrichment factors for deposition. Global biogeochemical cycles 22.

Sigler, J., Lee, X., Munger, W. (2003) Emission and long-range transport of gaseous mercury from a large-scale Canadian boreal forest fire. Environmental science & technology 37, 4343-4347.

Simon, M., Plummer, S., Fierens, F., Hoelzemann, J.J., Arino, O. (2004) Burnt area detection at global scale using ATSR-2: The GLOBSCAR products and their qualification. Journal of Geophysical Research: Atmospheres 109.

Sitch, S., Smith, B., Prentice, I.C., Arneth, A., Bondeau, A., Cramer, W., Kaplan, J., Levis, S., Lucht, W., Sykes, M.T. (2003) Evaluation of ecosystem dynamics, plant geography and terrestrial carbon cycling in the LPJ dynamic global vegetation model. Global Change Biology 9, 161-185.

Smith-Downey, N.V., Sunderland, E.M., Jacob, D.J. (2010) Anthropogenic impacts on global storage and emissions of mercury from terrestrial soils: Insights from a new global model. Journal of Geophysical Research: Biogeosciences 115.

Streets, D.G., Devane, M.K., Lu, Z., Bond, T.C., Sunderland, E.M., Jacob, D.J. (2011) All-time releases of mercury to the atmosphere from human activities. Environmental science & technology 45, 10485-10491.

Streets, D.G., Zhang, Q., Wu, Y. (2009) Projections of global mercury emissions in 2050. Environmental science & technology 43, 2983-2988.

Strode, S.A., Jaeglé, L., Selin, N.E., Jacob, D.J., Park, R.J., Yantosca, R.M., Mason, R.P., Slemr, F. (2007) Air-sea exchange in the global mercury cycle. Global biogeochemical cycles 21.

Suarez, M.J., daSilva, A., Dee, D., Bloom, S., Bosilovich, M., Pawson, S., Schubert, S., Wu, M.-L., Sienkiewicz, M., Stajner, I. (2005) Documentation and validation of the Goddard Earth Observing System (GEOS) data assimilation system, version 4.

Tansey, K., GrÉgoire, J.-M., Binaghi, E., Boschetti, L., Brivio, P.A., Ershov, D., Flasse, S., Fraser, R., Graetz, D., Maggi, M. (2004a) A global inventory of burned areas at 1 km

resolution for the year 2000 derived from SPOT VEGETATION data. Climatic Change 67, 345-377.

Tansey, K., Grégoire, J.M., Defourny, P., Leigh, R., Pekel, J.F., van Bogaert, E., Bartholomé, E. (2008) A new, global, multi-annual (2000–2007) burnt area product at 1 km resolution. Geophysical Research Letters 35.

Tansey, K., Grégoire, J.M., Stroppiana, D., Sousa, A., Silva, J., Pereira, J., Boschetti, L., Maggi, M., Brivio, P.A., Fraser, R. (2004b) Vegetation burning in the year 2000: Global burned area estimates from SPOT VEGETATION data. Journal of Geophysical Research: Atmospheres 109.

Thonicke, K., Venevsky, S., Sitch, S., Cramer, W. (2001) The role of fire disturbance for global vegetation dynamics: coupling fire into a Dynamic Global Vegetation Model. Global Ecology and Biogeography 10, 661-677.

Tilman, D., Fargione, J., Wolff, B., D'Antonio, C., Dobson, A., Howarth, R., Schindler, D., Schlesinger, W.H., Simberloff, D., Swackhamer, D. (2001) Forecasting agriculturally driven global environmental change. Science 292, 281-284.

Turetsky, M.R., Harden, J.W., Friedli, H.R., Flannigan, M., Payne, N., Crock, J., Radke, L. (2006) Wildfires threaten mercury stocks in northern soils. Geophysical Research Letters 33.

Van Der Werf, G.R., Randerson, J.T., Collatz, G.J., Giglio, L. (2003) Carbon emissions from fires in tropical and subtropical ecosystems. Global Change Biology 9, 547-562.

Van der Werf, G.R., Randerson, J.T., Giglio, L., Collatz, G., Mu, M., Kasibhatla, P.S., Morton, D.C., DeFries, R., Jin, Y.v., van Leeuwen, T.T. (2010) Global fire emissions and

the contribution of deforestation, savanna, forest, agricultural, and peat fires (1997–2009). Atmospheric Chemistry and Physics 10, 11707-11735.

van der Werf, G.R., Randerson, J.T., Giglio, L., Collatz, G.J., Kasibhatla, P.S., Arellano Jr, A.F. (2006) Interannual variability in global biomass burning emissions from 1997 to 2004. Atmospheric Chemistry and Physics 6, 3423-3441.

Varekamp, J.C., Buseck, P.R. (1986) Global mercury flux from volcanic and geothermal sources. Applied Geochemistry 1, 65-73.

Veiga, M.M., Maxson, P.A., Hylander, L.D. (2006) Origin and consumption of mercury in small-scale gold mining. Journal of Cleaner Production 14, 436-447.

Veiga, M.M., Meech, J.A., Oñate, N. (1994) Mercury pollution from deforestation. Nature 368, 816-817.

Weiss-Penzias, P., Jaffe, D., Swartzendruber, P., Hafner, W., Chand, D., Prestbo, E. (2007) Quantifying Asian and biomass burning sources of mercury using the Hg/CO ratio in pollution plumes observed at the Mount Bachelor Observatory. Atmospheric Environment 41, 4366-4379.

Wiedinmyer, C., Akagi, S., Yokelson, R.J., Emmons, L., Al-Saadi, J., Orlando, J., Soja, A. (2011) The Fire INventory from NCAR (FINN): a high resolution global model to estimate the emissions from open burning. Geoscientific Model Development 4, 625.

Wiedinmyer, C., Friedli, H. (2007) Mercury emission estimates from fires: an initial inventory for the United States. Environmental science & technology 41, 8092-8098.

Wiedinmyer, C., Quayle, B., Geron, C., Belote, A., McKenzie, D., Zhang, X., O'Neill, S., Wynne, K.K. (2006) Estimating emissions from fires in North America for air quality modeling. Atmospheric Environment 40, 3419-3432.

Wu, S., Mickley, L.J., Jacob, D.J., Logan, J.A., Yantosca, R.M., Rind, D. (2007) Why are there large differences between models in global budgets of tropospheric ozone? Journal of Geophysical Research: Atmospheres 112.

Wu, S., Mickley, L.J., Jacob, D.J., Rind, D., Streets, D.G. (2008a) Effects of 2000–2050 changes in climate and emissions on global tropospheric ozone and the policy-relevant background surface ozone in the United States. Journal of Geophysical Research: Atmospheres 113.

Wu, S., Mickley, L.J., Kaplan, J., Jacob, D.J. (2012) Impacts of changes in land use and land cover on atmospheric chemistry and air quality over the 21st century. Atmospheric Chemistry and Physics 12, 1597-1609.

Wu, S., Mickley, L.J., Leibensperger, E.M., Jacob, D.J., Rind, D., Streets, D.G. (2008b) Effects of 2000–2050 global change on ozone air quality in the United States. Journal of Geophysical Research: Atmospheres 113.

Yue, X., Mickley, L.J., Logan, J.A., Kaplan, J.O. (2013) Ensemble projections of wildfire activity and carbonaceous aerosol concentrations over the western United States in the mid-21st century. Atmospheric Environment 77, 767-780.

Zhang, H., Holmes, C., Wu, S. (2016) Impacts of changes in climate, land use and land cover on atmospheric mercury. Atmospheric Environment 141, 230-244.

Chapter 3: Wildfire Emissions of Atmospheric Constituents: Impacts of 2000s-2050s Global Change[2]

[2] The contents of this chapter will be submitted for publication as a journal article. Kumar, A., Wu, S., Wildfire Emissions of Atmospheric Constituents: Impacts of 2000s-2050s Global Change

3.1. Abstract

Wildfires emit a large number of atmospheric constituents. We study the potential effects of 2000s-2050s global change (following the IPCC A1B scenario) on wildfire emissions of important atmospheric constituents such as greenhouse gases (CO_2, CH_4, and N2O), tropospheric O_3 precursors (CO, NMVOCs, and NOx), particulate matter ($PM_{2.5}$), its components (BC, OC) and precursors (SO_2), organic acids (HCOOH) and mercury (Hg). Our results indicate a continuing increase in anthropogenic influence on wildfires in the coming decades. Greater human occupation of the African continent and the resulting increase in cropland coverage causes significant declines in wildfire emissions from the continent. Anthropogenic factors play an important role in the changes in emissions from other continents as well. Future changes in climate and land cover result in significant increases in global emissions for all the species. The global emissions of all the species show small changes due to very significant declines in African emissions suppressing the effects of much larger emissions increases in other continents. This highlights the dominant contribution and importance of Africa with respect to global wildfire emissions. We also discuss the possible implications of these future changes in wildfire emissions for future air quality, atmospheric chemistry/composition, climate and biogeochemical cycling of elements.

3.2. Introduction

Wildfires are episodic ecological disturbances the origins of which can be traced back to the late Silurian/early Devonian period (Gibling and Davies, 2012; Glasspool et al., 2004, 2006). They are caused by either natural events (e.g., lightning) (Price and Rind, 1994; Stocks et al., 2003; Veraverbeke et al., 2017) or anthropogenic activities (e.g. forest clearing to expand agricultural land use) (Bowman et al., 2011; Bowman et al., 2009; Crutzen and Andreae, 1990) with 80% of the burning occurring in the tropics (Hao and Liu, 1994). Wildfires play an important role in the Earth system. They are considered as major drivers of vegetation patterns in some ecosystems and compete with climatic effects in shaping biomes (Bond et al., 2005). Wildfires also act as sources of atmospheric trace gases (e.g. CO_2, CO, NO_x, CH_4), aerosols and organic compounds (alkanes, alkenes, HCOOH, HCHO). Thus, they exert a significant influence on atmospheric chemistry and composition, cause significant perturbations to the biogeochemical cycling of elements (e.g., carbon, nitrogen and mercury) (Crutzen and Andreae, 1990; Friedli et al., 2009b; Kumar et al., 2018; Seiler and Crutzen, 1980; Turetsky et al., 2006) and contribute to altering the Earth's radiation budget/climate at the global and regional scales (Christopher et al., 1998; Hobbs et al., 1997; Penner et al., 1992). Furthermore, wildfires are also associated with adverse human health effects/mortality (Johnston et al., 2011; Kim et al., 2015; Koplitz et al., 2016; Kunii et al., 2002; Kunzli et al., 2006; Liu et al., 2016; Marlier et al., 2013; Richardson et al., 2012; Sastry, 2002; Thelen et al., 2013), enormous economic losses (Brown et al., 2006; Butry et al., 2001; Hall, 2014), and alterations in land surface

albedo (Gatebe et al., 2014; Lyons et al., 2008; Myhre et al., 2005; Veraverbeke et al., 2012).

Climatic conditions (e.g. temperature, precipitation), biome characteristics/state (e.g. terrestrial vegetation type and availability) and anthropogenic influence (e.g. ignition and fire suppression) are critical factors that impact wildfire frequency, burned area and consequently the eventual emissions of various atmospheric species (Dale et al., 2001; Flannigan et al., 2009; Flannigan et al., 2005; Kloster et al., 2012; Pechony and Shindell, 2009; Pechony and Shindell, 2010). Meteorological conditions govern the frequency of natural ignition sources (e.g. lightning) and vegetation moisture content. Large-scale natural alterations in the climate system (e.g. El Nino) that result in drought like conditions can contribute to extreme fire years (Hess et al., 2001; Marlier et al., 2013; Van Der Werf et al., 2004; Voulgarakis et al., 2015). Terrestrial vegetation type/availability/continuity along with meteorological conditions are important factors influencing the fire spread after ignition and can affect the area burned by wildfires (Archibald et al., 2010; Giglio et al., 2006b; Kumar et al., 2018; Van Der Werf et al., 2003). Furthermore, human interactions with vegetated ecosystems is a major cause of wildfires (e.g. use of fire for forest clearing) while fires occurring in densely inhabited areas are more likely to be suppressed than the ones occurring in remote areas (Huang et al., 2015; Pechony and Shindell, 2009). Therefore, future changes in climate, terrestrial natural vegetation distribution/availability and human population patterns can significantly influence wildfires and wildfire emissions of atmospheric constituents (Huang et al., 2015; Kumar et al., 2018; Spracklen et al., 2009; Yue et al., 2015; Yue et al., 2013). For example, global cropland and pastureland area is

projected to increase in the 2050s (relative to the 2000s) (Tilman et al., 2001) which would result in less natural vegetation available for fires to burn. Changes in climate and atmospheric composition are expected to continue in the coming decades (IPCC, 2001) and could cause alterations in terrestrial ecosystems. For example, future increases in atmospheric CO_2 levels and changes in climate (e.g. temperature, precipitation) could significantly alter the natural vegetation distributions and extent relative to present day (Bachelet et al., 2003; Bachelet et al., 2001; Joos et al., 2001; Wu et al., 2012). Moreover, climate change could also influence wildfires through changes in lightning ignitions. For example, Price and Rind (1994) showed that a climate with double the CO_2 levels than present day could increase lightning caused fires by 44% in North America. Huang et al. (2015) predicted that 2000s-2050s global change following the IPCC A1B scenario would result in increasing global wildfire frequencies by 27% with climate change (19% increase in fire frequencies) and climate driven changes in land cover (+15%) being the major contributing factors. They also estimated that more frequent lightning strikes caused by changes in climate could increase global wildfire activity by 4% while anthropogenic land use change and shifts in human population density would contribute to reducing wildfire activity in the 2050s. Yue et al. (2015) found significant increases in summertime surface ozone (O_3) concentrations over North America due to the effects of climate change on wildfires in the 2050s.

In this work, we study the effects of 2000s-2050s global change on wildfire emissions of atmospheric species following the IPCC A1B scenario (IPCC, 2001). Wildfires emit a large number of atmospheric species. However, in this work we only consider species for which

wildfires constitute a significant source of emissions when compared to anthropogenic sources and which are of considerable importance with respect to climate change and air quality/atmospheric chemistry. The species are listed in Table 1.

3.3. Methodology

We follow the IPCC A1B scenario (IPCC, 2001) for 2000s-2050s global change and use a fire emissions model (Kumar et al., 2018) based on the classical biomass burning equation (Seiler and Crutzen, 1980) to estimate wildfire emissions (2000s and the 2050s) of the atmospheric constituents considered. The fire emissions model has a monthly temporal resolution and a spatial resolution of 4° x 5° (latitude x longitude). It includes burned area, vegetation areal coverage and density, combustion fractions/efficiencies and emission factors as inputs and accounts for variations in fire characteristics, climate, vegetation type and density across geographical regions. Global burned area estimates (2000s and the 2050s) for the model were predicted using regional regression tree relationships between burned area and fire frequencies. Figure 1 shows the global regions considered in the model. Global fire frequencies (2000s and 2050s) used to estimate burned area were based on a fire parameterization, which includes fire ignition agents (natural and anthropogenic) and incorporates the effects of fire suppression, fuel availability and climate on wildfires (Huang et al., 2015). The parameterization was used by Huang et al. (2015) to develop a suite of fire frequency scenarios considering 2000s-2050s global change (land cover change only (LC), land use change only (LU), Land use/Land cover only (LU/LC), climate

change only (CC), lightning ignition change only (LIGHT), population density change only (POPDENS) and effects of 2000s-2050s change in population density, land use/land cover, climate and ignition agents (referred to as the combined effects scenario here)). Global vegetation (tropical, temperate, boreal and grass) areal coverage data ((2000s and 2050s)) used in the model was simulated using the Lund-Potsdam-Jena Dynamic Global Vegetation Model (LPJ DGVM) (Gerten et al., 2004; Hickler et al., 2006; Schaphoff et al., 2006; Sitch et al., 2003; Thonicke et al., 2001; Wu et al., 2012) and cropland areal coverage data was from the IMAGE model (IMAGE Team, 2001; MNP, 2006). Vegetation density estimates for different global regions and vegetation types (tropical, temperate, boreal and grass) were from the terrestrial component of the Integrated Science Assessment Model (ISAM) model (Jain et al., 2006; Jain and Yang, 2005). Global simulated meteorology (2000s-2050s) was simulated using the GISS GCM v3 model (Wu et al., 2007; 2008a; 2008b). Combustion fractions/efficiencies were used from the work of Wiedinmyer et al. (2006). A detailed description of model development can be found in Kumar et al. (2018).

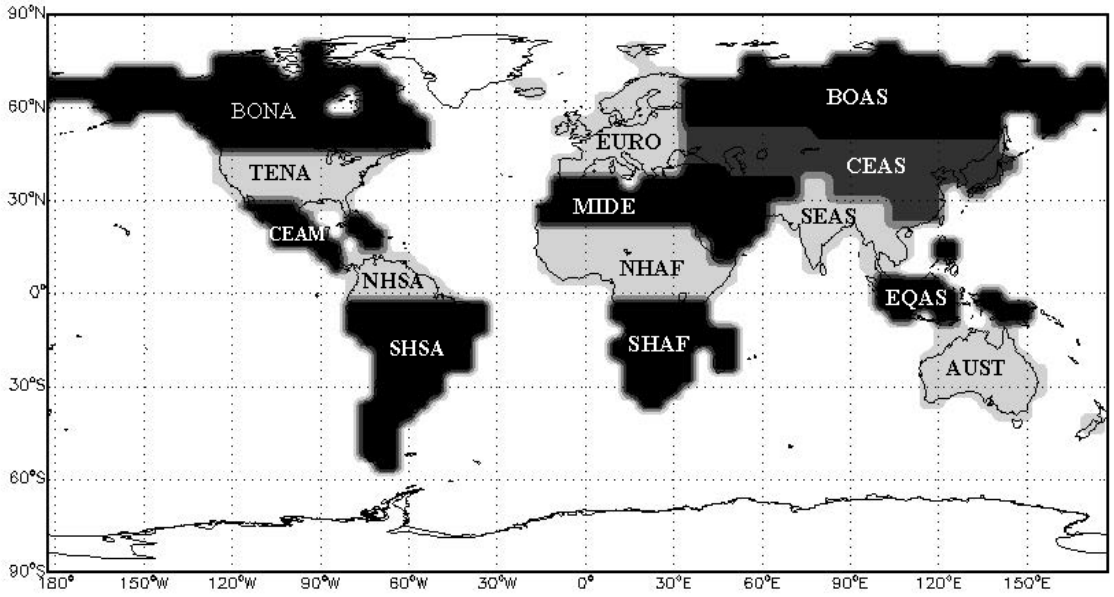

Figure 1: Definition of global regions used in the fire emissions model. BONA: Boreal North America, TENA: Temperate North America, CEAM: Central North America, NHSA: Northern Hemisphere South America, SHSA: Southern Hemisphere South America, EURO: Europe, MIDE: Middle East, NHAF: Northern Hemisphere Africa, SHAF: Southern Hemisphere Africa, BOAS: Boreal Asia, CEAS: Central Asia, SEAS: South East Asia, EQAS: Equatorial Asia, AUST: Australia.

We use emission factors for the species considered in this work from the compilation of Akagi et al. (2011) who have provided emission factors for 14 fuel/vegetation types. We use their estimates for tropical, temperate, boreal forests, grasslands and peatlands and supplement missing data with estimates from the Global Fire Emissions Database version with small fires (GFEDv4s) (Van der Werf et al., 2017) and Andreae and Merlet (2001). The emission factors for tropical, temperate, boreal forests and grasslands were assigned to the corresponding LPJ DGVM Plant Functional Types (PFTs) [*tropical: tropical broadleaved evergreen tree (TrBE), tropical broadleaved raingreen tree (TrBR),*

temperate (temperate needleleaved evergreen tree (TeNE), temperate broadleaved evergreen tree (TeBE), temperate broadleaved summergreen tree (TeBS), boreal (boreal needleleaved evergreen tree (BNE), boreal needleleaved summergreen tree (BNS) and grasslands (C3 and C4 herbs)]. However, to account for emissions due to peat burning, peatland emission factors were substituted for tropical forests in Equatorial Asia (EQAS) and boreal forests in North America and Asia (BONA, BOAS). The peatland emission factors as computed by Akagi et al. (2011) account for both peat and the forest overstory burning. Table 1 contains the atmospheric constituents considered in this study. Alkanes and alkenes are represented as lumped species while alkynes include acetylene only. The emission factors of the lumped alkane species were computed using a weighted summation of the emission factors of the individual species [*alkanes: ethane (C_2H_6), propane (C_3H_8), n-butane (C_4H_{10}), i-butane (C_4H_{10}), n-pentane (C_5H_{12}), i-pentane (C_5H_{12}), n-hexane (C_6H_{14}), heptane (C_7H_{16})*] and emissions are expressed as mass of carbon emitted. The weights are computed as the mass of carbon/mass of the compound (mass of nitrogen/mass of compound for nitrogen containing species). Emissions for alkenes [*ethylene (C_2H_4), propylene (C_3H_6),1-butene (C_4H_8), i-butene (C_4H_8),cis and trans 2-butene (C_4H_8), cis and trans 2-pentene (C_5H_{10}), 3-methyl-1-butene, 2-methyl-2-butene¸2-methyl-1-butene, 2-methyl-1-pentene)*,aromatic compounds [*benzene (C_6H_6), toluene (C_7H_8), xylene (C_8H_{10})*] and nitrogen [*ammonia (NH_3), nitrous acid (HONO), nitrogen oxide (NO_x), nitrous oxide (N_2O)*] were computed using the same methodology. These emission factors were input to the fire emissions model to obtain the emission estimates for all the species.

In this work, we present results for the 2000s and the 2050s combined effects scenario. The model was run for 5 years (1998-2002 for the 2000s and 2048-2052 for the 2050s) to obtain the emissions estimates reported. In addition, we also ran the model for the LC, LU, CC, LIGHT and POPDENS scenarios to determine the most important factors contributing to the emission changes in different regions/continents. The 2000s-2050s changes in wildfire frequencies for all the scenarios were reported in Section 1 and are discussed in detail in Huang et al. (2015). The estimated global burned area for the 2000s is 334 Mha [(51% (Africa (MIDE+NHAF+SHAF)), 23% (Eurasia (EURO+BOAS+CEAS+SEAS+EQAS)), 14% (South America (NHSA+SHSA)), 9% (Australia (AUST)), 3% (North America (BONA+TENA+CEAM))]. The 2000s-2050s changes in burned area for the LC, LU, LU/LC and CC scenarios are presented in Kumar et al. (2018). For the LIGHT scenario, global burned area is predicted to increase by 4% [+5% (North America, +3% (South America), +3% (Africa), +3% (Eurasia) and +17% (Australia)] while for the POPDENS scenario global burned area decreases by 13% [-4% (North America, -2% (South America), -27% (Africa), -0.8% (Eurasia) and +22% (Australia)]. Considering the combined effects of all the global change factors on wildfires (combined effects scenario), the global burned area in the 2050s increases by 9% [+34% (North America), +34% (South America), +2% (Africa), -7% (Eurasia), +85% (Australia)]. The emissions estimates for the species considered and the respective changes in the 2050s are discussed in the next section.

3.4. Results and Discussion

Table 1: Global wildfire emissions estimates (2000s) for the atmospheric species considered in this work.

Species[a]	Emissions (This work)	Literature range[b]
CO_2	7091	5716 – 9093
CO	424	271 - 568
CH_4	22	12.5 – 32.2
NH_3	10.5	4.2 – 7.7
SO_2	2.6	2.3 – 2.8
HONO	3.3	
NO_x	11.3	8.1 – 18.3
N_2O	1	0.9 – 1.4
$PM_{2.5}$	43	24.3 – 41
BC	2	1.8 – 4.8
OC	21	15.8 – 23.4
H_2	11	7.6 – 9.4
Alkanes	4.2	3.9 – 4
Alkenes	9	8 – 8.4
Acetylene	1.4	1.6
Aromatics	4.3	3
Formaldehyde	6.6	4.3 – 11.5

Acetone	2.5	2.5 – 3
Acetic acid	16	9.5 – 21.7
Formic acid	2.4	5.3
Carbon	2185	1741 – 2290
Nitrogen	15.5	
Mercury	612	104-1330

[a]All emissions estimates and ranges are in Tg year^{-1} except for mercury (Mg year^{-1})

[b]Data sources: (Andreae and Merlet, 2001; Bouwman et al., 1997; Brunke et al., 2001; Cofer III et al., 1991; De Simone et al., 2015; Ebinghaus et al., 2007; Friedli et al., 2009a; Friedli et al., 2001; Hoelzemann et al., 2004; Ito and Penner, 2004; Jain et al., 2006; Kaiser et al., 2012; Schultz et al., 2008; Sigler et al., 2003; Streets et al., 2009; Weiss-Penzias et al., 2007; Wiedinmyer et al., 2011)

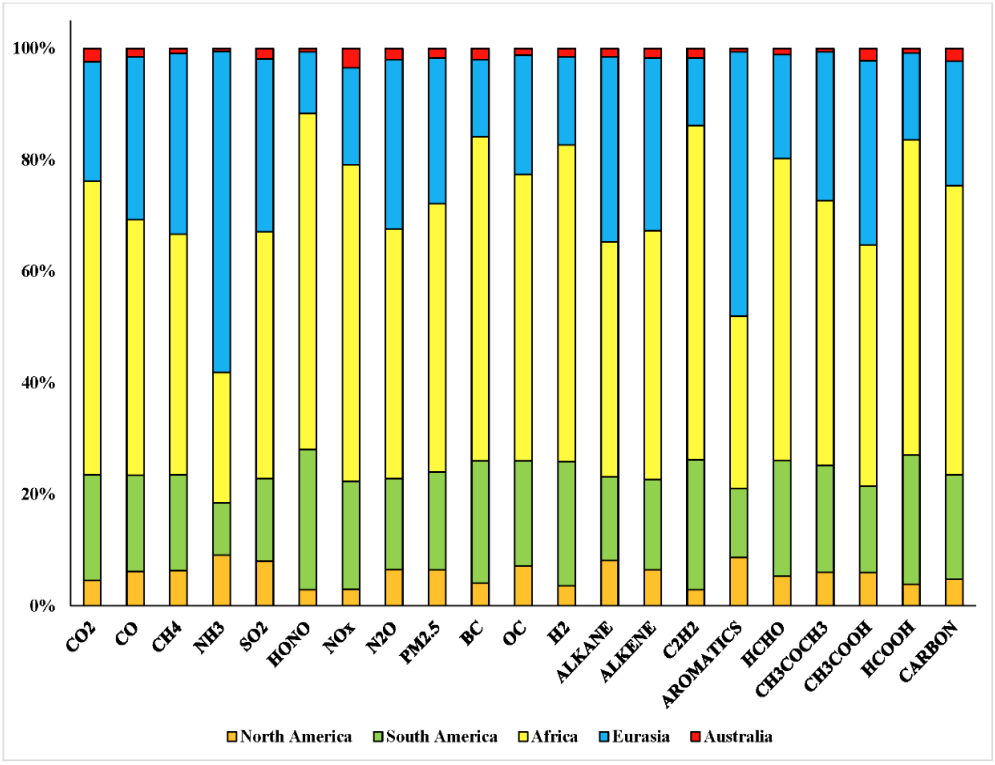

Figure 2: Geographical distribution of wildfire emissions (2000s) of the atmospheric species considered in this work.

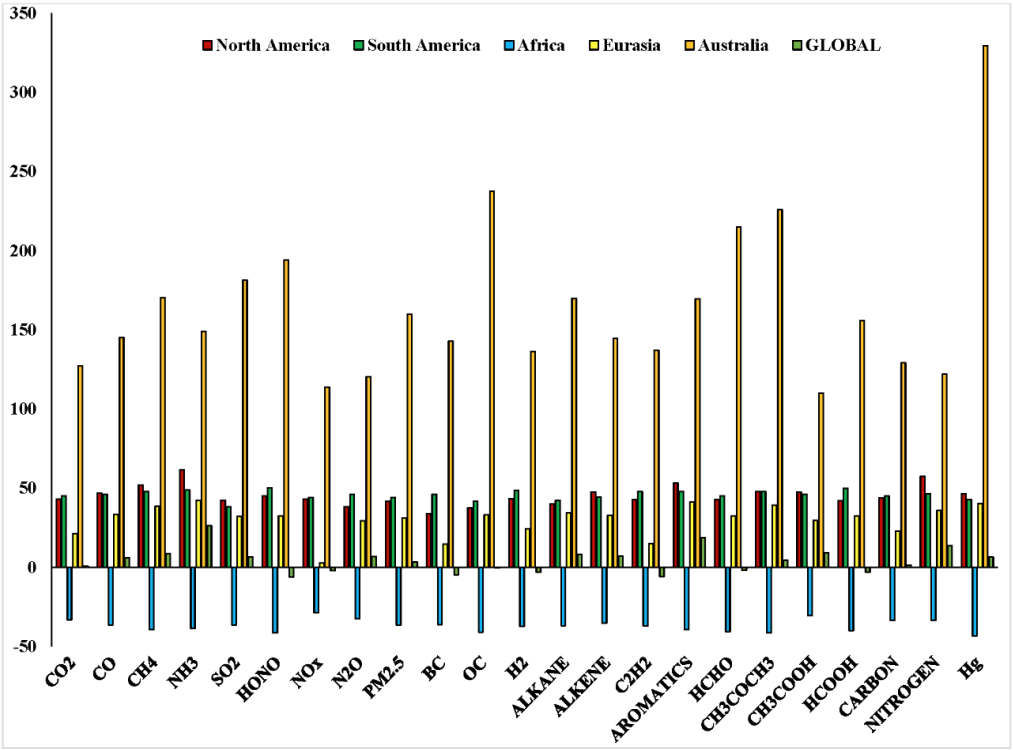

Figure 3: Changes in wildfire emissions of the atmospheric species considered in this work due to 2000s-2050s global change.

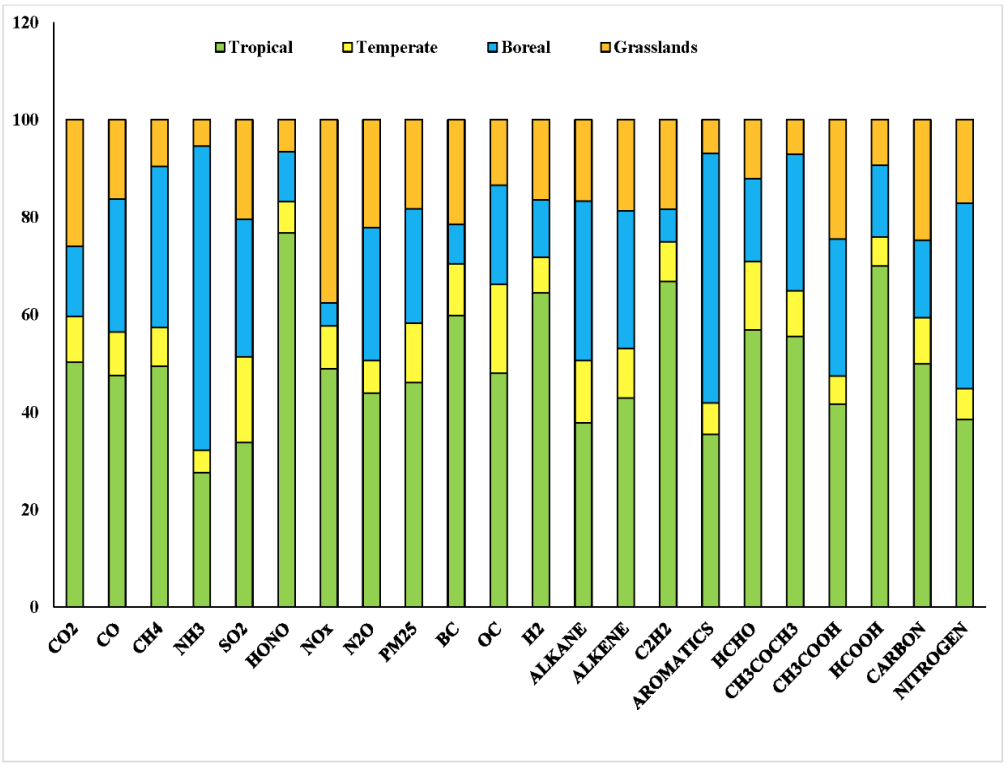

Figure 4: Vegetation distribution of wildfire emissions (2000s) of the atmospheric species considered in this work.

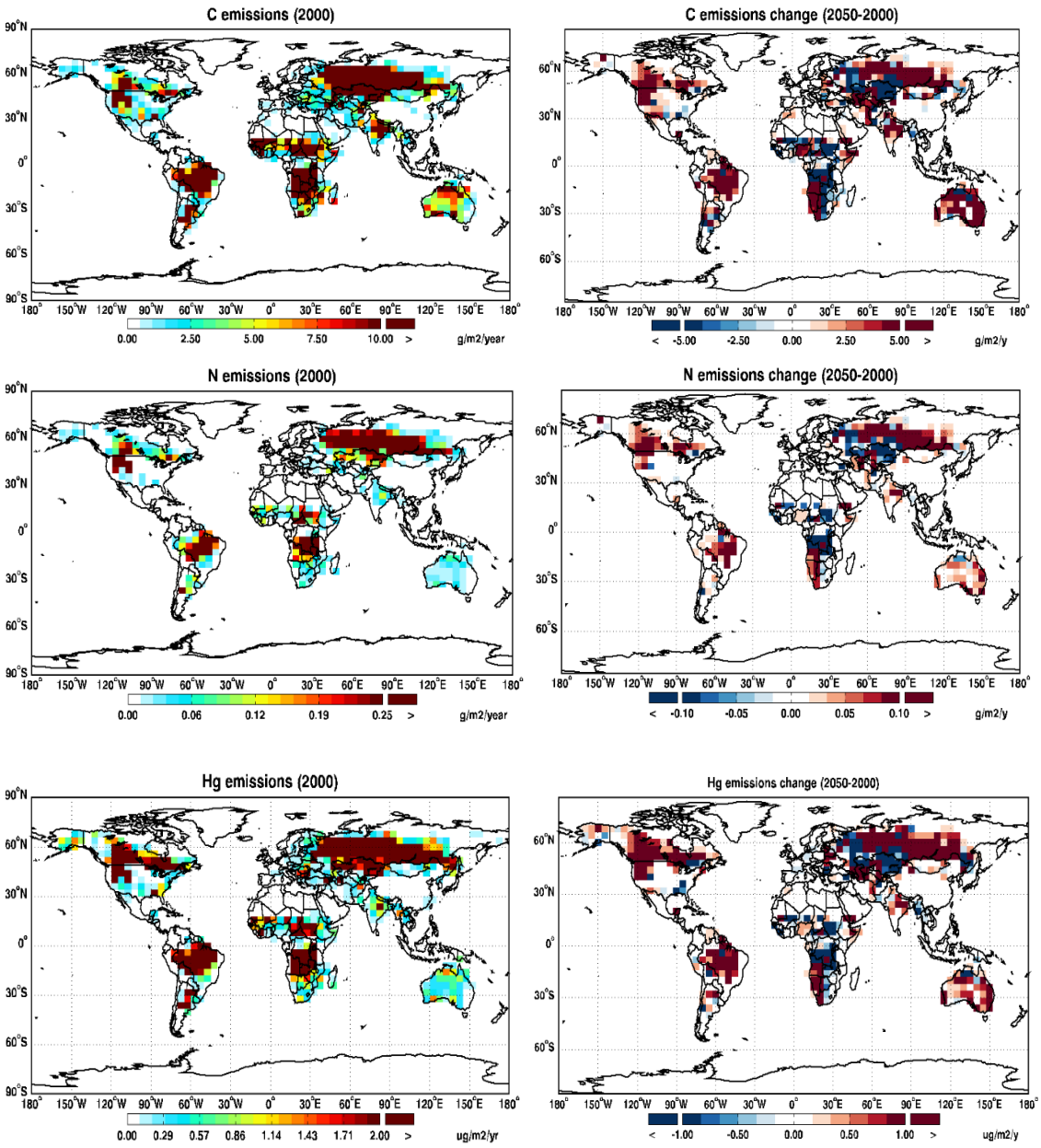

Figure 5: Changes in wildfire emissions of carbon, nitrogen and mercury for the 2000s and 2000s-2050s global change (Note the different scales and units in the plots).

Table 1 contains the global wildfire emissions estimates (for the 2000s) of the species considered in this work. The range of estimates available in the literature are also shown for comparison. The dominant species emitted from wildfires include important greenhouse gases [CO_2 (7091 Tg year^{-1}) and CH_4 (22 Tg year^{-1})], particulate matter [$PM_{2.5}$ (43 Tg year^{-1})], organic carbon aerosol [OC (21 Tg year^{-1})], tropospheric O_3 precursors [CO (424 Tg year^{-1}), NO_x (11 Tg year^{-1} as NO)], organic acids [acetic acid (CH_3COOH : 16 Tg year^{-1})], molecular hydrogen [H_2 (11 Tg year^{-1})] and ammonia [NH_3: (10.5 Tg year^{-1})]. In addition, relatively smaller amounts of some Non Methane Volatile Organic Compounds (NMVOCs) [alkanes (4 Tg year^{-1}), alkenes (9 Tg year^{-1}), aromatics (4 Tg year^{-1}), formaldehyde (HCHO) (7 Tg year^{-1}), acetone (CH_3COCH_3 (2.5 Tg year^{-1}))], aerosol precursors [SO_2 (2.6 Tg year^{-1})] , inorganic acids [HONO (3.3 Tg year^{-1})] and black carbon aerosol [BC: 2 Tg year^{-1}] are also emitted. Figure 2 shows the geographical distribution of the emissions for all the species. The present day emissions of mercury (Hg: 612 Mg year^{-1}) and geographical distribution has already been discussed in detail in Kumar et al. (2018) and hence is omitted here. A significant fraction (> 40%) of the global emissions for all the species is from Africa due to the high fire activity in the continent (> 50% of global annual burned area occurs in Africa [e.g. (Giglio et al., 2010b; Kumar et al., 2018; Randerson et al., 2012; Wiedinmyer et al., 2011)]). African emissions of highly oxidized species [e.g. CO_2 (53% of global emissions), NO_x (57%), HONO (60%)] and carbonaceous aerosols (BC: 58%, OC: 51%) are particularly high indicating the dominance of flaming combustion in African fires. Eurasia (11-58% of global emissions of the species) and South America (9-25%) are the other major sources of wildfire emissions of all the species. However, African emissions of NH_3 (23%) and aromatic hydrocarbons (31%)

constitute a minor fraction of the global emissions. 63% of global emissions of NH_3 and 50% of aromatic hydrocarbon emissions are estimated to originate in the boreal and tropical peatlands (BONA, BOAS, and EQAS). Peatlands also account for a significant fraction of global emissions of reduced carbon species such as CO (26%), CH_4 (32%), alkanes (33%) and alkenes (31%). These findings can be attributed to the dominance of smoldering combustion in peatlands, which results in higher emissions of reduced forms of carbon and nitrogen. Global carbon emissions (expressed as carbon equivalent emissions from CO_2 + CO + CH_4 + OC + BC + alkanes + alkenes + acetylene + aromatics) from wildfires are estimated as 2185 Tg C year $^{-1}$ while nitrogen emissions are 16 Tg N year^{-1} (expressed as nitrogen equivalent emissions from NH_3 + HONO + NO_x + N_2O). This spectrum of atmospheric species emitted and comparable emission magnitudes to anthropogenic sources emphasizes the important role of wildfires with respect to climate change at the regional, hemispheric and global scales, air quality, atmospheric chemistry, trace gas budgets and biogeochemical cycling of elements. Figure 4 shows the vegetation distribution of emissions for all the species considered in this work. The distribution for Hg is already presented by Kumar et al. (2018) and hence is omitted here. Tropical forests contribute the most to wildfire emissions with 50% or more of the global emissions for most species being emitted due to tropical forest burning (e.g. CO_2, NO_x, $PM_{2.5}$, BC, OC, H_2, HONO, HCOOH, HCHO, and C_2H_2). The total carbon emissions are also highest from tropical forest burning (50% of global emissions). Thus, wildfires in the tropics are of particular significance with respect to carbon cycle perturbations. The next most important biomes are grasslands (5-26% of global emissions for the species) followed by boreal (5-62%) and temperate forests (5-18%). Boreal forests account for particularly high fractions

of reduced species due to reasons explained earlier in this section. The minor contribution of temperate forests to global emissions of most species can be attributed to the relatively lower wildfire activity in the mid-latitudes as compared to that on the global scale.

Figures 3 and 5 show the predicted 2000s-2050s changes in global emissions of all the species considered in this work. On the global scale, these changes indicate that the future trajectory of global wildfire emissions of atmospheric constituents would be primarily influenced by developments in Africa. Global wildfire emissions of most species show increases between 0-10 % mainly due to the decline in emissions from Africa muting the significantly larger increases in other continents. For example, global CO_2 emissions show little change (+0.6%) due to a 33% decline in emissions from Africa countering the increases in other continents (North America: (+43%), South America: (+45%), Eurasia (+21%), Australia (+127%)). Global emissions of other important greenhouse gases (e.g. CH_4 (+8%) and N_2O (+7%)) are also predicted to increase in the 2050s with more pronounced changes at the continental scales. The consequences of a future increase in wildfire N_2O emissions would not be limited to the troposphere. A long lifetime and lack of sinks in the troposphere result in N_2O being transported to the stratosphere where it plays a major role in stratospheric O_3 destruction. Similar increases are predicted for other trace constituents [e.g. CO (+6%) and NMVOCs (e.g. alkanes: +8%, alkenes: +7%)], particulate matter [$PM_{2.5}$:+3.5%], aerosol precursors [SO_2:+6%], organic acids [CH_3COOH +9%] and Hg (+6%). However, global emissions of species for which the fraction of global emissions from Africa is very high [e.g. HONO (60%), NO_x (57%), BC (58%)] could decline in the 2050s [e.g. HONO (-6%), NO_x (-2%), H_2 (-3%), BC (-5%), HCOOH (-3%)]. On the other

hand, global emissions of species like NH_3 (+26%) and the aromatics (+19%) which have Africa as a minor source show much larger increases in the 2050s.

Following the IPCC A1B scenario (IPCC, 2001), 2000s-2050s global change is predicted to cause major alterations in global land cover (Wu et al., 2012) and climate (Wu et al., 2008a) while anthropogenic land use (Wu et al., 2012) and human population patterns (IMAGE Team, 2001) would also be starkly different from the 2000s. These impacts vary across continents with different global change components acting as key factors influencing wildfire emissions. In Africa, increase in anthropogenic land use and human occupancy of the continent act as major drivers contributing to the declines in wildfire emissions. A continual growth in cropland extent in the continent could result in significantly less natural vegetation availability than the 2000s. In addition, greater human population would increase the probability of wildfire suppression thereby inhibiting uncontrolled spreading after ignition. These factors outweigh the effects of a fire favorable climate and greater natural vegetation coverage due to climate driven alterations in land cover in the 2050s, both of which cause significant increases in wildfire emissions in the continent. Therefore, emissions from Africa are predicted to decline in the 2050s. On the contrary, wildfire emissions in South America and Australia are predicted to increase in the 2050s, driven by greater natural vegetation availability due to anthropogenic land use declines, favorable climate, increase in lightning frequency and greater anthropogenic ignitions associated with human population increases. Carbon emissions from South America and Australia are estimated to increase by 45% and 129%, respectively, along with significant increases in emissions of other atmospheric constituents as well.

Wildfire emissions from Africa and South America are critically important for the tropical atmospheric composition and climate [e.g. (Anderson et al., 1996; Andreae et al., 1994; Edwards et al., 2006; Mauzerall et al., 1998; Wai et al., 2014)]. Emissions from these continents constitute an important source of tropospheric O_3 precursors in the tropics and exert a significant influence on the O_3 levels [e.g. (Andreae et al., 1988; Krishnamurti et al., 1993; Roelofs et al., 1997; Thompson et al., 1996)]. Wildfire emissions contain O_3 precursors and result in enhancements of O_3 levels during wildfire events. Thus, a future decline in emissions of O_3 precursors [CH_4 (-40%), NO_x (-29%), NMVOCs (alkanes: -37%, alkenes: -35%)] from Africa could result in a reduction of tropical O_3 levels. In addition, reduction in emissions of HONO (-41%) [OH source along with O_3] and OH sinks [CH_4, CO (-37%), H_2 (-37%)] from Africa and corresponding rise in emissions from South America would also affect the hydroxyl (OH) radical abundance. The hydroxyl (OH) radical has the highest concentrations in the tropics due to high water vapor and solar radiation fluxes resulting in favorable conditions for ($O(^1D)+H_2O \rightarrow 2OH$) OH formation and regulates the oxidizing capacity of the tropical troposphere. Since the OH radical is responsible for the removal of several atmospheric trace constituents, alterations in its concentrations would affect the atmospheric lifetimes of atmospheric trace constituents and consequently their levels in the tropical troposphere. Furthermore, acidity in tropical precipitation arises primarily from organic acids (e.g. CH_3COOH, HCOOH) and nitric acid (HNO_3), the levels of which in the tropical troposphere are dependent on wildfire activity (Crutzen and Andreae, 1990). A decline in African emissions of organic acids (CH_3COOH: -31%, HCOOH: -40%)) and NO_x in the 2050s could contribute to reducing the acidity of tropical precipitation and the resulting adverse impacts on tropical ecosystems (e.g. foliar

damage). Lower emissions of aerosols ($PM_{2.5}$: -37%, BC: -36%, OC: -41%), their precursors (e.g. SO_2: -37%) from Africa could influence the climate in the tropics through alteration of the incoming solar radiation (absorption (e.g. BC) /scattering (e.g. SO_4^{2-})) while lower greenhouse gas emissions (CO_2, CH_4, N_2O) would act to alleviate warming effects in the tropics. Fewer aerosols would also result in reducing Cloud Condensation Nuclei (CCNs) which facilitate cloud formation and would thereby influence tropical precipitation patterns. However, the declines in African emissions are accompanied by a corresponding emissions rise in South America and Australia. Rise of tropospheric O_3 precursor emissions in South America (e.g. NO_x: +44%, CO: +46%, CH_4: +48%) and Australia [CO (+145%), CH_4 (+170%), NMVOCs (alkanes: 170%, alkenes: 144%) and NOx (114%)] would increase O_3 levels over these regions. O_3 production due to wildfire emissions in South America and the resulting vegetation damage can contribute to reducing the net primary productivity over the Amazon (Pacifico et al., 2015). A significant fraction of tropospheric O_3 levels over Australia can be attributed to wildfires (Hurst et al., 1994). Thus, higher O_3 levels in the future could have adverse effects on the Amazon forest vegetation and degrade air quality over both continents. Higher aerosol emissions from wildfires in South America ($PM_{2.5}$: +44%, BC: +46%, OC: +42%) and Australia ($PM_{2.5}$: +160%, BC: +143%, OC: +238%) could also have significant effects on the radiative forcing and air quality over these regions. In addition, pollution from African/South American/Australian fires can be transported long distances (e.g. South Atlantic, Indian Ocean) from the respective continents (Ansmann et al., 2009; Dirksen et al., 2009; Edwards et al., 2006; Staudt et al., 2002). The diverging emissions changes in these continents are

expected to have important implications for the transport of wildfire pollution to these remote regions.

Wildfire emissions from boreal forests are predicted to increase in the 2050s primarily driven by greater natural vegetation availability (increase in boreal forest coverage in the high latitudes) due to climate driven alterations in land cover, a warmer climate and the resulting higher lightning caused ignitions. In the mid-latitudes, emissions in North America could increase while a decline is predicted in Eurasia. In the North American mid-latitudes, climate (e.g. warmer and drier conditions in the US) and land cover change (e.g. increase in temperate forest coverage) together with increases in lightning frequencies drive the emissions increase outweighing the effects of increase in anthropogenic land use that would limit natural vegetation availability. Overall, carbon emissions from wildfires in North America could increase by 44% in the 2050s. In contrast, emissions are predicted to decline in the Asian mid-latitudes where anthropogenic land use could increase and in the Western parts of Russia where a reduction in boreal forest coverage decreases vegetation availability. In Equatorial Asia, higher precipitation in the 2050s results in a decline in wildfire emissions. These competing effects on wildfires in Eurasia result in an overall carbon emissions increase of 23% in the region (CO_2: 21%, CO: 34%, CH_4: 38%, BC: 15%, OC: 33%).

Higher boreal wildfire emissions in the 2050s could result in increased pollution not only at the local and regional scales but also at the hemispherical scale. Boreal wildfire events are accompanied by long-range transport of pollution in the Northern Hemisphere. Wildfire emissions from boreal North America can impact far away regions (e.g., US, North

Atlantic, Europe, Arctic) resulting in elevated pollution levels in these regions (Colarco et al., 2004; DeBell et al., 2004; Forster et al., 2001; Lapina et al., 2006; Real et al., 2007; Val Martin et al., 2008; Val Martin et al., 2006; Wotawa and Trainer, 2000). Boreal Asia wildfires also cause pollution transport to the Arctic, the remote Northern Pacific (Tanimoto et al., 2000), the Western United States (Bertschi et al., 2004; Bertschi and Jaffe, 2005; Jaffe et al., 2004), Alaska, Canada and East Asian countries (e.g. Korea) (Lee et al., 2005). Higher emissions of BC aerosols from boreal fires in the future could worsen the warming effects in the Arctic. BC aerosol emitted from boreal wildfires can be transported and deposited to the Arctic resulting in snow albedo reduction and accelerating snow melting (Stohl et al., 2006). Higher greenhouse gas emissions in the boreal regions would contribute to greater warming in these regions as well as globally. For example, an increase in burned area due to fires in boreal North America between the 1970s and 1990s corresponded with a 1°-1.6° rise in temperatures in the region (Kasischke et al., 1999). Boreal forests also act as major sinks of carbon and Hg (Turetsky et al., 2006; Yu et al., 2011; 2010). Thus, higher wildfire emissions of carbon and Hg from boreal forests in the future would also alter the biogeochemical cycling of these elements.

In the US, higher wildfire emissions of tropospheric O_3 precursors (e.g. NO_x, CH_4, NMVOCs, $PM_{2.5}$) could hamper the benefits achieved from controls on anthropogenic emissions of these species and have adverse effects on air quality with respect to O_3, CO, NOx and VOCs. Furthermore, higher emissions of aerosols ($PM_{2.5}$, BC, OC) would also contribute to deteriorating air quality while greater emissions of organic acids, SO_2 and NO_x could influence the acidity of precipitation over the US. Moreover, wildfires in

western US incur tremendous economic losses (Whitlock, 2004) and the situation would worsen with the significant increase in wildfires in the 2050s.

3.5. Conclusions

We estimated wildfire emissions (2000s) for important atmospheric constituents and the impacts of 2000s-2050s global change on these emissions following the IPCC A1B socioeconomic scenario. Our emission estimates for the 2000s show that Africa contributes significantly to the global wildfire emissions of all the atmospheric constituents considered owing to the high wildfire activity on the continent. Eurasia and South America are the other major contributors to global wildfire emissions of atmospheric constituents. In response to 2000s-2050s global change, wildfire emissions from Africa show a major decline while emissions in all other continents (North America, South America, Eurasia and Australia) are predicted to increase in the 2050s. Anthropogenic influence in the form of land use, population change and ignitions emerges as a very important factor driving the emissions decline in Africa and contributing to emissions increases in South America and Australia. Changes in climate and the resulting alterations in land cover and higher lightning ignitions in the 2050s also contribute significantly to changes in wildfire emissions in all the continents. These changes in wildfire emissions could have important implications for the future climate, atmospheric chemistry/air quality and biogeochemical cycling of carbon, nitrogen and mercury. Several studies in the past have solely focused on the influence of climate on future changes in wildfires. Our findings from this work indicate

that the anthropogenic influence in the form of land use and increasing population density would emerge as a dominant factor driving wildfire emissions in the coming decades.

Acknowledgements:

This study is supported by NSF (grant #1313755).

Competing interests:

The authors declare that they have no conflict of interest.

References

Akagi, S., Yokelson, R. J., Wiedinmyer, C., Alvarado, M., Reid, J., Karl, T., Crounse, J., and Wennberg, P.: Emission factors for open and domestic biomass burning for use in atmospheric models, Atmospheric Chemistry and Physics, 11, 4039-4072, 2011.

Anderson, B. E., Grant, W. B., Gregory, G. L., Browell, E. V., Collins, J. E., Sachse, G. W., Bagwell, D. R., Hudgins, C. H., Blake, D. R., and Blake, N. J.: Aerosols from biomass burning over the tropical South Atlantic region: Distributions and impacts, Journal of Geophysical Research: Atmospheres, 101, 24117-24137, 1996.

Andreae, M., Anderson, B., Blake, D., Bradshaw, J., Collins, J., Gregory, G., Sachse, G., and Shipham, M.: Influence of plumes from biomass burning on atmospheric chemistry over the equatorial and tropical South Atlantic during CITE 3, Journal of Geophysical Research: Atmospheres, 99, 12793-12808, 1994.

Andreae, M. O., Browell, E. V., Garstang, M., Gregory, G., Harriss, R., Hill, G., Jacob, D. J., Pereira, M., Sachse, G., and Setzer, A.: Biomass-burning emissions and associated haze layers over Amazonia, Journal of Geophysical Research: Atmospheres, 93, 1509-1527, 1988.

Andreae, M. O., and Merlet, P.: Emission of trace gases and aerosols from biomass burning, Global biogeochemical cycles, 15, 955-966, 2001.

Ansmann, A., Baars, H., Tesche, M., Müller, D., Althausen, D., Engelmann, R., Pauliquevis, T., and Artaxo, P.: Dust and smoke transport from Africa to South America: Lidar profiling over Cape Verde and the Amazon rainforest, Geophysical Research Letters, 36, 2009.

Archibald, S., Nickless, A., Govender, N., Scholes, R., and Lehsten, V.: Climate and the inter-annual variability of fire in southern Africa: a meta-analysis using long-term field data and satellite-derived burnt area data, Global Ecology and Biogeography, 19, 794-809, 2010.

Bachelet, D., Neilson, R. P., Lenihan, J. M., and Drapek, R. J.: Climate change effects on vegetation distribution and carbon budget in the United States, Ecosystems, 4, 164-185, 2001.

Bachelet, D., Neilson, R. P., Hickler, T., Drapek, R. J., Lenihan, J. M., Sykes, M. T., Smith, B., Sitch, S., and Thonicke, K.: Simulating past and future dynamics of natural ecosystems in the United States, Global Biogeochemical Cycles, 17, 2003.

Bertschi, I., Jaffe, D. A., Jaeglé, L., Price, H., and Dennison, J.: PHOBEA/ITCT 2002 airborne observations of transpacific transport of ozone, CO, volatile organic compounds, and aerosols to the northeast Pacific: Impacts of Asian anthropogenic and Siberian boreal fire emissions, Journal of Geophysical Research: Atmospheres, 109, 2004.

Bertschi, I. T., and Jaffe, D. A.: Long-range transport of ozone, carbon monoxide, and aerosols to the NE Pacific troposphere during the summer of 2003: Observations of smoke plumes from Asian boreal fires, Journal of Geophysical Research: Atmospheres, 110, 2005.

Bond, W. J., Woodward, F. I., and Midgley, G. F.: The global distribution of ecosystems in a world without fire, New phytologist, 165, 525-538, 2005.

Bouwman, A., Lee, D., Asman, W., Dentener, F., Van Der Hoek, K., and Olivier, J.: A global high-resolution emission inventory for ammonia, Global biogeochemical cycles, 11, 561-587, 1997.

Bowman, D. M., Balch, J. K., Artaxo, P., Bond, W. J., Carlson, J. M., Cochrane, M. A., D'Antonio, C. M., DeFries, R. S., Doyle, J. C., and Harrison, S. P.: Fire in the Earth system, science, 324, 481-484, 2009.

Bowman, D. M., Balch, J., Artaxo, P., Bond, W. J., Cochrane, M. A., D'antonio, C. M., DeFries, R., Johnston, F. H., Keeley, J. E., and Krawchuk, M. A.: The human dimension of fire regimes on Earth, Journal of biogeography, 38, 2223-2236, 2011.

Brown, I. F., Schroeder, W., Setzer, A., De Los Rios Maldonado, M., Pantoja, N., Duarte, A., and Marengo, J.: Monitoring fires in southwestern Amazonia rain forests, Eos, Transactions American Geophysical Union, 87, 253-259, 2006.

Brunke, E. G., Labuschagne, C., and Slemr, F.: Gaseous mercury emissions from a fire in the Cape Peninsula, South Africa, during January 2000, Geophysical Research Letters, 28, 1483-1486, 2001.

Butry, D. T., Mercer, E., Prestemon, J. P., Pye, J. M., and Holmes, T. P.: What is the price of catastrophic wildfire?, Journal of Forestry, 99, 9-17, 2001.

Christopher, S. A., Wang, M., Berendes, T. A., Welch, R. M., and Yang, S.-K.: The 1985 biomass burning season in South America: Satellite remote sensing of fires, smoke, and regional radiative energy budgets, Journal of Applied Meteorology, 37, 661-678, 1998.

Cofer III, W., Levine, J., Winstead, E., and Stocks, B.: New estimates of nitrous oxide emissions from biomass burning, Nature, 349, 689, 1991.

Colarco, P., Schoeberl, M., Doddridge, B., Marufu, L., Torres, O., and Welton, E.: Transport of smoke from Canadian forest fires to the surface near Washington, DC: Injection height, entrainment, and optical properties, Journal of Geophysical Research: Atmospheres, 109, 2004.

Crutzen, P. J., and Andreae, M. O.: Biomass burning in the tropics: Impact on atmospheric chemistry and biogeochemical cycles, Science, 250, 1669-1679, 1990.

Dale, V. H., Joyce, L. A., McNulty, S., Neilson, R. P., Ayres, M. P., Flannigan, M. D., Hanson, P. J., Irland, L. C., Lugo, A. E., and Peterson, C. J.: Climate change and forest disturbances: climate change can affect forests by altering the frequency, intensity, duration, and timing of fire, drought, introduced species, insect and pathogen outbreaks, hurricanes, windstorms, ice storms, or landslides, BioScience, 51, 723-734, 2001.

De Simone, F., Cinnirella, S., Gencarelli, C. N., Yang, X., Hedgecock, I. M., and Pirrone, N.: Model study of global mercury deposition from biomass burning, Environmental science & technology, 49, 6712-6721, 2015.

DeBell, L. J., Talbot, R. W., Dibb, J. E., Munger, J. W., Fischer, E. V., and Frolking, S. E.: A major regional air pollution event in the northeastern United States caused by extensive forest fires in Quebec, Canada, Journal of Geophysical Research: Atmospheres, 109, 2004.

Dirksen, R. J., Folkert Boersma, K., De Laat, J., Stammes, P., Van Der Werf, G. R., Val Martin, M., and Kelder, H. M.: An aerosol boomerang: Rapid around-the-world transport of smoke from the December 2006 Australian forest fires observed from space, Journal of Geophysical Research: Atmospheres, 114, 2009.

Ebinghaus, R., Slemr, F., Brenninkmeijer, C., Van Velthoven, P., Zahn, A., Hermann, M., O'Sullivan, D., and Oram, D.: Emissions of gaseous mercury from biomass burning in South America in 2005 observed during CARIBIC flights, Geophysical Research Letters, 34, 2007.

Edwards, D., Emmons, L., Gille, J., Chu, A., Attié, J. L., Giglio, L., Wood, S., Haywood, J., Deeter, M., and Massie, S.: Satellite-observed pollution from Southern Hemisphere biomass burning, Journal of Geophysical Research: Atmospheres, 111, 2006.

Flannigan, M. D., Logan, K. A., Amiro, B. D., Skinner, W. R., and Stocks, B.: Future area burned in Canada, Climatic change, 72, 1-16, 2005.

Flannigan, M. D., Krawchuk, M. A., de Groot, W. J., Wotton, B. M., and Gowman, L. M.: Implications of changing climate for global wildland fire, International journal of wildland fire, 18, 483-507, 2009.

Forster, C., Wandinger, U., Wotawa, G., James, P., Mattis, I., Althausen, D., Simmonds, P., O'Doherty, S., Jennings, S. G., and Kleefeld, C.: Transport of boreal forest fire emissions from Canada to Europe, Journal of Geophysical Research: Atmospheres, 106, 22887-22906, 2001.

Friedli, H., Arellano, A., Cinnirella, S., and Pirrone, N.: Initial estimates of mercury emissions to the atmosphere from global biomass burning, Environ. Sci. Technol, 43, 3507-3513, 2009a.

Friedli, H., Arellano, A., Cinnirella, S., and Pirrone, N.: Initial estimates of mercury emissions to the atmosphere from global biomass burning, Environmental science & technology, 43, 3507-3513, 2009b.

Friedli, H. R., Radke, L. F., and Lu, J. Y.: Mercury in smoke from biomass fires, Geophysical Research Letters, 28, 3223-3226, 2001.

Gatebe, C., Ichoku, C., Poudyal, R., Román, M., and Wilcox, E.: Surface albedo darkening from wildfires in northern sub-Saharan Africa, Environmental Research Letters, 9, 065003, 2014.

Gerten, D., Schaphoff, S., Haberlandt, U., Lucht, W., and Sitch, S.: Terrestrial vegetation and water balance—hydrological evaluation of a dynamic global vegetation model, Journal of Hydrology, 286, 249-270, 2004.

Gibling, M. R., and Davies, N. S.: Palaeozoic landscapes shaped by plant evolution, Nature Geoscience, 5, 99, 2012.

Giglio, L., Van der Werf, G., Randerson, J., Collatz, G., and Kasibhatla, P.: Global estimation of burned area using MODIS active fire observations, Atmospheric Chemistry and Physics, 6, 957-974, 2006.

Giglio, L., Randerson, J., Van der Werf, G., Kasibhatla, P., Collatz, G., Morton, D., and DeFries, R.: Assessing variability and long-term trends in burned area by merging multiple satellite fire products, Biogeosciences, 7, 1171-1186, 2010.

Glasspool, I. J., Edwards, D., and Axe, L.: Charcoal in the Silurian as evidence for the earliest wildfire, Geology, 32, 381-383, 2004.

Glasspool, I. J., Edwards, D., and Axe, L.: Charcoal in the Early Devonian: a wildfire-derived Konservat–Lagerstätte, Review of Palaeobotany and Palynology, 142, 131-136, 2006.

Hall, J. R.: The total cost of fire in the United States, National Fire Protection Association, 2014.

Hao, W. M., and Liu, M. H.: Spatial and temporal distribution of tropical biomass burning, Global biogeochemical cycles, 8, 495-503, 1994.

Hess, J. C., Scott, C. A., Hufford, G. L., and Fleming, M. D.: El Nino and its impact on fire weather conditions in Alaska, International Journal of Wildland Fire, 10, 1-13, 2001.

Hickler, T., Prentice, I. C., Smith, B., Sykes, M. T., and Zaehle, S.: Implementing plant hydraulic architecture within the LPJ Dynamic Global Vegetation Model, Global Ecology and Biogeography, 15, 567-577, 2006.

Hobbs, P. V., Reid, J. S., Kotchenruther, R. A., Ferek, R. J., and Weiss, R.: Direct radiative forcing by smoke from biomass burning, Science, 275, 1777-1778, 1997.

Hoelzemann, J. J., Schultz, M. G., Brasseur, G. P., Granier, C., and Simon, M.: Global Wildland Fire Emission Model (GWEM): Evaluating the use of global area burnt satellite data, Journal of Geophysical Research: Atmospheres, 109, 2004.

Huang, Y., Wu, S., and Kaplan, J. O.: Sensitivity of global wildfire occurrences to various factors in the context of global change, Atmospheric Environment, 121, 86-92, 2015.

Hurst, D. F., Griffith, D. W., and Cook, G. D.: Trace gas emissions from biomass burning in tropical Australian savannas, Journal of Geophysical Research: Atmospheres, 99, 16441-16456, 1994.

IMAGE Team, H.: The IMAGE 2.2 implementation of the SRES scenarios: a comprehensive analysis of emissions, climate change and impacts in the 21st century, RIVM CD-ROM Publication, 481508018, 2001.

IPCC: Climate Change 2001: The Scientific Basis, contribution of Working Group I to the Third Assessment Report of the Intergovernmental Panel on Climate Change, edited by: Houghton, J. T., Ding, Y., Griggs, D. J., Noguer, M., van der, P. J. Linden, Cambridge University Press, Cambridge United Kingdom and New York, NY, USA, 2001.

Ito, A., and Penner, J. E.: Global estimates of biomass burning emissions based on satellite imagery for the year 2000, Journal of Geophysical Research: Atmospheres, 109, 2004.

Jaffe, D., Bertschi, I., Jaeglé, L., Novelli, P., Reid, J. S., Tanimoto, H., Vingarzan, R., and Westphal, D. L.: Long-range transport of Siberian biomass burning emissions and impact on surface ozone in western North America, Geophysical Research Letters, 31, 2004.

Jain, A. K., and Yang, X.: Modeling the effects of two different land cover change data sets on the carbon stocks of plants and soils in concert with CO2 and climate change, Global Biogeochemical Cycles, 19, 2005.

Jain, A. K., Tao, Z., Yang, X., and Gillespie, C.: Estimates of global biomass burning emissions for reactive greenhouse gases (CO, NMHCs, and NOx) and CO2, Journal of Geophysical Research: Atmospheres, 111, 2006.

Johnston, F., Hanigan, I., Henderson, S., Morgan, G., and Bowman, D.: Extreme air pollution events from bushfires and dust storms and their association with mortality in Sydney, Australia 1994–2007, Environmental research, 111, 811-816, 2011.

Joos, F., Prentice, I. C., Sitch, S., Meyer, R., Hooss, G., Plattner, G. K., Gerber, S., and Hasselmann, K.: Global warming feedbacks on terrestrial carbon uptake under the Intergovernmental Panel on Climate Change (IPCC) emission scenarios, Global Biogeochemical Cycles, 15, 891-907, 2001.

Kaiser, J., Heil, A., Andreae, M., Benedetti, A., Chubarova, N., Jones, L., Morcrette, J.-J., Razinger, M., Schultz, M., and Suttie, M.: Biomass burning emissions estimated with a global fire assimilation system based on observed fire radiative power, Biogeosciences, 9, 527, 2012.

Kasischke, E. S., Bergen, K., Fennimore, R., Sotelo, F., Stephens, G., Janetos, A., and Shugart, H. H.: Satellite imagery gives clear picture of Russia's boreal forest fires, Eos, Transactions American Geophysical Union, 80, 141-147, 1999.

Kim, P. S., Jacob, D. J., Mickley, L. J., Koplitz, S. N., Marlier, M. E., DeFries, R. S., Myers, S. S., Chew, B. N., and Mao, Y. H.: Sensitivity of population smoke exposure to fire locations in Equatorial Asia, Atmospheric Environment, 102, 11-17, 2015.

Kloster, S., Mahowald, N., Randerson, J., and Lawrence, P.: The impacts of climate, land use, and demography on fires during the 21st century simulated by CLM-CN, Biogeosciences, 9, 2012.

Koplitz, S. N., Mickley, L. J., Marlier, M. E., Buonocore, J. J., Kim, P. S., Liu, T., Sulprizio, M. P., DeFries, R. S., Jacob, D. J., and Schwartz, J.: Public health impacts of the severe haze in Equatorial Asia in September–October 2015: demonstration of a new framework for informing fire management strategies to reduce downwind smoke exposure, Environmental Research Letters, 11, 094023, 2016.

Krishnamurti, T., Fuelberg, H., Sinha, M., Oosterhof, D., Bensman, E., and Kumar, V.: The meteorological environment of the tropospheric ozone maximum over the tropical South Atlantic Ocean, Journal of Geophysical Research: Atmospheres, 98, 10621-10641, 1993.

Kumar, A., Wu, S., Huang, Y., Liao, H., and Kaplan, J. O.: Mercury from wildfires: Global emission inventories and sensitivity to 2000–2050 global change, Atmospheric Environment, 173, 6-15, 2018.

Kunii, O., Kanagawa, S., Yajima, I., Hisamatsu, Y., Yamamura, S., Amagai, T., and Ismail, I. T. S.: The 1997 haze disaster in Indonesia: its air quality and health effects, Archives of Environmental Health: An International Journal, 57, 16-22, 2002.

Kunzli, N., Avol, E., Wu, J., Gauderman, W. J., Rappaport, E., Millstein, J., Bennion, J., McConnell, R., Gilliland, F. D., and Berhane, K.: Health effects of the 2003 Southern

California wildfires on children, American journal of respiratory and critical care medicine, 174, 1221-1228, 2006.

Lapina, K., Honrath, R., Owen, R., Val Martin, M., and Pfister, G.: Evidence of significant large-scale impacts of boreal fires on ozone levels in the midlatitude Northern Hemisphere free troposphere, Geophysical Research Letters, 33, 2006.

Lee, K. H., Kim, J. E., Kim, Y. J., Kim, J., and von Hoyningen-Huene, W.: Impact of the smoke aerosol from Russian forest fires on the atmospheric environment over Korea during May 2003, Atmospheric Environment, 39, 85-99, 2005.

Liu, J. C., Mickley, L. J., Sulprizio, M. P., Dominici, F., Yue, X., Ebisu, K., Anderson, G. B., Khan, R. F., Bravo, M. A., and Bell, M. L.: Particulate air pollution from wildfires in the Western US under climate change, Climatic change, 138, 655-666, 2016.

Lyons, E. A., Jin, Y., and Randerson, J. T.: Changes in surface albedo after fire in boreal forest ecosystems of interior Alaska assessed using MODIS satellite observations, Journal of Geophysical Research: Biogeosciences, 113, 2008.

Marlier, M. E., DeFries, R. S., Voulgarakis, A., Kinney, P. L., Randerson, J. T., Shindell, D. T., Chen, Y., and Faluvegi, G.: El Niño and health risks from landscape fire emissions in southeast Asia, Nature climate change, 3, 131-136, 2013.

Mauzerall, D. L., Logan, J. A., Jacob, D. J., Anderson, B. E., Blake, D. R., Bradshaw, J. D., Heikes, B., Sachse, G. W., Singh, H., and Talbot, B.: Photochemistry in biomass burning plumes and implications for tropospheric ozone over the tropical South Atlantic, Journal of Geophysical Research: Atmospheres, 103, 8401-8423, 1998.

MNP: Integrated modelling of global environmental change, an overview of IMAGE 2.4. edited by: Bouwman, A. F., Kram,T., and Klein Goldewijk, K, Netherlands Environmental Assessment Agency (MNP), Bilthoven, The Netherlands, 2006.

Myhre, G., Govaerts, Y., Haywood, J. M., Berntsen, T. K., and Lattanzio, A.: Radiative effect of surface albedo change from biomass burning, Geophysical Research Letters, 32, 2005.

Pacifico, F., Folberth, G., Sitch, S., Haywood, J., Rizzo, L., Malavelle, F., and Artaxo, P.: Biomass burning related ozone damage on vegetation over the Amazon forest: a model sensitivity study, Atmospheric Chemistry and Physics, 15, 2791-2804, 2015.

Pechony, O., and Shindell, D.: Fire parameterization on a global scale, Journal of Geophysical Research: Atmospheres, 114, 2009.

Pechony, O., and Shindell, D. T.: Driving forces of global wildfires over the past millennium and the forthcoming century, Proceedings of the National Academy of Sciences, 107, 19167-19170, 2010.

Penner, J. E., Dickinson, R. E., and O'Neill, C. A.: Effects of aerosol from biomass burning on the global radiation budget, Science, 256, 1432-1434, 1992.

Price, C., and Rind, D.: The impact of a 2× CO2 climate on lightning-caused fires, Journal of Climate, 7, 1484-1494, 1994.

Randerson, J., Chen, Y., Werf, G., Rogers, B., and Morton, D.: Global burned area and biomass burning emissions from small fires, Journal of Geophysical Research: Biogeosciences, 117, 2012.

Real, E., Law, K. S., Weinzierl, B., Fiebig, M., Petzold, A., Wild, O., Methven, J., Arnold, S., Stohl, A., and Huntrieser, H.: Processes influencing ozone levels in Alaskan forest fire

plumes during long-range transport over the North Atlantic, Journal of Geophysical Research: Atmospheres, 112, 2007.

Richardson, L. A., Champ, P. A., and Loomis, J. B.: The hidden cost of wildfires: Economic valuation of health effects of wildfire smoke exposure in Southern California, Journal of Forest Economics, 18, 14-35, 2012.

Roelofs, G. J., Lelieveld, J., Smit, H. G., and Kley, D.: Ozone production and transports in the tropical Atlantic region during the biomass burning season, Journal of Geophysical Research: Atmospheres, 102, 10637-10651, 1997.

Sastry, N.: Forest fires, air pollution, and mortality in Southeast Asia, Demography, 39, 1-23, 2002.

Schaphoff, S., Lucht, W., Gerten, D., Sitch, S., Cramer, W., and Prentice, I. C.: Terrestrial biosphere carbon storage under alternative climate projections, Climatic Change, 74, 97-122, 2006.

Schultz, M. G., Heil, A., Hoelzemann, J. J., Spessa, A., Thonicke, K., Goldammer, J. G., Held, A. C., Pereira, J., and van Het Bolscher, M.: Global wildland fire emissions from 1960 to 2000, Global Biogeochemical Cycles, 22, 2008.

Seiler, W., and Crutzen, P. J.: Estimates of gross and net fluxes of carbon between the biosphere and the atmosphere from biomass burning, Climatic change, 2, 207-247, 1980.

Sigler, J., Lee, X., and Munger, W.: Emission and long-range transport of gaseous mercury from a large-scale Canadian boreal forest fire, Environmental science & technology, 37, 4343-4347, 2003.

Sitch, S., Smith, B., Prentice, I. C., Arneth, A., Bondeau, A., Cramer, W., Kaplan, J., Levis, S., Lucht, W., and Sykes, M. T.: Evaluation of ecosystem dynamics, plant geography and

terrestrial carbon cycling in the LPJ dynamic global vegetation model, Global Change Biology, 9, 161-185, 2003.

Spracklen, D. V., Mickley, L. J., Logan, J. A., Hudman, R. C., Yevich, R., Flannigan, M. D., and Westerling, A. L.: Impacts of climate change from 2000 to 2050 on wildfire activity and carbonaceous aerosol concentrations in the western United States, Journal of Geophysical Research: Atmospheres, 114, 2009.

Staudt, A. C., Jacob, D. J., Logan, J. A., Bachiochi, D., Krishnamurti, T., and Poisson, N.: Global chemical model analysis of biomass burning and lightning influences over the South Pacific in austral spring, Journal of Geophysical Research: Atmospheres, 107, 2002.

Stocks, B., Mason, J., Todd, J., Bosch, E., Wotton, B., Amiro, B., Flannigan, M., Hirsch, K., Logan, K., and Martell, D.: Large forest fires in Canada, 1959–1997, Journal of Geophysical Research, 108, 8149, 2003.

Stohl, A., Andrews, E., Burkhart, J., Forster, C., Herber, A., Hoch, S., Kowal, D., Lunder, C., Mefford, T., and Ogren, J.: Pan-Arctic enhancements of light absorbing aerosol concentrations due to North American boreal forest fires during summer 2004, Journal of Geophysical Research: Atmospheres, 111, 2006.

Streets, D. G., Zhang, Q., and Wu, Y.: Projections of global mercury emissions in 2050, Environmental science & technology, 43, 2983-2988, 2009.

Tanimoto, H., Kajii, Y., Hirokawa, J., Akimoto, H., and Minko, N. P.: The atmospheric impact of boreal forest fires in far eastern Siberia on the seasonal variation of carbon monoxide: Observations at Rishiri, a northern remote island in Japan, Geophysical Research Letters, 27, 4073-4076, 2000.

Thelen, B., French, N. H., Koziol, B. W., Billmire, M., Owen, R. C., Johnson, J., Ginsberg, M., Loboda, T., and Wu, S.: Modeling acute respiratory illness during the 2007 San Diego wildland fires using a coupled emissions-transport system and generalized additive modeling, Environmental Health, 12, 94, 2013.

Thompson, A., Pickering, K., McNamara, D., Schoeberl, M., Hudson, R., Kim, J., Browell, E., Kirchhoff, V., and Nganga, D.: Where did tropospheric ozone over southern Africa and the tropical Atlantic come from in October 1992? Insights from TOMS, GTE TRACE A, and SAFARI 1992, Journal of Geophysical Research: Atmospheres, 101, 24251-24278, 1996.

Thonicke, K., Venevsky, S., Sitch, S., and Cramer, W.: The role of fire disturbance for global vegetation dynamics: coupling fire into a Dynamic Global Vegetation Model, Global Ecology and Biogeography, 10, 661-677, 2001.

Tilman, D., Fargione, J., Wolff, B., D'Antonio, C., Dobson, A., Howarth, R., Schindler, D., Schlesinger, W. H., Simberloff, D., and Swackhamer, D.: Forecasting agriculturally driven global environmental change, Science, 292, 281-284, 2001.

Turetsky, M. R., Harden, J. W., Friedli, H. R., Flannigan, M., Payne, N., Crock, J., and Radke, L.: Wildfires threaten mercury stocks in northern soils, Geophysical Research Letters, 33, 2006.

Val Martin, M., Honrath, R., Owen, R. C., Pfister, G., Fialho, P., and Barata, F.: Significant enhancements of nitrogen oxides, black carbon, and ozone in the North Atlantic lower free troposphere resulting from North American boreal wildfires, Journal of Geophysical Research: Atmospheres, 111, 2006.

Val Martin, M., Honrath, R., Owen, R., and Lapina, K.: Large-scale impacts of anthropogenic pollution and boreal wildfires on the nitrogen oxides over the central North Atlantic region, Journal of Geophysical Research: Atmospheres, 113, 2008.

Van Der Werf, G. R., Randerson, J. T., Collatz, G. J., and Giglio, L.: Carbon emissions from fires in tropical and subtropical ecosystems, Global Change Biology, 9, 547-562, 2003.

Van Der Werf, G. R., Randerson, J. T., Collatz, G. J., Giglio, L., Kasibhatla, P. S., Arellano, A. F., Olsen, S. C., and Kasischke, E. S.: Continental-scale partitioning of fire emissions during the 1997 to 2001 El Nino/La Nina period, Science, 303, 73-76, 2004.

Van der Werf, G. R., Randerson, J. T., Giglio, L., Leeuwen, T. T. v., Chen, Y., Rogers, B. M., Mu, M., van Marle, M. J., Morton, D. C., and Collatz, G. J.: Global fire emissions estimates during 1997–2016, Earth System Science Data, 9, 697-720, 2017.

Veraverbeke, S., Verstraeten, W. W., Lhermitte, S., Van De Kerchove, R., and Goossens, R.: Assessment of post-fire changes in land surface temperature and surface albedo, and their relation with fire–burn severity using multitemporal MODIS imagery, International Journal of Wildland Fire, 21, 243-256, 2012.

Veraverbeke, S., Rogers, B. M., Goulden, M. L., Jandt, R. R., Miller, C. E., Wiggins, E. B., and Randerson, J. T.: Lightning as a major driver of recent large fire years in North American boreal forests, Nature Climate Change, 7, 529, 2017.

Voulgarakis, A., Marlier, M. E., Faluvegi, G., Shindell, D. T., Tsigaridis, K., and Mangeon, S.: Interannual variability of tropospheric trace gases and aerosols: The role of biomass burning emissions, Journal of Geophysical Research: Atmospheres, 120, 7157-7173, 2015.

Wai, K., Wu, S., Kumar, A., and Liao, H.: Seasonal variability and long-term evolution of tropospheric composition in the tropics and Southern Hemisphere, Atmospheric Chemistry and Physics, 14, 4859, 2014.

Weiss-Penzias, P., Jaffe, D., Swartzendruber, P., Hafner, W., Chand, D., and Prestbo, E.: Quantifying Asian and biomass burning sources of mercury using the Hg/CO ratio in pollution plumes observed at the Mount Bachelor Observatory, Atmospheric Environment, 41, 4366-4379, 2007.

Whitlock, C.: Land management: Forests, fires and climate, Nature, 432, 28, 2004.

Wiedinmyer, C., Quayle, B., Geron, C., Belote, A., McKenzie, D., Zhang, X., O'Neill, S., and Wynne, K. K.: Estimating emissions from fires in North America for air quality modeling, Atmospheric Environment, 40, 3419-3432, 2006.

Wiedinmyer, C., Akagi, S., Yokelson, R. J., Emmons, L., Al-Saadi, J., Orlando, J., and Soja, A.: The Fire INventory from NCAR (FINN): a high resolution global model to estimate the emissions from open burning, Geoscientific Model Development, 4, 625, 2011.

Wotawa, G., and Trainer, M.: The influence of Canadian forest fires on pollutant concentrations in the United States, Science, 288, 324-328, 2000.

Wu, S., Mickley, L. J., Jacob, D. J., Logan, J. A., Yantosca, R. M., and Rind, D.: Why are there large differences between models in global budgets of tropospheric ozone?, Journal of Geophysical Research: Atmospheres, 112, 2007.

Wu, S., Mickley, L. J., Jacob, D. J., Rind, D., and Streets, D. G.: Effects of 2000–2050 changes in climate and emissions on global tropospheric ozone and the policy-relevant

background surface ozone in the United States, Journal of Geophysical Research: Atmospheres, 113, 2008a.

Wu, S., Mickley, L. J., Leibensperger, E. M., Jacob, D. J., Rind, D., and Streets, D. G.: Effects of 2000–2050 global change on ozone air quality in the United States, Journal of Geophysical Research: Atmospheres, 113, 2008b.

Wu, S., Mickley, L. J., Kaplan, J., and Jacob, D. J.: Impacts of changes in land use and land cover on atmospheric chemistry and air quality over the 21st century, Atmospheric Chemistry and Physics, 12, 1597-1609, 2012.

Yu, Z., Loisel, J., Brosseau, D. P., Beilman, D. W., and Hunt, S. J.: Global peatland dynamics since the Last Glacial Maximum, Geophysical Research Letters, 37, 2010.

Yu, Z., Beilman, D., Frolking, S., MacDonald, G. M., Roulet, N. T., Camill, P., and Charman, D.: Peatlands and their role in the global carbon cycle, Eos, Transactions American Geophysical Union, 92, 97-98, 2011.

Yue, X., Mickley, L. J., Logan, J. A., and Kaplan, J. O.: Ensemble projections of wildfire activity and carbonaceous aerosol concentrations over the western United States in the mid-21st century, Atmospheric Environment, 77, 767-780, 2013.

Yue, X., Mickley, L., Logan, J., Hudman, R., Martin, M. V., and Yantosca, R.: Impact of 2050 climate change on North American wildfire: consequences for ozone air quality, Atmospheric Chemistry and Physics, 15, 10033-10055, 2015.

Chapter 4: Mercury Pollution in the Arctic from Wildfires: Source Attribution for the 2000s[3]

[3] The contents of this chapter will be submitted for publication as a journal article. *Kumar, A., Wu, S., Mercury Pollution in the Arctic from Wildfires: Source Attribution for the 2000s*

4.1. Abstract

Mercury (Hg) is a global environmental pollutant that has wildfires as an important source. Hg contamination of the Arctic is a cause of concern and can primarily be attributed to long-range transport from lower latitude sources. In this work, we estimate the contribution of wildfires to Hg pollution in the Arctic (66° N to 90° N) using a new global Hg wildfire emissions inventory and an atmospheric chemical transport model (GEOS-Chem). Our results show that wildfires contribute 10% of annual Hg deposition to the Arctic. Eurasia contributes 5.3% of annual Hg deposition followed by Africa (2.5%) and North America (1%). The substantial contributions of Eurasia and North America can be attributed to Hg emissions from the boreal forest fires. We also find that wildfires result in significant Hg deposition to the Arctic across all seasons (winter: 8.3%, spring: 7%, summer: 11%, fall: 14.6%) with year round contributions from Africa and the highest deposition occurring during the boreal fire season. These findings quantify the significance of wildfires as a source of Arctic Hg contamination and the highlight the importance of mobilization of sequestered Hg from boreal forests for the Arctic.

4.2. Introduction

Mercury (Hg) is a toxic pollutant that poses a significant threat to human health. It has a ubiquitous presence in the atmosphere and undergoes repeated cycling between the air and surface reservoirs resulting in considerable persistence in the environment. Due to its air-surface exchange characteristics and persistent nature, recent work has grouped it with other pollutants exhibiting similar characteristics [e.g. Polycyclic Aromatic Hydrocarbons (PAHs) and Polychlorinated Biphenyl compounds (PCBs)] with the collection referred to as Atmosphere-Surface-Exchangeable Pollutants (ASEPs) (Perlinger et al., 2014; 2016). Methyl mercury (CH_3Hg) is the most toxic Hg species (Jæger et al., 2009; Sanfeliu et al., 2003; Wolfe et al., 1998). It can have serious effects on human health with fish consumption being the main route of exposure (Díez, 2008; Harada, 1995; Inskip and Piotrowski, 1985; Jacobson et al., 2015; Matsumoto et al., 1965; Mergler et al., 2007). CH_3Hg is formed in terrestrial and aquatic environments by methylation of inorganic Hg (Beckert et al., 1974; Gabriel and Williamson, 2004). Atmospheric Hg inputs (dry and wet deposition), which are dependent on Hg emissions from anthropogenic sources, wildfires) and re-emission of previously deposited Hg, result in inorganic Hg enrichment of both terrestrial and aquatic environments (Driscoll et al., 2007; Grigal, 2002, 2003). The atmosphere also serves as a medium for long-range transport of Hg species [e.g. Hg(0)] to remote regions where subsequent Hg deposition degrades the previously pristine ecosystems (Driscoll et al., 2013; Grigal, 2002).

Hg pollution in the Arctic is a cause of concern due to its adverse impacts on human health in the region. With no major local Hg sources, the most likely cause of Hg pollution in the Arctic is long-range transport of pollution from the lower-latitudes (Landers et al., 1995). Several past studies have reported the transport of lower-latitude pollution (including Hg) to the Arctic [e.g. (Barrie et al., 1981; Barrie, 1986; Dastoor et al., 2015; Durnford et al., 2010; Eckhardt et al., 2007; Koch and Hansen, 2005; Law and Stohl, 2007; Octaviani et al., 2015; Shindell et al., 2008)]. Hg transported from lower-latitude sources to the Arctic followed by the processes of deposition, chemical transformation, bioaccumulation and biomagnification has contributed to high levels in Arctic wildlife species and the indigenous population [(AMAP, 2011; Bjerregaard and Hansen, 2000; Van Oostdam et al., 1999; Walker et al., 2006)]. Obrist et al. (2017) showed that Hg uptake by Arctic Tundra vegetation could contribute to elevated levels of Hg in the Arctic, with the Tundra being a major sink for Hg emitted at the mid-latitudes. Dastoor et al. (2015) estimated that global anthropogenic Hg emissions could account for 30% of Hg deposition to the Canadian Arctic. Pacyna and Keeler (1995) estimated that Hg emissions from Eurasia and North America could contribute 60 to 80 tons of Hg to the Arctic region annually.

Wildfires are an important source of Hg to the atmosphere with estimated global emissions equivalent to 8% of all natural and anthropogenic Hg emissions (Friedli et al., 2009a). These episodic disturbances are accompanied by high temperatures and burning of biomass, which results in re-mobilization of Hg previously sequestered in terrestrial environments to the atmosphere (Artaxo et al., 2000; Friedli et al., 2003b; Friedli et al., 2001; Kohlenberg et al., 2018; Sigler et al., 2003; Veiga et al., 1994; Woodruff et al., 2001).

Their role in Arctic Hg pollution is important because firstly, wildfire emissions comprise almost exclusively of elemental mercury [Hg(0)] (Friedli et al., 2001), which has an atmospheric lifetime ranging from years to months (Horowitz et al., 2017; Macdonald et al., 2000; Schroeder and Munthe, 1998) enabling it to be transported long distances from the source regions. Particulate bound Hg [Hg(P)] could account for a reasonable fraction of emissions depending on fuel moisture content, however global estimates of Hg(P) are very small (4-5 Mg $year^{-1}$) (Obrist et al., 2007). Secondly, boreal forests in the high latitudes can store substantial amounts of Hg and wildfires are a frequent disturbance in these ecosystems resulting in significant Hg atmospheric emissions (Turetsky et al., 2006). Therefore, it is imperative to quantify the impacts wildfires have on Hg pollution in the Arctic.

Global wildfire emissions of Hg have been quite uncertain (range: 104-1330 Mg Hg $year^{-1}$) (Brunke et al., 2001; De Simone et al., 2015; Ebinghaus et al., 2007; Friedli et al., 2009a; 2003a; Sigler et al., 2003; Weiss-Penzias et al., 2007). Thus, their contribution to Arctic Hg pollution is unknown. To our knowledge, no study so far has attempted to determine the source attribution of Hg pollution in the Arctic due to wildfires using a global Hg wildfire emissions inventory. This study employs GEOS-Chem, a three-dimensional global model of atmospheric chemistry and transport with a recently developed global Hg wildfire emissions inventory to determine the contribution of global and continental Hg wildfire emissions to Hg deposition in the Arctic.

4.3. Methodology

4.3.1. Global Hg Wildfire Emissions Inventory

We use the global Hg wildfire emissions inventory developed by Kumar et al. (2018). The inventory spans the years 1998-2002 (representing the 2000s) and has a monthly temporal and 4° x 5° (latitude x longitude) spatial resolution. Hg emissions were estimated using a fire emissions model (Kumar et al., 2018) based on the classical biomass burning equation (Seiler and Crutzen, 1980). The model includes burned area, vegetation areal coverage and density, combustion fractions and biome specific Hg emission factors as inputs and accounts for variations in fire characteristics, climate, vegetation type and density across geographical regions. Figure 1 shows the geographical regions defined in the model. Burned area estimates for the 2000s were predicted using regression tree relationships between burned area and fire frequencies. Global fire frequencies were based on a fire parameterization, which incorporates the effects of fire ignition agents (natural and anthropogenic) and suppression, fuel availability and climate (Huang et al., 2015). Global vegetation (tropical, temperate, boreal and grass) areal coverage was simulated using the Lund-Potsdam-Jena Dynamic Global Vegetation Model (LPJ DGVM) (Gerten et al., 2004; Hickler et al., 2006; Sitch et al., 2003; Thonicke et al., 2001; Wu et al., 2012) and cropland areal coverage data was from the IMAGE model (IMAGE Team, 2001). Available biomass density estimates for different geographical regions and vegetation types (tropical, temperate, boreal and grasslands) were from the terrestrial component of the Integrated Science Assessment (ISAM) model (Jain et al., 2006; Jain and Yang, 2005). A detailed

description of model development can be found in Kumar et al. (2018). Global Hg emissions for the 2000s (1998-2002 average) are estimated to be 612 Mg year^{-1} with Africa, Eurasia, South America and North America being the major source regions.

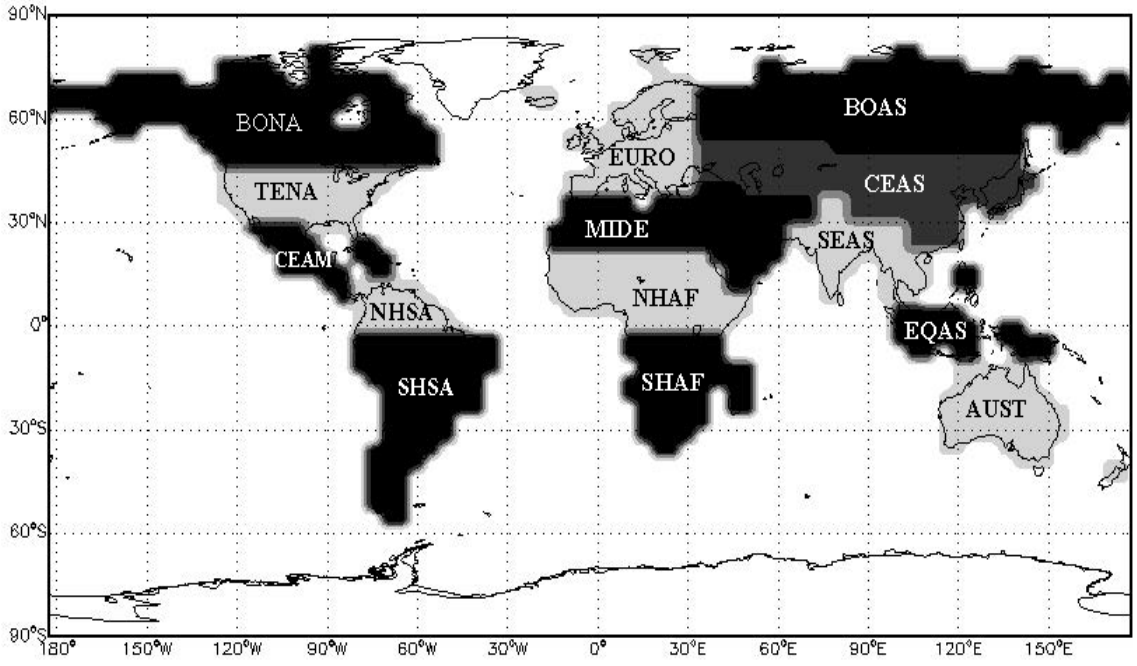

Figure 1: Definition of global regions used in the fire emissions model development. BONA: Boreal North America, TENA: Temperate North America, CEAM: Central North America, NHSA: Northern Hemisphere South America, SHSA: Southern Hemisphere South America, EURO: Europe, MIDE: Middle East, NHAF: Northern Hemisphere Africa, SHAF: Southern Hemisphere Africa, BOAS: Boreal Asia, CEAS: Central Asia, SEAS: South East Asia, EQAS: Equatorial Asia, AUST: Australia.

4.3.2. GEOS-Chem Hg Simulation

We use the global Hg simulation (Amos et al., 2012; Corbitt et al., 2011; Holmes et al., 2010; Selin et al., 2007; Selin et al., 2008; Strode et al., 2007) in the GEOS-Chem model of atmospheric chemistry and transport (Bey et al., 2001). The global Hg simulation in GEOS-Chem is available at spatial resolutions of 2° x 2.5° and 4° x 5° (latitude x longitude). It simulates three mercury species (elemental Hg (Hg(0)), divalent Hg (Hg(II), particulate bound Hg (Hg(P)) and includes Hg cycling amongst fully coupled atmospheric, terrestrial and oceanic reservoirs. The model includes both primary (anthropogenic + natural) and secondary Hg emissions. Anthropogenic Hg emissions are based on Pacyna et al. (2010) and updated following Streets et al. (2009) (Corbitt et al., 2011). Biomass burning emissions are calculated using a fixed Hg/CO emission ratio (Holmes et al., 2010; Selin et al., 2008). Biomass burning emissions comprise exclusively of Hg(0) (Selin et al., 2008). Natural emissions include geogenic sources, ocean and land re-emissions (soil emissions, prompt recycling of newly deposited Hg). Atmospheric Hg sinks in the model include dry and wet deposition of the Hg species. Deposition of Hg(0), Hg(II) and Hg(P) to terrestrial surfaces follows the resistance-in-series formulation of Wesely (1989). Dry deposition of Hg(0) to oceans is based on the bidirectional exchange model of Soerensen et al. (2010). Sea salt aerosol uptake of Hg(II) (function of wind speed, relative humidity and mixing depth) is included as a sink in the marine boundary layer (Holmes et al., 2010; Holmes et al., 2009). Wet deposition of Hg(II) and Hg(P) consists of scavenging in wet convective updrafts and rainout and washout in large scale precipitation (Amos et al., 2012; Holmes et al., 2010; Liu et al., 2001; Wang et al., 2011). Atmospheric chemistry of Hg in

the model involves gas phase oxidation of Hg(0) to Hg(II) driven by bromine (Br) atoms and in-cloud aqueous phase photochemical reduction of Hg(II) to Hg(0) (Holmes et al., 2006; Selin et al., 2008). GEOS-Chem is capable of simulating the Arctic springtime Hg depletion events driven by Br oxidation of Hg(0) (Holmes et al., 2010). Hg(II) partitioning from gas phase to particulate phase [Hg(P)] is parameterized as a function of temperature and particulate matter concentration (Amos et al., 2012).

In this work, we use the GEOS-Chem Hg simulation at a spatial resolution of 4° x 5° (model version: v9-02) driven with the GEOS-5 meteorology fields and Hg wildfire emissions inventory from Kumar et al. (2018) [Section 2.1]. We perform seven simulations (including a control run) to determine the contributions of different wildfire emissions source continents to Hg deposition in the Arctic. Table 1 lists the simulations along with the respective descriptions. These simulations consisted of a control (Control (with wildfire emissions for the 2000s)) and no wildfires (No Global) simulation together with simulations having emissions from individual continents absent [e.g. No North America simulations had zero emissions from North America]. For all the seven simulations, we simulate meteorology years 2006-2010 with the first year used for model initialization. The results presented here are averages of the years 2007-2010. The Arctic region is defined as extending from 66° N to 90° N and 180° W to 180° E. The deposition archived from the simulations is the sum of dry (Hg(0) + Hg(II) + Hg(P)) and wet deposition (Hg(II) + Hg(P)). The contribution of each continent is calculated as shown in Eq. (1).

$$\mathbf{Contribution_{Continent}} = \left(\frac{\mathbf{Hg\ Deposition_{Control} - Hg\ Deposition_{Sensitivity}}}{\mathbf{Hg\ Deposition_{Control}}}\right) * \mathbf{100} \quad (1)$$

Where:

$\mathbf{Contribution_{Continent}}$: Percentage contribution of Hg wildfire emissions in the continent to Hg deposition in the Arctic (Continent=North America, South America, Eurasia, Africa, Australia)

$\mathbf{Hg\ Deposition_{Control}}$: Annual total Hg deposition over the Arctic for the control run

$\mathbf{Hg\ Deposition_{Sensitivity}}$: Annual total Hg deposition over the Arctic for the sensitivity runs (Sensitivity = No Global, No North America, No South America, No Eurasia, No Africa, No Australia)

Table 1: Description of the simulations performed to determine the contribution of wildfire emissions (global/continental) on Hg deposition in the Arctic.

Simulation	Description
Control	With global Hg wildfire emissions for the 2000s
No Global	No wildfire emissions globally
No North America	No wildfire emissions from North America (BONA, TENA, CEAM)
No South America	No wildfire emissions from South America (NHSA, SHSA)
No Africa	No wildfire emissions from Africa (MIDE, NHAF, SHAF)
No Eurasia	No wildfire emissions from Eurasia (EURO, BOAS, CEAS, SEAS, EQAS)
No Australia	No wildfire emissions from Australia (AUST)

4.4. Hg deposition to the Arctic due to wildfires (2000s)

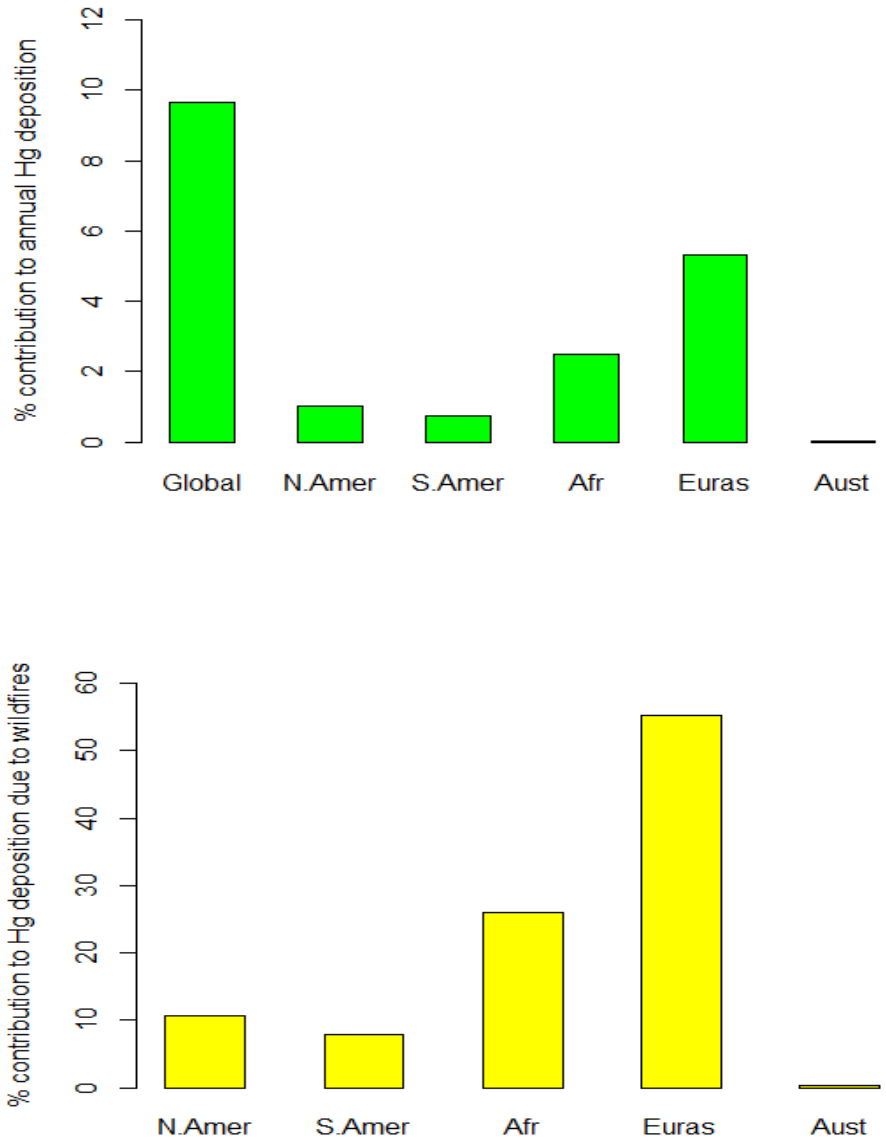

Figure 2: (a) Percentage contribution of global and continental wildfire emissions to annual deposition to the Arctic, (b) percentage contribution of different regions/continents to annual deposition due to wildfires in the Arctic.

Figure 2(a) shows the percentage of annual Hg deposition to the Arctic due to wildfires (global and continental) while Figure 2(b) shows the contribution of different continents to the annual wildfire deposition. Global wildfire Hg emissions are estimated to contribute ~10% of the annual Hg deposition to the Arctic. A significant fraction (~9%) of this Hg originates from wildfires in Eurasia (5% of annual Hg deposition), Africa (2.3%) and North America (1%), which collectively account for ~83% of global Hg wildfire emissions (Kumar et al., 2018). Considering the deposition due to wildfires only [Figure 2(b)], these continents account for 92% of the annual deposition to the Arctic (Eurasia: 55%, Africa: 26%, North America: 11%). The significant contributions of North America and Eurasia can be primarily attributed to wildfires in the boreal parts of these continents. Wildfires in boreal forests (BONA + BOAS) account for 41% of the global Hg wildfire emissions with Eurasian boreal forests emitting 31% of global emissions due to the significantly higher fire activity in the region as compared to boreal North America (Kumar et al., 2018). This distribution is also reflected in the relatively minor contribution of wildfires in North America to annual Arctic deposition (1%) as compared to that of Eurasia (5.3%). Major tropical wildfire emissions sources such as South America and Africa also contribute to Arctic Hg enrichment annually, accounting for 3.3% of total deposition and 34% of deposition due to wildfires. This could be attributed to the long atmospheric lifetime of Hg(0), which is the primary species emitted from wildfires enabling it to be transported far away from the source regions. Wildfires in Australia account for < 1% of global Hg emissions (Kumar et al., 2018), which results in the negligible contributions (< 0.1%) of the continent to Arctic Hg deposition.

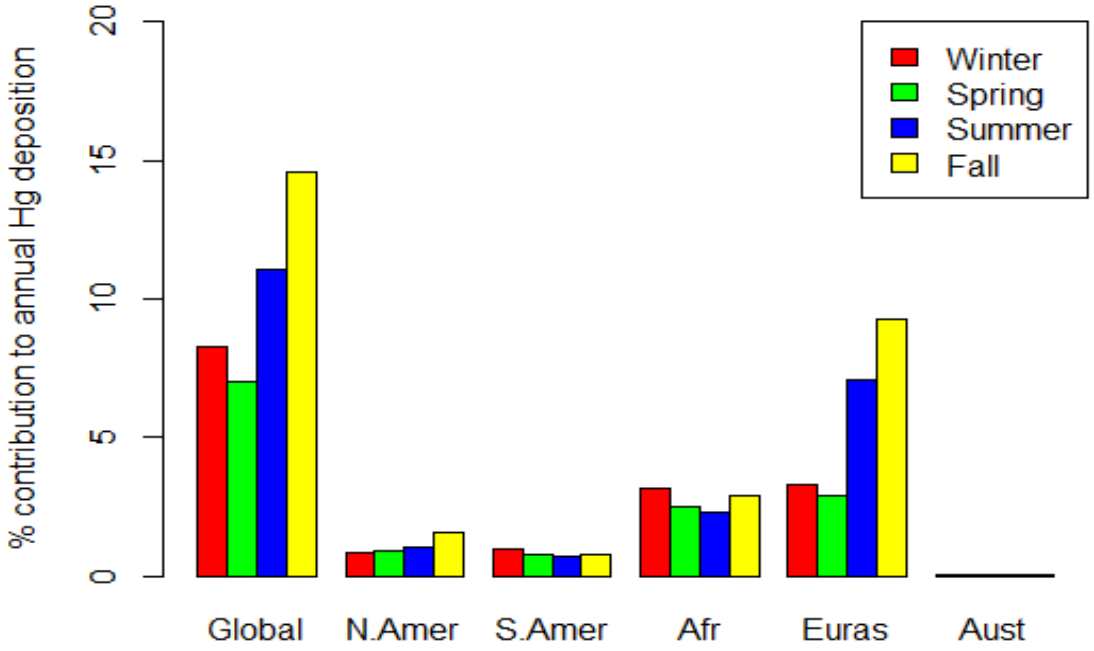

Figure 3: Seasonal contribution of wildfire emissions (global and continental) to annual total Hg deposition in the Arctic.

Figure 3 shows the seasonal variation in contributions of wildfires to Hg deposition in the Arctic (winter: December-January-February, spring: March-April-May, summer: June-July-August, fall: September-October-November).Wildfires are a year-round phenomenon with some part of the globe experiencing fires in a given season. This is shown by the consistent Hg deposition in the Arctic due to wildfires across all seasons. Global wildfire emissions cause the maximum Hg deposition during the fall (15%) and summer (11%) with relatively smaller inputs during the spring (7%) and winter (8%). The peak contributions

during the summer and fall months coincide with the onset of the burning season in the boreal forests. Therefore, the contributions of North America (summer: 1%, fall: 1.5%) and Eurasia (summer: 7%, fall: 9%) in these seasons are higher than in the winter (North America: 0.8%, Eurasia: 3%) and spring (North America: 0.9%, Eurasia: 2.9%). The dominant role of boreal fires in Eurasia can be observed here as well with > 50% of the deposition during summer and fall being caused by them. African wildfire emissions result in a consistent year round Hg enrichment of the Arctic with similar contributions across all seasons (2.3% - 3.1%), which can be attributed to the consistent fire activity occurring in the continent in a year. During winter and spring, Africa and Eurasia are the major contributors to Arctic Hg deposition. These findings indicate that wildfires play a major role in Hg enrichment of the Arctic year round.

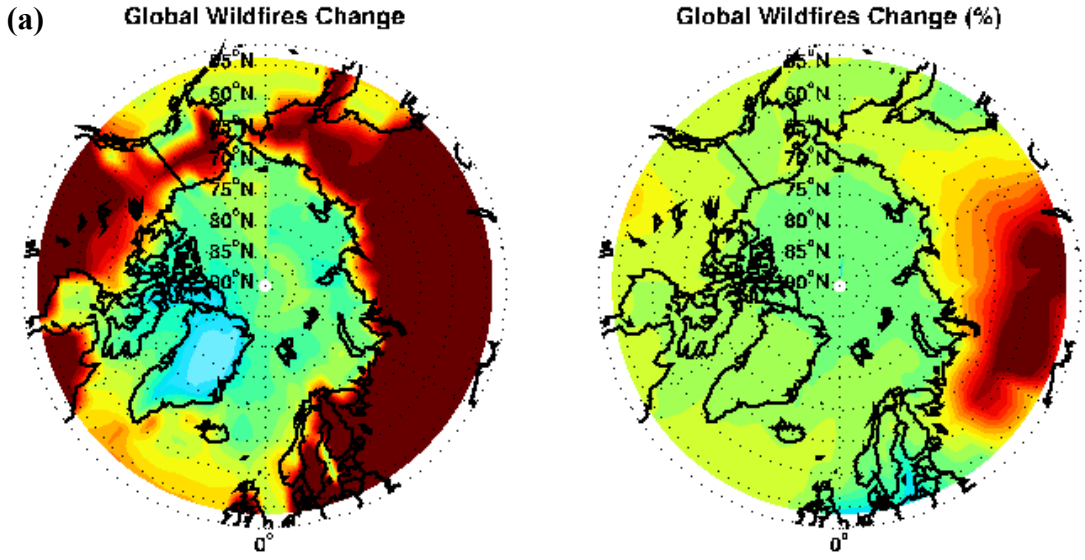

(b)

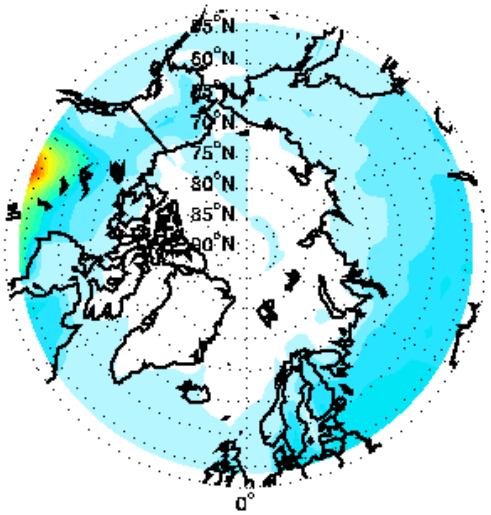
North America Change
65°N
60°N
70°N
75°N
80°N
85°N
90°N
0°

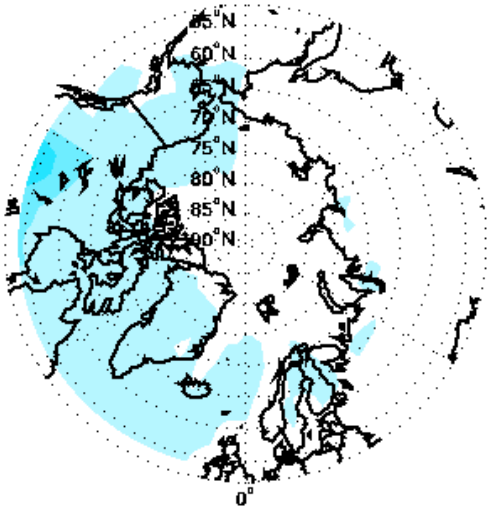
North America Change (%)
65°N
60°N
70°N
75°N
80°N
85°N
90°N
0°

(c)

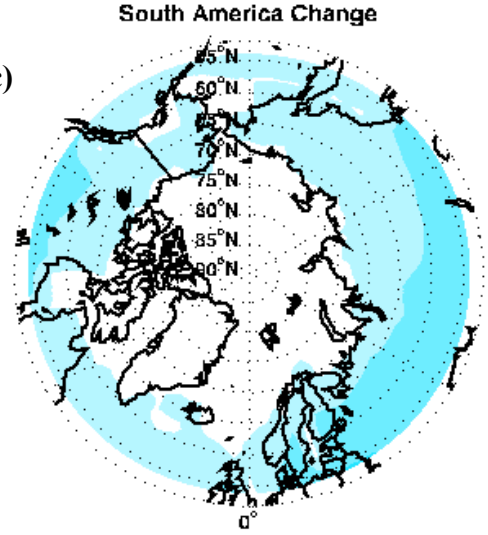
South America Change
65°N
60°N
70°N
75°N
80°N
85°N
90°N
0°

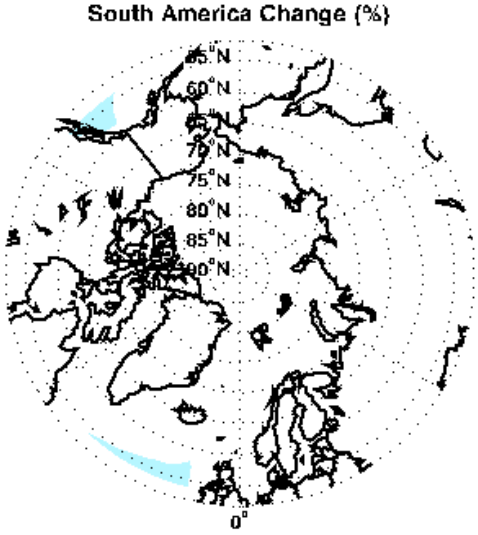
South America Change (%)
65°N
60°N
70°N
75°N
80°N
85°N
90°N
0°

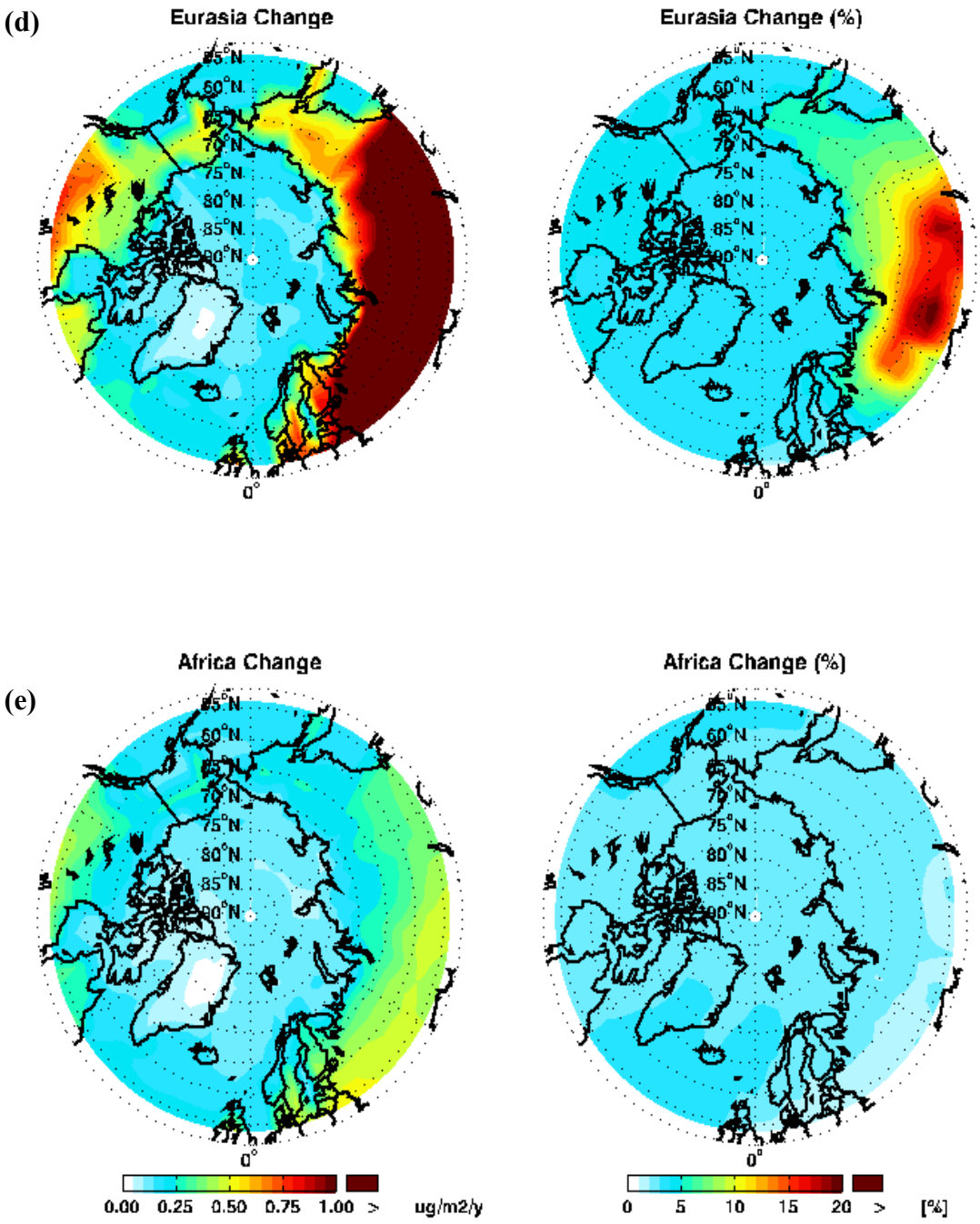

Figure 4: Spatial distribution of contribution to Arctic Hg deposition in the absence of global (a) and continental (North America (b), Eurasia (c), South America (d), and Africa (e) Hg wildfire emissions.

Figure 4 shows the spatial distribution of contributions of global and continental Hg wildfire emissions to annual Arctic Hg deposition (Australia is omitted due to negligible contributions). Wildfires make significant contributions to annual Hg deposition throughout the Arctic [Figure 4(a)]. Deposition is particulary high in the Eurasian parts due to the high Hg emissions from the boreal forests in the region. Other parts of the Arctic receive much lower inputs. Deposition to the Arctic Tundra region (North of 70° latitude) ranges from 5-10% [Figure 4(a)] with substantial differences between the North American and Russian Tundra reflecting the differences in the magnitude of emissions in the two regions. Obrist et al. (2017) identified Hg (0) atmospheric deposition to the Arctic Tundra to be a major driver of Arctic Hg contamination with deposition amplifying during the vegetation-growing season. Since wildfires emit Hg mainly as Hg (0) and considering that boreal forest emissions (the major wildfire source of Hg deposition to the Arctic) increase significantly during the vegetation growing season (e.g. summer) in the Tundra, wildfires cause Hg inputs to the Arctic when it can have the most significant impacts on the Arctic ecosystems. Figures 4(b) - 4(e) show the spatial distribution of contributions of emissions from different continents to the Arctic. Emissions from Africa make uniform contributions throughout the Arctic region [Figure 4(e)] while Eurasian emissions also increase Hg deposition in other parts of the Arctic (e.g. North America). These results further emphasize the importance of long-range transport of Hg to the Arctic from far away regions.

4.5. Conclusions

We studied the source attribution (2000s) for Hg deposition to the Arctic due to wildfires in this study. We used a new global Hg wildfire emissions inventory to drive the atmospheric Hg simulation in a global model of atmospheric chemistry and transport (GEOS-Chem). A suite of simulations were performed with wildfire emissions turned off globally and from individual wildfire emissions source continents. Global wildfire Hg emissions are estimated to contribute 10% of annual Hg deposition to the Arctic. At the continental scale, Eurasia contributes 5.3% of annual Hg deposition followed by Africa (2.5%) and North America (1%). The substantial contributions of Eurasia and North America can be primarily attributed to wildfire emissions from the boreal forests in these continents. We also find that wildfires result in significant Hg deposition to the Arctic across all seasons (winter: 8.3%, spring: 7%, summer: 11%, fall: 14.6%) with the highest deposition occurring during the boreal fire season (summer and fall). Several studies have highlighted the importance of boreal forests as important sinks of Hg in the high latitudes and the implications of mobilization of this Hg. Our estimates of more than 50% of wildfire caused deposition to the Arctic emerging from Eurasia and North America where boreal forests are the major Hg source provide quantitative evidence supporting these earlier studies. In addition, due to the significantly higher contribution to Hg deposition as compared to boreal forests in North America, boreal forests in Asia could be identified as the major biome driving Arctic Hg pollution due to wildfires.

References

AMAP (2011) AMAP Assessment 2011: Mercury in the Arctic. Arctic Monitoring and Assessment Programme (AMAP), 193.

Amos, H.M., Jacob, D.J., Holmes, C., Fisher, J.A., Wang, Q., Yantosca, R.M., Corbitt, E.S., Galarneau, E., Rutter, A., Gustin, M. (2012) Gas-particle partitioning of atmospheric Hg (II) and its effect on global mercury deposition. Atmospheric Chemistry and Physics 12, 591-603.

Artaxo, P., de Campos, R.C., Fernandes, E.T., Martins, J.V., Xiao, Z., Lindqvist, O., Fernández-Jiménez, M.T., Maenhaut, W. (2000) Large scale mercury and trace element measurements in the Amazon basin. Atmospheric Environment 34, 4085-4096.

Barrie, L., Hoff, R., Daggupaty, S. (1981) The influence of mid-latitudinal pollution sources on haze in the Canadian Arctic. Atmospheric Environment (1967) 15, 1407-1419.

Barrie, L.A. (1986) Arctic air pollution: an overview of current knowledge. Atmospheric Environment (1967) 20, 643-663.

Beckert, W., Moghissi, A., Au, F., Bretthauer, E., McFarlane, J. (1974) Formation of methylmercury in a terrestrial environment. Nature 249, 674.

Bey, I., Jacob, D.J., Yantosca, R.M., Logan, J.A., Field, B.D., Fiore, A.M., Li, Q., Liu, H.Y., Mickley, L.J., Schultz, M.G. (2001) Global modeling of tropospheric chemistry with

assimilated meteorology: Model description and evaluation. Journal of Geophysical Research: Atmospheres 106, 23073-23095.

Bjerregaard, P., Hansen, J.C. (2000) Organochlorines and heavy metals in pregnant women from the Disko Bay area in Greenland. Science of The Total Environment 245, 195-202.

Brunke, E.G., Labuschagne, C., Slemr, F. (2001) Gaseous mercury emissions from a fire in the Cape Peninsula, South Africa, during January 2000. Geophysical Research Letters 28, 1483-1486.

Corbitt, E.S., Jacob, D.J., Holmes, C.D., Streets, D.G., Sunderland, E.M. (2011) Global source–receptor relationships for mercury deposition under present-day and 2050 emissions scenarios. Environmental science & technology 45, 10477-10484.

Dastoor, A., Ryzhkov, A., Durnford, D., Lehnherr, I., Steffen, A., Morrison, H. (2015) Atmospheric mercury in the Canadian Arctic. Part II: Insight from modeling. Science of The Total Environment 509, 16-27.

De Simone, F., Cinnirella, S., Gencarelli, C.N., Yang, X., Hedgecock, I.M., Pirrone, N. (2015) Model study of global mercury deposition from biomass burning. Environmental science & technology 49, 6712-6721.

Díez, S., (2008) Human health effects of methylmercury exposure, Reviews of Environmental Contamination and Toxicology. Springer, pp. 111-132.

Driscoll, C.T., Han, Y.-J., Chen, C.Y., Evers, D.C., Lambert, K.F., Holsen, T.M., Kamman, N.C., Munson, R.K. (2007) Mercury contamination in forest and freshwater ecosystems in the northeastern United States. BioScience 57, 17-28.

Driscoll, C.T., Mason, R.P., Chan, H.M., Jacob, D.J., Pirrone, N. (2013) Mercury as a global pollutant: sources, pathways, and effects. Environmental science & technology 47, 4967-4983.

Durnford, D., Dastoor, A., Figueras-Nieto, D., Ryjkov, A. (2010) Long range transport of mercury to the Arctic and across Canada. Atmospheric Chemistry and Physics 10, 6063-6086.

Ebinghaus, R., Slemr, F., Brenninkmeijer, C., Van Velthoven, P., Zahn, A., Hermann, M., O'Sullivan, D., Oram, D. (2007) Emissions of gaseous mercury from biomass burning in South America in 2005 observed during CARIBIC flights. Geophysical Research Letters 34.

Eckhardt, S., Breivik, K., Stohl, A. (2007) Record high peaks in PCB concentrations in the Arctic atmosphere due to long-range transport of biomass burning emissions. Atmospheric Chemistry and Physics 7, 4527-4536.

Friedli, H., Arellano, A., Cinnirella, S., Pirrone, N. (2009) Initial estimates of mercury emissions to the atmosphere from global biomass burning. Environmental science & technology 43, 3507-3513.

Friedli, H., Radke, L., Lu, J., Banic, C., Leaitch, W., MacPherson, J. (2003a) Mercury emissions from burning of biomass from temperate North American forests: laboratory and airborne measurements. Atmospheric Environment 37, 253-267.

Friedli, H., Radke, L., Prescott, R., Hobbs, P., Sinha, P. (2003b) Mercury emissions from the August 2001 wildfires in Washington State and an agricultural waste fire in Oregon and atmospheric mercury budget estimates. Global Biogeochemical Cycles 17.

Friedli, H.R., Radke, L.F., Lu, J.Y. (2001) Mercury in smoke from biomass fires. Geophysical Research Letters 28, 3223-3226.

Gabriel, M.C., Williamson, D.G. (2004) Principal biogeochemical factors affecting the speciation and transport of mercury through the terrestrial environment. Environmental geochemistry and health 26, 421-434.

Gerten, D., Schaphoff, S., Haberlandt, U., Lucht, W., Sitch, S. (2004) Terrestrial vegetation and water balance—hydrological evaluation of a dynamic global vegetation model. Journal of Hydrology 286, 249-270.

Grigal, D. (2002) Inputs and outputs of mercury from terrestrial watersheds: a review. Environmental Reviews 10, 1-39.

Grigal, D. (2003) Mercury sequestration in forests and peatlands. Journal of environmental quality 32, 393-405.

Harada, M. (1995) Minamata disease: methylmercury poisoning in Japan caused by environmental pollution. Critical reviews in toxicology 25, 1-24.

Hickler, T., Prentice, I.C., Smith, B., Sykes, M.T., Zaehle, S. (2006) Implementing plant hydraulic architecture within the LPJ Dynamic Global Vegetation Model. Global Ecology and Biogeography 15, 567-577.

Holmes, C.D., Jacob, D.J., Corbitt, E.S., Mao, J., Yang, X., Talbot, R., Slemr, F. (2010) Global atmospheric model for mercury including oxidation by bromine atoms. Atmospheric Chemistry and Physics 10, 12037-12057.

Holmes, C.D., Jacob, D.J., Mason, R.P., Jaffe, D.A. (2009) Sources and deposition of reactive gaseous mercury in the marine atmosphere. Atmospheric Environment 43, 2278-2285.

Holmes, C.D., Jacob, D.J., Yang, X. (2006) Global lifetime of elemental mercury against oxidation by atomic bromine in the free troposphere. Geophysical Research Letters 33.

Horowitz, H.M., Jacob, D.J., Zhang, Y., Dibble, T.S., Slemr, F., Amos, H.M., Schmidt, J.A., Corbitt, E.S., Marais, E.A., Sunderland, E.M. (2017) A new mechanism for atmospheric mercury redox chemistry: implications for the global mercury budget. Atmospheric Chemistry and Physics 17, 6353-6371.

Huang, Y., Wu, S., Kaplan, J.O. (2015) Sensitivity of global wildfire occurrences to various factors in the context of global change. Atmospheric Environment 121, 86-92.

IMAGE Team, H. (2001) The IMAGE 2.2 implementation of the SRES scenarios: a comprehensive analysis of emissions, climate change and impacts in the 21st century. RIVM CD-ROM Publication 481508018.

Inskip, M., Piotrowski, J. (1985) Review of the health effects of methylmercury. Journal of Applied Toxicology 5, 113-133.

Jacobson, J.L., Muckle, G., Ayotte, P., Dewailly, É., Jacobson, S.W. (2015) Relation of prenatal methylmercury exposure from environmental sources to childhood IQ. Environmental health perspectives 123, 827.

Jæger, I., Hop, H., Gabrielsen, G.W. (2009) Biomagnification of mercury in selected species from an Arctic marine food web in Svalbard. Science of The Total Environment 407, 4744-4751.

Jain, A.K., Tao, Z., Yang, X., Gillespie, C. (2006) Estimates of global biomass burning emissions for reactive greenhouse gases (CO, NMHCs, and NOx) and CO2. Journal of Geophysical Research: Atmospheres 111.

Jain, A.K., Yang, X. (2005) Modeling the effects of two different land cover change data sets on the carbon stocks of plants and soils in concert with CO2 and climate change. Global Biogeochemical Cycles 19.

Koch, D., Hansen, J. (2005) Distant origins of Arctic black carbon: a Goddard Institute for Space Studies ModelE experiment. Journal of Geophysical Research: Atmospheres 110.

Kohlenberg, A.J., Turetsky, M.R., Thompson, D.K., Branfireun, B.A., Mitchell, C.P. (2018) Controls on boreal peat combustion and resulting emissions of carbon and mercury. Environmental Research Letters 13, 035005.

Kumar, A., Wu, S., Huang, Y., Liao, H., Kaplan, J.O. (2018) Mercury from wildfires: Global emission inventories and sensitivity to 2000–2050 global change. Atmospheric Environment 173, 6-15.

Landers, D., Ford, J., Gubala, C., Monetti, M., Lasorsa, B., Martinson, J. (1995) Mercury in vegetation and lake sediments from the US Arctic. Water, Air, and Soil Pollution 80, 591-601.

Law, K.S., Stohl, A. (2007) Arctic air pollution: Origins and impacts. science 315, 1537-1540.

Liu, H., Jacob, D.J., Bey, I., Yantosca, R.M. (2001) Constraints from 210Pb and 7Be on wet deposition and transport in a global three-dimensional chemical tracer model driven by assimilated meteorological fields. Journal of Geophysical Research: Atmospheres 106, 12109-12128.

Macdonald, R.W., Barrie, L.A., Bidleman, T.F., Diamond, M.L., Gregor, D.J., Semkin, R.G., Strachan, W., Li, Y.F., Wania, F., Alaee, M. (2000) Contaminants in the Canadian Arctic: 5 years of progress in understanding sources, occurrence and pathways. Science of The Total Environment 254, 93-234.

Matsumoto, H., Koya, G., Takeuchi, T. (1965) Fetal minamata disease. Journal of Neuropathology and Experimental Neurology 24, 563-574.

Mergler, D., Anderson, H.A., Chan, L.H.M., Mahaffey, K.R., Murray, M., Sakamoto, M., Stern, A.H. (2007) Methylmercury exposure and health effects in humans: a worldwide concern. AMBIO: A Journal of the Human Environment 36, 3-11.

Obrist, D., Agnan, Y., Jiskra, M., Olson, C.L., Colegrove, D.P., Hueber, J., Moore, C.W., Sonke, J.E., Helmig, D. (2017) Tundra uptake of atmospheric elemental mercury drives Arctic mercury pollution. Nature 547, 201.

Obrist, D., Moosmüller, H., Schürmann, R., Chen, L.-W.A., Kreidenweis, S.M. (2007) Particulate-phase and gaseous elemental mercury emissions during biomass combustion: controlling factors and correlation with particulate matter emissions. Environmental science & technology 42, 721-727.

Octaviani, M., Stemmler, I., Lammel, G., Graf, H.F. (2015) Atmospheric transport of persistent organic pollutants to and from the Arctic under present-day and future climate. Environmental science & technology 49, 3593-3602.

Pacyna, E.G., Pacyna, J., Sundseth, K., Munthe, J., Kindbom, K., Wilson, S., Steenhuisen, F., Maxson, P. (2010) Global emission of mercury to the atmosphere from anthropogenic sources in 2005 and projections to 2020. Atmospheric Environment 44, 2487-2499.

Pacyna, J., Keeler, G.J., (1995) Sources of mercury in the Arctic, Mercury as a Global Pollutant. Springer, pp. 621-632.

Perlinger, J., Urban, N., Obrist, D., Wu, S., (2014) The Role of Biogeochemical Cycling of Atmosphere-surface Exchangeable Pollutants (ASEPs) in the Dynamic Coupled Human-Natural ASEP System, AGU Fall Meeting Abstracts.

Perlinger, J.A., Gorman, H.S., Norman, E.S., Obrist, D., Selin, N.E., Urban, N.R., Wu, S., (2016) Measurement and Modeling of Atmosphere-Surface Exchangeable Pollutants (ASEPs) To Better Understand their Environmental Cycling and Planetary Boundaries. ACS Publications.

Sanfeliu, C., Sebastià, J., Cristòfol, R., Rodríguez-Farré, E. (2003) Neurotoxicity of organomercurial compounds. Neurotoxicity research 5, 283-305.

Schroeder, W.H., Munthe, J. (1998) Atmospheric mercury—an overview. Atmospheric Environment 32, 809-822.

Seiler, W., Crutzen, P.J. (1980) Estimates of gross and net fluxes of carbon between the biosphere and the atmosphere from biomass burning. Climatic change 2, 207-247.

Selin, N.E., Jacob, D.J., Park, R.J., Yantosca, R.M., Strode, S., Jaeglé, L., Jaffe, D. (2007) Chemical cycling and deposition of atmospheric mercury: Global constraints from observations. Journal of Geophysical Research: Atmospheres 112.

Selin, N.E., Jacob, D.J., Yantosca, R.M., Strode, S., Jaeglé, L., Sunderland, E.M. (2008) Global 3-D land-ocean-atmosphere model for mercury: Present-day versus preindustrial cycles and anthropogenic enrichment factors for deposition. Global Biogeochemical Cycles 22.

Shindell, D., Chin, M., Dentener, F., Doherty, R., Faluvegi, G., Fiore, A., Hess, P., Koch, D., MacKenzie, I., Sanderson, M. (2008) A multi-model assessment of pollution transport to the Arctic. Atmospheric Chemistry and Physics 8, 5353-5372.

Sigler, J., Lee, X., Munger, W. (2003) Emission and long-range transport of gaseous mercury from a large-scale Canadian boreal forest fire. Environmental science & technology 37, 4343-4347.

Sitch, S., Smith, B., Prentice, I.C., Arneth, A., Bondeau, A., Cramer, W., Kaplan, J., Levis, S., Lucht, W., Sykes, M.T. (2003) Evaluation of ecosystem dynamics, plant geography and terrestrial carbon cycling in the LPJ dynamic global vegetation model. Global Change Biology 9, 161-185.

Soerensen, A.L., Sunderland, E.M., Holmes, C.D., Jacob, D.J., Yantosca, R.M., Skov, H., Christensen, J.H., Strode, S.A., Mason, R.P. (2010) An improved global model for air-sea exchange of mercury: High concentrations over the North Atlantic. Environmental science & technology 44, 8574-8580.

Streets, D.G., Zhang, Q., Wu, Y. (2009) Projections of global mercury emissions in 2050. Environmental science & technology 43, 2983-2988.

Strode, S.A., Jaeglé, L., Selin, N.E., Jacob, D.J., Park, R.J., Yantosca, R.M., Mason, R.P., Slemr, F. (2007) Air-sea exchange in the global mercury cycle. Global Biogeochemical Cycles 21.

Thonicke, K., Venevsky, S., Sitch, S., Cramer, W. (2001) The role of fire disturbance for global vegetation dynamics: coupling fire into a Dynamic Global Vegetation Model. Global Ecology and Biogeography 10, 661-677.

Turetsky, M.R., Harden, J.W., Friedli, H.R., Flannigan, M., Payne, N., Crock, J., Radke, L. (2006) Wildfires threaten mercury stocks in northern soils. Geophysical Research Letters 33.

Van Oostdam, J., Gilman, A., Dewailly, E., Usher, P., Wheatley, B., Kuhnlein, H., Neve, S., Walker, J., Tracy, B., Feeley, M. (1999) Human health implications of environmental contaminants in Arctic Canada: a review. Science of The Total Environment 230, 1-82.

Veiga, M.M., Meech, J.A., Oñate, N. (1994) Mercury pollution from deforestation. Nature 368, 816.

Walker, J.B., Houseman, J., Seddon, L., McMullen, E., Tofflemire, K., Mills, C., Corriveau, A., Weber, J.-P., LeBlanc, A., Walker, M. (2006) Maternal and umbilical cord blood levels of mercury, lead, cadmium, and essential trace elements in Arctic Canada. Environmental research 100, 295-318.

Wang, Q., Jacob, D.J., Fisher, J.A., Mao, J., Leibensperger, E., Carouge, C., Sager, P.L., Kondo, Y., Jimenez, J., Cubison, M. (2011) Sources of carbonaceous aerosols and deposited black carbon in the Arctic in winter-spring: implications for radiative forcing. Atmospheric Chemistry and Physics 11, 12453-12473.

Weiss-Penzias, P., Jaffe, D., Swartzendruber, P., Hafner, W., Chand, D., Prestbo, E. (2007) Quantifying Asian and biomass burning sources of mercury using the Hg/CO ratio in pollution plumes observed at the Mount Bachelor Observatory. Atmospheric Environment 41, 4366-4379.

Wesely, M. (1989) Parameterization of surface resistances to gaseous dry deposition in regional-scale numerical models. Atmospheric Environment (1967) 23, 1293-1304.

Wolfe, M.F., Schwarzbach, S., Sulaiman, R.A. (1998) Effects of mercury on wildlife: a comprehensive review. Environmental toxicology and chemistry 17, 146-160.

Woodruff, L., Harden, J., Cannon, W., Gough, L., (2001) Mercury loss from the forest floor during wildland fire, AGU Fall Meeting Abstracts.

Wu, S., Mickley, L.J., Kaplan, J., Jacob, D.J. (2012) Impacts of changes in land use and land cover on atmospheric chemistry and air quality over the 21st century. Atmospheric Chemistry and Physics 12, 1597-1609.

Permission for Reproducing Chapter 2

From: Permissions Helpdesk <permissionshelpdesk@elsevier.com>

To: Aditya Kumar <adityak@mtu.edu>

Mar 1, 2018, 11:42 AM

Dear Aditya,

As an Elsevier journal author, you retain the right to Include the article in a thesis or dissertation (provided that this is not to be published commercially) whether in full or in part, subject to proper acknowledgment; seehttps://www.elsevier.com/about/our-business/policies/copyright/personal-use for more information. As this is a retained right, no written permission from Elsevier is necessary.

If I may be of further assistance, please let me know.

Best of luck with your dissertation and best regards,

Laura

Laura Stingelin
Permissions Helpdesk Associate

ELSEVIER | Global E-Operations Books
+1 215-239-3867 office

l.stingelin@elsevier.com
Contact the Permissions Helpdesk
+1 800-523-4069 x3808 | permissionshelpdesk@elsevier.com

From: Aditya Kumar [mailto:adityak@mtu.edu]

Sent: Wednesday, February 28, 2018 2:13 PM

To: Permissions Helpdesk <permissionshelpdesk@elsevier.com>

Subject: Including published article in doctoral dissertation

Dear Sir/Ma'am,

My name is Aditya Kumar and I am writing to request permission for a journal article titled "Mercury from wildfires: Global emission inventories and sensitivity to 2000–2050 global change" published in Atmospheric Environment (publication date: 2018/1/1, Volume 173, Pages 6-15) to be included in my doctoral dissertation. The paper is attached with this message. I am the lead author in this publication. It is required by my graduate school to include a no-objection letter from the journal in my dissertation. Hence, I would request you to please provide some form of no objection documentation that I can include in my dissertation.

Thanks,

Sincerely,

Aditya Kumar